

ESTIMATION OF CROP WATER REQUIREMENT IN RICE USING SATELLITE DATA AND GIS

by
CHINNU RAJU
(2019-11-186)



DEPARTMENT OF AGRICULTURAL METEOROLOGY
COLLEGE OF AGRICULTURE
VELLANIKKARA, THRISSUR – 680 656
KERALA, INDIA
2021

ESTIMATION OF CROP WATER REQUIREMENT IN RICE USING SATELLITE DATA AND GIS

by
CHINNU RAJU
(2019-11-186)

THESIS

Submitted in partial fulfillment of the requirement for the degree of

MASTER OF SCIENCE IN AGRICULTURE

Faculty of Agriculture
Kerala Agricultural University



**DEPARTMENT OF AGRICULTURAL METEOROLOGY
COLLEGE OF AGRICULTURE**

VELLANIKKARA, THRISSUR – 680 656

KERALA, INDIA

2021

DECLARATION

I hereby declare that this thesis entitled “**ESTIMATION OF CROP WATER REQUIREMENT IN RICE USING SATELLITE DATA AND GIS**” is a bonafide record of research work done by me during the course of research and the thesis has not previously formed the basis for the award to me of any degree, diploma, associateship, fellowship or other similar title, of any other University or Society.

Vellanikkara

Date: 29.11.2021


CHINNU RAJU
(2019-11-186)

CERTIFICATE

Certified that this thesis entitled “**ESTIMATION OF CROP WATER REQUIREMENT IN RICE USING SATELLITE DATA AND GIS**” is a bonafide record of research work done independently by **Ms. Chinnu Raju (2019-11-186)** under my guidance and supervision and that it has not previously formed the basis for the award of any degree, diploma, fellowship or associateship to her.

Vellanikkara

Date: 29/11/2021


Dr. Ajith K.

(Chairman, Advisory Committee)

Assistant Professor

Agricultural Meteorology

RARS, Kumarakom

CERTIFICATE

We, the undersigned members of the advisory committee of **Ms. Chinnu Raju (2019-11-186)**, a candidate for the degree of **Master of Science in Agriculture** with major field in Agricultural Meteorology, agree that this thesis entitled **“ESTIMATION OF CROP WATER REQUIREMENT IN RICE USING SATELLITE DATA AND GIS”** may be submitted by **Ms. Chinnu Raju** in partial fulfillment of the requirement for the degree.

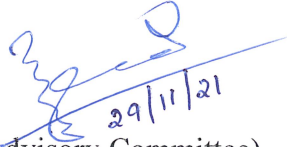
Dr. Ajith K.

(Chairman, Advisory Committee)

Assistant Professor

Agricultural Meteorology

RARS, Kumarakom



Dr. B. Ajithkumar

(Member, Advisory Committee)

Associate Professor and Head

Dept. of Agricultural Meteorology

College of Agriculture, Vellanikkara



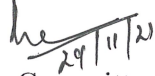
Dr. Anitha S.

(Member, Advisory Committee)

Professor (Agronomy) and Head

Instructional Farm, KAU

Vellanikkara



Dr. Divya Vijayan V.

(Member, Advisory Committee)

Assistant Professor (Soil Science)

STCR (Soil Test Crop Response)

College of Agriculture, Vellanikkara



ACKNOWLEDGEMENT

*First and foremost, I humbly bow my head before the **Almighty** and my parents who enabled me to pursue this work in to successful completion*

*It is with immense pleasure I wish to express my deep sense of whole hearted gratitude, indebtedness and heartfelt thanks to my major advisor, **Dr. Ajith K.**, Assistant Professor of Agricultural meteorology, for his expert guidance, constant inspiration, affectionate advices, untiring interest, unreserved help, abiding patience, constructive criticism, valuable suggestions and above all, the understanding and wholehearted co-operation rendered throughout the course of my study. This work would not have been possible without his unfailing support in the preparation of the manuscript. I am so grateful that he is my teacher.*

*I owe my most sincere gratitude to **Dr. B. Ajithkumar**, Associate Professor and Head, Department of Agricultural meteorology, and member of my advisory committee for his meticulous help in improving my presentation skills, expert advice and constant encouragement throughout my course of study. I thank him for having shaped me to take up a good career in Agricultural Meteorology*

*I sincerely thank **Dr. Anitha S.**, Professor and Head, Instructional Farm, KAU and member of my advisory committee for her timely support, enthusiasm and valuable suggestions. I am also thankful to her for helping me make necessary corrections in my thesis and enrich my ideas.*

*I am indeed grateful to **Dr. Divya Vijayan V.**, Assistant Professor, Department of Soil Science and Agricultural Chemistry and member of my advisory committee for her timely advice and unfailing support. Her suggestions and constructive comments were valuable for the smooth conduct of my research work.*

*I am deeply indebted to **Dr. P. Lincy Davis**, Assistant Professor, Department of Agricultural meteorology, for her well-timed guidance, critical evaluation, constant encouragement and moral support rendered during the conduct of my study.*

*I am deeply obliged to **Mr. Arjun Vysakh**, Assistant Professor, Department of Agricultural meteorology, for his valuable suggestions and support rendered*

throughout the course of study. It is with my heartfelt feelings, I wish to express my sincere thanks to **Dr. Shajeesh Jan P.** Assistant Professor of Agricultural meteorology, for his guidance and support.

I would like to acknowledge the help extended by each of the non-teaching staffs especially **Gangadharan sir, Paulose sir, Sreejith chettan, Shahimol chechi, Deena chechi, Likhitha chechi, Swathy chechi, Suchitra chechi, Mini chechi and Bindhu chechi.**

More personally I am thankful forever to all my loving friends **Abin, Riya and Sona,** for the joyous company, sincere love and support in different stages of the study. Special words of thanks to my seniors **Aswathy chechi, Harithalekshmi chechi, Vinu chettan, Haritha Raj chechi and Anunayana chechi** for their valuable advice, prompt help and co-operation during the entire period of study. I would like to express my sincere thanks to my young sisters **Arsha, Anusha and Sowmya** for all the support throughout my work.

I express my great pleasure to extend indebtedness to **Dr. Sharon C. L.,** P.G. academic officer, College of Horticulture for her whole-hearted co-operation and gracious help rendered during the last two years.

I am thankful to **Mr. Aravind K. S. and Mrs. Rejitha** of Students' Computer Club, College of Agriculture for rendering necessary help whenever needed. I am thankful to remember the services rendered by all the staff members of College Library, Office of COA, Vellanikkara, and Central Library, KAU. I am thankful to Kerala Agricultural University for the technical and financial assistance for persuasion of my study and research work.

Above all, with gratitude and affection, I recall the moral support, boundless affection, constant encouragement and motivation of my father **Mr. Raju Paulose,** my mother **Mrs. Elsy Raju,** my sister **Chinchu Raju** and my **grandparents** without which this endeavour would never have become a reality. Thanking the Almighty.


Chinnu Raju

CONTENTS

CHAPTER NO.	TITLE	PAGE NO.
1	INTRODUCTION	1-2
2	REVIEW OF LITERATURE	3-18
3	MATERIALS AND METHODS	19-33
4	RESULTS	34-83
5	DISCUSSION	84-94
6	SUMMARY	95-96
	REFERENCES	i-xv
	APPENDICES	
	ABSTRACT	

LIST OF TABLES

Table No.	Title	Page No.
3.1	Sentinel-2 data acquisition schedule	21
3.2	Band designation for Sentinel-2	22
3.3	Rice area validation points	23
3.4	Non rice area validation points in Palakkad district	24
3.5	Confusion matrix for validation of rice area	26
3.6	Interpretation of Kappa coefficient	27
3.7	MOD13Q1 NDVI data acquisition schedule	30
4.1	Confusion matrix for accuracy assessment of rice classification	35
4.2	Ground truth locations in the study area	37
4.3	Relationship between maximum NDVI and rice yield	38
4.4	NDVI values corresponding to the age of the plant extracted for each location in Alathur block from MOD13Q1 images	39
4.5	NDVI values corresponding to the age of the plant extracted for each location in Nenmara block from MOD13Q1 images	40
4.6	NDVI values corresponding to the age of the plant extracted for each location in Kollengode block from MOD13Q1 images	41
4.7	NDVI values corresponding to the age of the plant extracted for each location in Chittur block from MOD13Q1 images	42
4.8	NDVI values corresponding to the age of the plant extracted for each location in Kuzhalmannam block from MOD13Q1 images	43
4.9	K_c table value corresponding to the age of the rice plant	44
4.10	K_c table values corresponding to age of the crop for Alathur block	45
4.11	K_c table values corresponding to age of the crop for Nenmara block	46
4.12	K_c table values corresponding to age of the crop for Kollengode block	47

LIST OF TABLES (Contd.)

Table No.	Title	Page No.
4.13	K _c table values corresponding to age of the crop for Chittur block	48
4.14	K _c table values corresponding to age of the crop for Kuzhalmannam block	49
4.15	K _c (Table value) and K _c (Predicted) value for Alathur block	51
4.16	K _c (Table value) and K _c (Predicted) value for Nenmara block	53
4.17	K _c (Table value) and K _c (Predicted) value for Kollengode block	54
4.18	K _c (Table value) and K _c (Predicted) value for Chittur block	55
4.19	K _c (Table value) and K _c (Predicted) value for Kuzhalmannam block	56
4.20	Weekly ET _o of Alathur block during the crop period	58
4.21	Monthly ET _o of Alathur block during the crop period	59
4.22	Monthly ET _o of Nenmara block during the crop period	59
4.23	Weekly ET _o of Nenmara block during the crop period	61
4.24	Weekly ET _o of Kollengode block during the crop period	62
4.25	Monthly ET _o of Kollengode block during the crop period	63
4.26	Weekly ET _o of Chittur block during the crop period	65
4.27	Weekly ET _o of Kuzhalmannam block during the crop period	66
4.28	Monthly ET _o of Chittur block during the crop period	67
4.29	Monthly ET _o of Kuzhalmannam block during the crop period	67
4.30	Effective rainfall in Alathur block during the crop period	68
4.31	Effective rainfall in Nenmara block during the crop period	68
4.32	Effective rainfall in Kollengode block during the crop period	69
4.33	Effective rainfall in Chittur block during the crop period	69
4.34	Effective rainfall in Kuzhalmannam block during the crop period	69
4.35	Irrigation requirement in Alathur block	72

LIST OF TABLES (Contd.)

Table No.	Title	Page No.
4.36	Irrigation requirement in Nenmara block	75
4.37	Irrigation requirement in Kollengode block	77
4.38	Irrigation requirement in Chittur block	79
4.39	Irrigation requirement in Kuzhalmannam block	81

LIST OF FIGURES

Figure No.	Title	Between pages
3.1	Location map of Palakkad district	19-20
3.2	Sentinel-2 image acquisition and coverage on Palakkad district from https://earthexplorer.usgs.gov .	20-21
3.3	MOD13Q1 NDVI acquisition and coverage on Palakkad district from http://lpdaac.usgs.gov .	29-30
3.4	MODIS downloaded image in sinusoidal projection	30-31
3.5	MODIS reprojected image	31-32
3.6	MODIS-NDVI retrieved	31-32
3.7	Temporal variation of NDVI with crop stages in rice	31-32
4.1	Mosaicked composite image of the study area	34-35
4.2	Land use classification of study area	34-35
4.3	Rice area map of the study area in Palakkad district	34-35
4.4	Rice area map validation points for rice and non-rice classes across the study area in Palakkad	34-35
4.5	NDVI - K_c relationship	50-51
4.6	K_c map of 305 th Julian day 2020 representing the early vegetative stage of the crop	83-84
4.7	K_c map of 321 st Julian day 2020 representing the early vegetative stage of the crop	83-84
4.8	K_c map of 337 th Julian day 2020 representing the late vegetative stage of the crop	83-84
4.9	K_c map of 363 rd Julian day 2020 representing the late vegetative stage of the crop	83-84
4.10	K_c map of 1 st Julian day 2021 representing the reproductive stage of the crop	83-84

LIST OF FIGURES (Contd.)

Figure No.	Title	Between pages
4.11	K _c map of 17 th Julian day 2021 representing the reproductive stage of the crop	83-84
4.12	K _c map of 33 rd Julian day 2021 representing the maturity stage of the crop	83-84
4.13	K _c map of 49 th Julian day 2021 representing the maturity stage of the crop	83-84
4.14	Crop water demand map for early vegetative stage of the crop	83-84
4.15	Crop water demand map for late vegetative stage of the crop	83-84
4.16	Crop water demand map for reproductive stage of the crop	83-84
4.17	Crop water demand map for maturity stage of the crop	83-84
5.1	Correlation between maximum NDVI and rice yield	85-86
5.2	Relationship of NDVI and K _c with age of the plant in Alathur block	86-87
5.3	Relationship of NDVI and K _c with age of the plant in Nenmara block	87-88
5.4	Relationship of NDVI and K _c with age of the plant in Kollengode block	87-88
5.5	Relationship of NDVI and K _c with age of the plant in Chittur block	87-88
5.6	Relationship of NDVI and K _c with age of the plant in Kuzhalmannam block	87-88
5.7	Relationship of K _c table value and K _c predicted value in Alathur block	87-88
5.8	Relationship of K _c table value and K _c predicted value in Nenmara block	88-89
5.9	Relationship of K _c table value and K _c predicted value in Kollengode block	88-89
5.10	Relationship of K _c table value and K _c predicted value in Chittur block	88-89
5.11	Relationship of K _c table value and K _c predicted value in Kuzhalmannam block	88-89
5.12	Weekly reference evapotranspiration (ET _o) of Alathur block during the crop growth period	89-90

LIST OF FIGURES (Contd.)

Figure No.	Title	Between pages
5.13	Weekly reference evapotranspiration (ET_o) of Nenmara block during the crop growth period	89-90
5.14	Weekly reference evapotranspiration (ET_o) of Kollengode block during the crop growth period	89-90
5.15	Weekly reference evapotranspiration (ET_o) of Chittur block during the crop growth period	89-90
5.16	Weekly reference evapotranspiration (ET_o) of Kuzhalmannam block during the crop growth period	89-90
5.17	Distribution of monthly rainfall, effective rainfall, reference evapotranspiration and crop evapotranspiration of rice in Alathur block	92-93
5.18	Stagewise irrigation requirement in Alathur block during <i>mundakan</i> season 2020-21	92-93
5.19	Distribution of monthly rainfall, effective rainfall, reference evapotranspiration and crop evapotranspiration of rice in Nenmara block	92-93
5.20	Stagewise irrigation requirement in Nenmara block during <i>mundakan</i> season 2020-21	92-93
5.21	Distribution of monthly rainfall, effective rainfall, reference evapotranspiration and crop evapotranspiration of rice in Kollengode block	92-93
5.22	Stagewise irrigation requirement in Kollengode block during <i>mundakan</i> season 2020-21	92-93
5.23	Distribution of monthly rainfall, effective rainfall, reference evapotranspiration and crop evapotranspiration of rice in Chittur block	92-93
5.24	Stagewise irrigation requirement in Chittur block during <i>mundakan</i> season 2020-21	92-93
5.25	Distribution of monthly rainfall, effective rainfall, reference evapotranspiration and crop evapotranspiration of rice in Kuzhalmannam block	92-93
5.26	Stagewise irrigation requirement in Kuzhalmannam block during <i>mundakan</i> season	92-93
5.27	Comparison of K_c values corresponding to rice and non-rice area	92-93

LIST OF PLATES

Plate No.	Title	Between pages
I	Land based observations in rice fields at Palakkad	23-24
II	Collection of information regarding plant height and leaf area index	23-24
III	Rice fields located by GPS and Google earth in five blocks of Palakkad district	23-24
IV	Crop cutting experiment at Palakkad	38-39

Introduction

1. INTRODUCTION

Water scarcity has become a major concern in agriculture along with climate change and projected precipitation shifts. Hence, available water resources should be effectively utilised in-order to avoid wastage of irrigation water in fields. Conventionally, irrigation scheduling is done based on the irrigator's personal expertise, plant appearance, neighbour observation or just irrigating whenever water is available. However, a number of irrigation scheduling strategies based on soil water monitoring, plant monitoring and a water balancing approach have been developed over the years. Many scientists developed empirical equations to calculate potential evapotranspiration, reference crop evapotranspiration and crop evapotranspiration based on weather variables.

Further, irrigation models like CROPWAT, AQUACROP, APSIM *etc.* were developed by scientists for the estimation of crop water requirement and irrigation requirements based on crop, soil and climate data. These models could also be used to calculate scheme of water supply under different cropping patterns and management conditions. CROPWAT model can be effectively used to evaluate farmer's irrigation practices and estimate crop performance under irrigated and rainfed conditions (FAO, 1992). The models serve as a farm management tool, helping farm managers to take decisions regarding whether to irrigate, how much water to be used *etc.* (Ullasa, 2019). But, these methods of estimating crop water requirement have limitations because they are recognized as point-based methods and cannot be used at a regional scale. To arrive at water conservation, it is necessary to monitor irrigation scheduling over large areas by adopting new technologies for estimating crop water demands accurately.

Irrigation planning and management is based on the demand and supply of irrigation water over space and time. Information regarding crop type, acreage, yield and growing condition is useful for irrigation studies. Remote sensing has recently been popular in large-scale crop acreage estimation due to its broad swath and ability to give accurate and fast geographical and temporal information on crop growth conditions. Delineating rice areas aids in determining the current status of rice cultivation and it will be helpful in assessing the quantity of irrigation water required

over a large area in a particular season. It also aids policymakers in developing new plans and policies to assist farmers and urge them to produce more. On account of large areas involved, dynamic changes and time constraints, remote sensing has been proven to be more effective tool for irrigation studies than traditional methods which are time consuming and cumbersome. Remote sensing is effective in timely estimation of crop areas, estimating water demand over space and time, monitor crop condition during growing season, forecast yield of the crop before the end of the season and evaluating the overall performance of irrigation projects.

Development of innovative water saving techniques is the greatest challenge in front of scientists (Ullasa, 2019). In order to overcome this, an integrated, multidisciplinary and participatory approach should be followed for management of water resources in future. The combination of remote sensing and agrometeorological techniques is considered as a promising method in irrigation scheduling and management of cropped areas.

Judicious choice of irrigation strategies based on satellite data and land-based observations is an effective tool to overcome the water scarcity faced during late *mundakan* and *puncha* seasons in Kerala. The crop evapotranspiration (ET_c) maps developed from K_c maps will depict the spatial and temporal distribution of crop water requirements during the growing season. Hence the study is proposed with the objective of developing crop water demand maps of selected rice area by establishing a relationship between Normalized Difference Vegetation Index (NDVI) and crop coefficient (K_c) values. This will help the planners and farmers in better management of available irrigation water so as to maximise food production and to fulfil the demands of growing population.

Review of literature

2. REVIEW OF LITERATURE

Water is an inevitable component for agricultural production and it plays a vital role in ensuring food security. According to the world bank, agriculture accounts for 70% of total water withdrawals globally. United Nations Food and Agriculture Organisation (FAO) pointed out that, approximately 60 % of the water taken up for agriculture is being wasted, largely due to inefficient applications. As per the report of Department of Water Resources, River Development & Ganga Rejuvenation, agriculture accounts for 80 % of total fresh water consumption in India. Crops like rice, wheat and sugarcane constitute 91 % of crop production in India, among these, sugarcane uses less water than global average, but in the case of wheat and rice, water usage is higher than global average (NWM, 2021). Rice is primarily produced under flooded conditions, but it is not an aquatic plant. Rice water use needs to be investigated under climate change conditions due to decreasing trends in availability of fresh water for agriculture coupled with increasing world population (Djaman *et al.*, 2019). Different methods have been employed to estimate the crop water requirement based on crop evapotranspiration *viz.*, empirical methods, lysimeters, crop weather models, agro-meteorological methods, remote sensing *etc.* Research works carried out on these aspects are reviewed and presented in this chapter.

2.1. Irrigation scheduling based on crop water requirement in rice

Irrigation is the process through which controlled water supply is provided into the root zone of the crop to supplement the moisture requirement of plants. Irrigation scheduling is the process of determining correct frequency and duration of watering (Thomas, 2010). It influences the agronomic and economic viability of farms through improved crop yields and effective utilisation of available water. The amount of irrigation water to be applied depends on the soil water status and crop water requirement (Smith, 1992). Crop water requirement (CWR) refers to the quantity of water required by the crop or cropping system during a given period of time for the normal growth of the crop under fields conditions. It is the sum total of water used for meeting the consumptive use of the crop, unavoidable losses of water during irrigation and water used for other operations like land preparation, puddling, transplanting *etc.* Consumptive use or crop water use represents the water loss from a cropped field

through evapotranspiration and metabolic activities of the plant. The water utilized for metabolic activities is usually less than 1 % of total crop water use so, consumptive use can be taken as equivalent to crop evapotranspiration. The crop water requirement is met through irrigation, effective rainfall and soil profile contribution (Thomas, 2010). The water requirement of the crop is normally expressed in mm/day, mm/week or mm/month. The factors affecting CWR are type of crop and cultivar, growth stage of the crop, ground cover, climate *etc.* Recently, new technologies and services have been developed to improve irrigation water management, precise irrigation scheduling and early warning systems for identifying water stress in field scale (Lorite, 2018).

Among cereals, rice has a high demand for water, particularly in the reproductive stage *ie*; from panicle initiation to early grain development stage. Irrigated rice receives 34-43 % of the world's total irrigation water, which is equivalent to 24-30 % of the entire world's fresh water resources. Evapotranspiration (ET), accounts for up to 80% of the water used by the rice crop. Seasonal actual evapotranspiration (ET_a) in rice was reported to be 540-730 mm in India (Chahal *et al.*, 2007), while 400-700 mm in Philippines (Tabbal *et al.*, 2002). This quantity depends on seasonal conditions such as temperature, humidity, wind and sunshine hours as well as the length of the growing period. The longer the crop growth period the higher will be the water requirement. A general rule is that a rice crop will need approximately 10 mm of water per day. Therefore, a crop that matures in 100 days will require approximately 1000 mm of water while a crop that matures in 150 days will require 50 % more. According to IRRI, around 1300-1500 mm is the typical amount of water needed for irrigated rice in Asia (IRRI, 2021).

Irrigation requirement for rice cultivation have been studied by scientists all over the world, the crop water requirement in Tanzania was estimated to be 2300 mm (Mdemu *et al.*, 2004), but in the sub-tropical and semiarid regions of Pakistan 1200 to 1600 mm was reported. In Italy, the water requirement of rice was reported in amounts ranging from 700 to 800 mm (Spanu *et al.*, 2009). The irrigation water requirement of rice for the wet and dry seasons in Senegal river basin, of Africa was studied by Hargreaves *et al.* (1986) and they reported that, 1788 and 2030 mm of irrigation water has to be supplied in the respective seasons. But recent studies

conducted in this region reported 1110 to 1300 mm (de Vries *et al.*, 2010) and 863 to 1198 mm irrigation requirement which is slightly lesser than the earlier estimated values. Rice seasonal irrigation water requirements ranged from 962 to 1114 mm in Taiwan (Kuo *et al.*, 2006). Terjung *et al.* (1984) estimated rice irrigation water requirement of more than 1000 mm in northwest China and 500 mm in south and central China. The net irrigation water required for cultivating Boro rice in western region of Bangladesh was 849 mm (Hossain *et al.*, 2017). The variation in irrigation requirement in rice from one region to another, could be ascribed to the changes in prevailing weather conditions.

2.2. Influence of weather variables on crop evapotranspiration

Evapotranspiration is a key factor in irrigation planning and regional water allocation. The changes in meteorological factors as a result of climate change will have an impact on evapotranspiration and agricultural water needs (Dharshana *et al.*, 2013). The meteorological variables like air temperature, sunshine hours, relative humidity, wind speed and evaporation influence the rate of evapotranspiration. Among the weather parameters, most important ones determining rate of evapotranspiration are air temperature and sunshine hours as per studies conducted in China (Gao *et al.*, 2006), southwest England (Ishak *et al.*, 2010) and Israel (Cohen *et al.*, 2002). But, according to the evapotranspiration studies conducted in Australia (Rayner, 2007), Tibetan Plateau (Zhang *et al.*, 2007), Iran (Dinpashoh *et al.*, 2011) and North East India (Jhajharia *et al.*, 2011) wind speed is the major factor influencing evapotranspiration. Chattopadhyay and Hulme (1997) reported that relative humidity is the most important weather variable governing evapotranspiration in India, whereas, it is maximum temperature in China (Cong and Yang, 2009) and western half of Iran (Tabari *et al.*, 2011). These studies indicate that the critical weather variable influencing evapotranspiration varies from place to place.

Saxena *et al.* (2020) analysed the trends in reference evapotranspiration (ET_o) estimated using Penman-Monteith equation over arid, semi-arid and humid regions of northwest (NW) India during 1985-2018, and observed that the average annual ET_o was lowest in semi-arid region and highest in arid region. The results indicated a significant decrease in ET_o on annual basis for most of the locations and NW India as

a whole. Such negative trends in ET_o , according to Bandyopadhyay *et al.* (2009), are due to a considerable constant decrease in wind speed and solar radiation, as well as a significant increase in relative humidity in these regions over the years. Hence, any change in climate of a region creates variations in evapotranspiration rate and in turn the crop water requirement.

2.3. Estimation of Crop evapotranspiration

2.3.1. Crop evapotranspiration based on empirical equations

Scientists were interested in developing methods and formulas to estimate crop evapotranspiration since 1940's. Evapotranspiration is mainly of two types, Potential evapotranspiration (PET) and Actual evapotranspiration (AET) (Mahi and Kingra, 2018). The concept of Potential evapotranspiration (PET) was introduced by Thornthwaite in 1943 and later by Penman in 1948 (Rao, 2008). Potential evapotranspiration refers to the loss of water from a large area, uniformly covered with actively growing vegetation in a region where there is no shortage of water (Thomas, 2010). The potential evapotranspiration rate is completely dependent on weather parameters and is not influence by soil or plant factors. While, the term actual evapotranspiration indicates the total amount of water used by a crop for evaporation and transpiration during it's entire crop growth period. AET is dependent on the amount of water available to the plant. If sufficient water is available to the crop, actual evapotranspiration becomes equal to potential evapotranspiration, if moisture is limiting it will be less than PET (Mahi and Kingra, 2018).

Potential evapotranspiration (PET) could be estimated by direct and indirect methods. The direct methods include soil moisture sampling, using equipments fixed in soil like atmometers, pans and lysimeters. Indirect methods use empirical equations to calculate PET based on weather variables (Mahi and Kingra, 2018). Indirect methods are generally classified in to three, based on the number of weather variable considered as input, they are (i) methods based on only one weather parameter (*eg*; Thornthwaite's method), (ii) methods based on two weather parameters (*eg*; Makkink method, Jensen-Haise method, Blaney-Criddle method *etc.* and (iii) combination methods based on all important weather parameters (*eg*; FAO Penman-Montieth

method) (Mavi, 2018). Thornthwaite's empirical method of estimating potential evapotranspiration (PET) has been preferred by several scientists in India to Penman's theoretical combination approach, because of the former's simplicity. But, when Kumar *et al.* (1986) compared the performance of Thornthwaite's method and Penman method in India and observed that Thornthwaite's method gave considerably higher estimates of PET and showed lower inter-annual variability than Penman's method during the southwest monsoon season.

Later, Papadopoulou *et al.* (2003) conducted a study to compare the potential evapotranspiration and its spatial distribution in Greece estimated using Thornthwaite equation, Blaney-Criddle formula and Hargreaves method. They reported that for Thornthwaite and Blaney-Criddle methods, potential evapotranspiration was found to be slightly higher in the eastern part of the country and Hargreaves method overestimated potential evapotranspiration as compared to the other two methods.

The mass transfer-based model is one of the most widely used models to estimate reference crop evapotranspiration. The common mass transfer-based models are Papadakis (1966), Rohwer (1931), Dalton (1802), Ivanov Romanenko (1961), Meyer (1926), Trabert (1896) and WMO (1966) methods. Acheampong (1986) considered the Penman, Thornthwaite, and Papadakis models for the estimation of the reference crop evapotranspiration for Ghana, among the three methods considered the modified Penman method was found to be most suitable. Rawat *et al.* (2019) estimated crop evapotranspiration (ET_c) of rabi crops in Haryana with the help of models like, Surface Energy Balance Algorithm for Land (SEBAL), Makkink model, Hargreaves and Samani model, Camargo method and Jensen-Haise model. Among the different models used in the study Makkink model showed good agreement with evapotranspiration obtained from FAO Penman-Monteith equation.

Food and Agricultural organisation conducted a study for examining the efficiency of 20 different evapotranspiration formulas and it was observed that modified Penman method overestimated potential evapotranspiration while, Penman-Monteith method showed a stable tendency from humid to dry weather condition (Yoo *et al.*, 2006). Hence, Penman-Monteith method was accepted as a standard method to estimate PET. This method considers weather parameters like net radiation, air

temperature, vapour pressure deficit and wind speed to estimate evapotranspiration and showed very good results as compared to lysimeter readings obtained for Alfalfa in Canada (Sentelhas, 2010). Yoo *et al.* (2006) compared the potential evapotranspiration estimated using modified Penman method and Penman-Monteith method for 30 years in 9 regions of Korea. In all the growing seasons, PET estimated by modified Penman method was 17.2 % higher than Penman-Monteith method average.

2.3.2. Crop evapotranspiration based on pan evaporation data

The pan evaporation method has been widely adopted in Agro-meteorological stations, for estimating crop evapotranspiration. The evaporation from a free water surface is multiplied with a constant value *ie*; pan factor (K_p), to get evapotranspiration from the green grass cover (Allen *et al.*, 1997). Allen *et al.* (1998) suggested the use of Penman-Monteith equation as standard method to estimate crop evapotranspiration (ET_c) in many areas of the world. However, the major disadvantage of this method is that air temperature, relative humidity, wind speed and solar radiation are required, which are not easily detectable in many meteorological stations. Therefore, estimation of ET_c is often based on pan evaporation (E_{pan}) measurements due to low cost, simplicity of the measuring equipment, simple data interpretation and application as well as, suitability for locations with limited availability of meteorological data (Trajkovic, 2009). Gundekar *et al.* (2008) observed high correlation between E_{pan} and ET_c values when the measuring systems were properly installed and maintained.

Mushtaq *et al.* (2020) estimated the crop evapotranspiration (ET_c) in apple using daily pan evaporation data recorded with the help of USWB class A pan evaporimeter in Jammu and Kashmir. The results showed that irrigation requirement for apple based on pan evaporation method ranged from 1.25 litre plant⁻¹ day⁻¹ to 7.08 litre plant⁻¹ day⁻¹ in April and July months respectively. Pan evaporation method for estimation of water requirement has been successful in saffron (Ahmad *et al.*, 2017), wheat (Kingra and Mahey, 2009) and most of the solanaceous vegetable crops (Ahmad *et al.*, 2019).

2.3.3. Crop evapotranspiration estimation using lysimeter

Evapotranspiration could be estimated with high precision using lysimeter and remote sensing techniques (Valipour, 2014). Kingra and Mahey (2009) did a comparative evaluation of different methods like lysimeter, open pan evaporimeter and modified Penman method to compute evapotranspiration at different phenological stages in wheat. They reported that during initial stages of crop growth, evapotranspiration estimated by lysimeter is less as compared to other methods, but, with an increase in the leaf area index of the crop, evapotranspiration estimated using lysimeter increases as compared to open pan evaporimeter and modified Penman method. When the crop approaches senescence and maturity, again lysimeter evapotranspiration is lower than open pan evaporimeter and modified Penman method. Evaporation from pan evaporimeter is controlled by the climatic parameters, thus with increase in temperature in the months of March and April, the pan evaporation and PET also increased, whereas, lysimeter evapotranspiration depends on crop characteristics and it is highest when the leaf area index is maximum. Maina *et al.* (2014) estimated crop evapotranspiration in the paddy fields of Australia using lysimeter and it was used to estimate the actual crop water requirement of MR219 rice (*Oryza sativa*) variety.

2.3.4. Crop coefficient approach to estimate crop evapotranspiration

The crop coefficient (K_c) is a key factor in scheduling irrigation of crops based on crop evapotranspiration. The crop coefficient value varies depending on crop type, crop growth stage, prevailing climate, soil characteristics *etc.* The K_c is minimum at emergence, it increases with canopy development and is maximum at grain filling. This seasonal distribution of K_c values can be represented as a function of time (in the day) or may be related to parameters of the crop (Rawat *et al.*, 2019). The product of crop coefficient and reference crop evapotranspiration gives crop evapotranspiration of concerned crop.

According a study done by Djaman *et al.* (2019) in Africa, rice K_c values during the crop development, mid-season and late season stages were 1.01, 1.31 and 1.12 respectively. Tyagi *et al.* (2000) conducted experiments on rice during rainy

season (July to October) in Karnal, India and estimated crop coefficient values of rice corresponding to the four crop growth stages (initial, crop development, reproductive and maturity) as 1.15, 1.23, 1.14 and 1.02 respectively. Allen et al. (1998) recommended rice K_c values of 1.05, 1.20 and 0.90-0.60 for the crop development, mid-season and late season stages under continuous flooding irrigation conditions in Italy. The K_c values of 0.92, 1.06, and 1.03 were reported for sprinkler irrigated rice under semi-arid climate in Spain (Moratiel and Martinez-Cob, 2013). In California, Montazar *et al.* (2017) derived paddy rice K_c values of 1.10, 1.00, and 0.80 for the initial, midseason and late season stages. According to a study done by Lee and Huang (2014), K_c value of 0.5 was observed 0-15 days after sowing (DAS), 0.8 (15-35 DAS), 1.2 (35-45 DAS), 1.3 (45-75 DAS), 1.2 (75-90 DAS), 1.1 (90-105 DAS), 0.7 (105-120 DAS) in Northern Taiwan.

2.4. Crop water requirement estimation

2.4.1. Integration of crop simulation models and remote sensing techniques

Crop weather models could be used to simulate the crop evapotranspiration and schedule irrigation based on agricultural water requirements under different cropping patterns (Sheng *et al.*, 2001). The Land and Water Development Division of FAO developed a model named CROPWAT to determine crop evapotranspiration and yield responses to water supplied to the crop (FAO, 1992). Several researchers have used the CROPWAT model for analysing crop water requirements in different parts of the world (Kar and Verma, 2005). Gowda *et al.* (2013) reported that water requirement in maize varied with planting dates and water requirement was more for late planted crops as compared to early planted crops, as per the study conducted using CROPWAT model in northern zone of Karnataka. Vysak *et al.* (2016) conducted a study using CROPWAT model to evaluate crop water requirement of rice at different planting dates in Thrissur district of Kerala. They observed that the crop water requirement increased with delay in planting, due to rise in maximum temperature and reduction in effective rainfall. The late planted (after July 5th) rice was found to have more water requirement than early planted crop especially in mid-season stage, which is the critical stage of irrigation. The water stress at this stage may lead to the low grain yield for late planted crops.

The Water Unit at the FAO (Food and Agriculture Organization) has developed another model named AQUACROP which simulates the crop biomass, grain yield, actual evapotranspiration, canopy cover as well as soil water content dynamics accurately under full irrigation and fertility conditions. The maize growth, yield and crop water use under different water stress conditions in Nebraska, USA was studied using AquaCrop model by Sandhu and Irmak (2019). The model simulated crop evapotranspiration accurately. Pirmoradian and Davatgar (2019) simulated irrigation requirement in rice using AquaCrop model in paddy fields of Guilan in northern Iran. The simulated total irrigation water requirement in wet, normal and dry years, were 6750, 8050 and 8760 m³ ha⁻¹, respectively. There are other simulation models like APSIM, HYDROLOGIC, HYDRUS, CROPCYST, EPIC, STICS *etc.* used for assessing water stress and irrigation scheduling in various crops.

The lack of trustworthy historical data for model calibrations is a persistent barrier for crop simulation models, especially for future projection of crop performance estimations and impact assessments under varying conditions. In some circumstances, the quantity and quality of available input data may not be sufficient to drive most crop models. Even when a good crop simulation model is chosen, data limitations limit the model's ability to make accurate estimates (Kephe *et al.*, 2021). The integration of crop simulation models and remote sensing helps to overcome this draw back. Through remote sensing regional scale data is made available with good accuracy.

2.4.2. Crop water requirement estimation based on remote sensing

The crop evapotranspiration (ET_c) can be measured using traditional methods such as the Bowen ratio, eddy covariance, water balance and at field scale using lysimeter systems, yet, these methods are unable to provide distributed or regional scale evapotranspiration (Bala *et al.*, 2015). Advanced geo spatial techniques could be used to estimate crop water requirements on a regional scale with limited time (Javed and Ahamad, 2020). Remote sensing imagery from cameras on board satellites, aerial platforms, airplanes or similar systems has been recognized as an exceptional tool to produce spatial information about crop evapotranspiration. The lack of availability of

timely images at the required spatial resolution, captured during the crop growth period, has been hindering the use of remote sensing approaches in agriculture. In remote sensing, timeliness, frequency and spatial resolution of the data are important. These restrictions are being removed by developments in communication technology and computation, as well as a significant change in the National Aeronautics and Space Administration's (NASA) data policy, which now allows open and free access to georeferenced Landsat images in near real time through the Internet. The European Space Agency (ESA) adopted the same data policy, allowing free and open access to the 10-m imagery acquired by Sentinel-2 through the Internet. This revolutionised the satellite-based remote sensing system for spatial resolutions of 10-30 m. Furthermore, a rising number of commercial sensors, such as WorldView2, PLEIADES, DMC, and DEIMOS, with very high spatial resolution of 1-5 m, are ready to give regular land observations with increasing capabilities (Calera *et al.*, 2017).

2.4.2.1. MODIS - NDVI

Vegetation activity is monitored on a large scale using normalized difference vegetation index (NDVI) time-series datasets acquired by sensors onboard satellites with short revisit periods, particularly National Oceanic and Atmospheric Administration (NOAA) Advanced Very High-Resolution Radiometer (AVHRR) (Prince and Goward, 1995). National Aeronautics and Space Administration (NASA) launched TERRA and AQUA satellites in 1999 and 2002, respectively, which consist of Moderate Resolution Imaging Spectroradiometer (MODIS) sensors which has improved calibration and atmospheric correction as compared to the AVHRR sensors. The MODIS NDVI can be considered as a successor to 20-year NOAA-AVHRR derived NDVI time series, to provide a longer-term data record for operational monitoring studies. The AVHRR-NDVI has been widely used earlier, in various operational applications, including famine early warning systems, land cover classification, health and epidemiology, drought detection, land degradation, deforestation, change detection and monitoring (Cihlar *et al.*, 1997).

A vegetation Index is a mathematical combination of two or more spectral bands that enhances the contrast between vegetation (having high reflectance) and bare soil, man-made structures *etc.* More than one hundred vegetation indices have

been derived from multispectral imagery (Xue and Su, 2017). Among different vegetation indices, Normalized Difference Vegetation Index (NDVI) has been one of the most commonly used vegetation indices in remote sensing since its introduction in 1970s. Studies have demonstrated that NDVI is effective to differentiate savannah, dense forest, non-forest and agricultural fields and it is also useful in distinguishing evergreen forest and seasonal forest types (Pettorelli *et al.*, 2005). NDVI helps to estimate several vegetation properties, like the Leaf area Index (LAI) (Tian *et al.*, 2015), biomass, chlorophyll content in the leaves (Pastor-Guzman *et al.*, 2015), plant productivity (Vicente-Serrano *et al.*, 2016), fractional vegetation cover (Dutrieux *et al.*, 2015) and plant stress (Chavez *et al.*, 2015). The value of NDVI ranges from -1 to +1. NDVI for bare soil ranges from -0.1-0.2, whereas, for dense vegetation it occurs between 0.5-0.8. NDVI is sensitive to fractional changes in vegetation cover until a full cover is reached, any further increase in LAI results in very small increase in NDVI value (Carlson and Ripley, 1997).

The Moderate Resolution Imaging Spectroradiometer (MODIS) VI products can be used to monitor photosynthetic activity based on the spatial and temporal comparisons of global vegetation conditions (Justice *et al.*, 1998). Huete *et al.* (2002) compared two vegetation indices (VI) obtained from MODIS sensor, with the NOAA-14, 1 km AVHRR-NDVI for twelve months at four test sites representing semi-arid grass/shrub, savanna and tropical forest biomes. The vegetation indices considered for the study were the normalized difference vegetation index (NDVI) and enhanced vegetation index (EVI), produced at 1 km and 500 m resolutions and 16-day compositing periods by MODIS sensor. The airborne-measured, top-of-canopy reflectance showed a good correspondence with VI values obtained from MODIS sensor.

The MODIS standard VI products include two, gridded vegetation indices (NDVI, EVI) and quality analysis (QA) with statistical data that indicate the quality of the VI product and input reflectance data (Huete *et al.*, 2002). For production purposes the MODIS VIs are output in tile units that are approximately 1200 by 1200 km in the integerized sinusoidal (ISIN) grid projection. When mosaicked, all tiles cover the terrestrial Earth and the MODIS VI can be generated globally every 16 days interval.

The VI products rely on the level 2 daily surface reflectance product (MOD09 series), which are corrected for molecular scattering, ozone absorption and aerosols (Vermote, *et al.*, 2002). There is some production of the 250m MODIS VI products (MOD13Q1) over a limited set of tiles (Huete *et al.*, 2002).

For compositing, only the higher quality, cloud-free, filtered data are retained. Low quality data contains cloud-contaminated pixels and extreme off-nadir sensor view angles whereas, best quality pixels are cloud-free and nadir-view pixels with minimal residual atmospheric aerosols (van Leeuwen *et al.*, 1999). MODIS is a whiskbroom sensor, which causes the pixel size to increase with scan angle by a factor of four (Huete *et al.*, 2002).

Several researchers have explored the utility of open-source MODIS-NDVI in agriculture. Beck *et al.* (2006) observed that Moderate Resolution Imaging Spectroradiometer (MODIS) NDVI method is very effective in estimating biophysical parameters and monitoring vegetation phenology at very high latitudes of Norway. In Argentina, Lopresti *et al.* (2015) calibrated and validated an empirical model with field-observed wheat yields and MODIS-NDVI data and the results showed an R^2 value of 0.75. Mkhabela *et al.* (2011) observed that MODIS-NDVI could be effectively used to predict crop yield in Canadian Prairies. The crop acreage estimation and yield forecasting of rice using MODIS-NDVI and LANDSAT images in Thanjavur district of Tamil Nadu during ‘*samba*’ rice season during 2016-2017 and the NDVI showed highest exponential relationship with rice yield (Ajith *et al.*, 2017). Mehaboob *et al.*, (2016) has done a similar study to estimate rice area and yield in Bangladesh.

Research works are now focused on the applicability of MODIS-NDVI in irrigation studies by using satellite derived NDVI for the development of crop coefficient (K_c) values on spatial scale. It involves different methods like, establishing empirical relationships with vegetation indices (Ray and Dadhwal, 2001), exploiting the relationships existing between vegetation spectral reflectance and some parameters like albedo, leaf area, canopy surface roughness by using analytical approaches, or by deriving the K_c from the ratio of actual evapotranspiration estimated through remotely sensed surface energy balance models and reference

evapotranspiration (Tasumi and Allen, 2007). The advantage of the first strategy is that, by assuming an average seasonal trend of crop development, it is possible to estimate seasonal or monthly K_c values for the whole studied area. But the second strategy can provide more realistic estimates of K_c by taking in to account the spatial variability. The third one is the least expensive in terms of remote sensing data requirements (Casa *et al.*, 2008). Remote sensing-based vegetation indices are used for calculating K_c at the field scale for different crops, namely wheat, beans (Duchemin *et al.*, 2006), potato (Jayanthi *et al.*, 2007), maize (Hunsaker *et al.*, 2005), sugar beet and green bean (Koksal, 2008), soybean, sorghum, corn and alfalfa (Singh and Irmak, 2008), cotton (Hunsaker *et al.*, 2005), irrigated sorghum (Bashir *et al.*, 2007) and paddy crop (Mishra *et al.*, 2005).

Parmar and Gontia (2016) developed a simple linear regression model to establish a relationship between a NDVI derived from Landsat images and the crop coefficient (K_c) for the Ozat-II canal command of Junagadh district of Gujarat State, India. The NDVI- K_c equation was found to be useful for estimation of crop evapotranspiration for summer groundnut during the entire crop growth period. Remote sensing based crop coefficient estimation was done for irrigated and rainfed maize in USA by establishing a linear regression equation with MODIS-NDVI retrieved during the crop period. The validation of NDVI- K_c model yielded an R^2 value of 0.90, the regional scale crop evapotranspiration was estimated based on K_c values derived and reference evapotranspiration (Kamble *et al.*, 2013).

2.5. Remote sensing for crop area delineation

According to European commission (2018), agricultural areas refer to land suitable for agricultural practices, which include arable land, permanent cropland and permanent grassland. Agricultural field boundaries (AFB) can be conceptualized as the natural disruptions that partition locations where a change of crop type occurs or comparable crops naturally detach (Rydberg *et al.*, 2001). The boundaries of agricultural fields are important features that define agricultural units and allow one to spatially aggregate information about fields and their characteristics. This information includes location, shape, spatial extent and field characteristics such as crop type, soil type, fertility and yield. Traditionally, AFB were established through surveying

techniques, which are laborious, costly, and time-consuming. Currently, the availability of very high resolution (VHR) satellite imageries and the advancement in deep learning-based image analysis have shown potential for the automated delineation of agricultural field boundaries (Persello *et al.*, 2019).

Several remote sensing technologies for determining farmland extent have been investigated. It has been observed that using multi-temporal images with higher spatial resolution produces better results than using mono-temporal images with lesser resolution (Shimada *et al.*, 2014). Scientists tested several earth observation methodologies to automatically delineate crop field boundaries from multi-temporal Sentinel-2 imagery, which uses edge detection and image segmentation to delimit agricultural fields, orchards, and vineyards from multiple images acquired throughout the growing season. The Sentinel-2 images produced promising results (Zhan *et al.*, 2021). The utilisation of multi-temporal high spatial resolution data, on the other hand, results in a massive increase in data volume, limiting the size of the research region to the data storage and processing capabilities of the local general-purpose computer (Xiao *et al.*, 2021).

Remote sensing-based methods could be effectively used for mapping rice area and forecasting rice production (Noureldin, 2013). Remote sensing technology helps in spatial coverage over a large geographic area under low cost during all seasons except monsoon (Mosleh *et al.*, 2015). The satellite data are currently available in open-source platforms in a time bound manner, this also enhances the application of satellite-based information in different sectors including agriculture. Nayak (2006), developed rice map of Hirakud command area of Orissa, total crop delineated was 2624 ha against the agriculture department data of 2604 ha. Raza *et al.*, (2018) conducted a study in Punjab area of Pakistan, using Landsat 8 thermal for rice area delineation and growth variability maps were generated. The total area under investigation was 13,657 km² out of which 931.61 km² (6.8%) was found to be least suitable, 3316.69 km² (24.2%) was moderately suitable, 6019.63 km² (44%) was highly suitable and 3395.28 km² (24.85%) was not suitable for rice crop cultivation. Mostafa (2015), mapped the rice area in Bangladesh using Moderate Resolution Imaging Spectroradiometer (MODIS)-derived 16-day composite of NDVI at 250m

spatial resolution and the results were in good agreement with ground-based estimates at both country level and district level. Ajith *et al.* (2017) estimated area under rice during the Samba season in the Thanjavur district of Tamil Nadu using cloud free mono temporal Landsat 8 OLI images and the total area estimated was 1,09,799 ha during 2015-16 period. The potential of combined use of Sentinel-1/2 images for rice area mapping in China was studied by Xiao *et al.* (2021) and produced promising results.

2.5.1. Sentinel-2 images

The first Sentinel satellite, Sentinel-1A, was launched in 2014 by the Copernicus Program, which is run by the European Space Agency (ESA). Sentinel-1, 2, 3, and 5 are among the Copernicus satellite missions that have been launched so far. The launch of the multispectral instruments in Sentinel-2 satellite was a key contribution to the Copernicus Programme. Sentinel-2A and Sentinel-2B are twin satellites that make up the Sentinel-2 constellation (Phiri *et al.*, 2020). The Sentinel-2 satellites have multispectral imaging instruments (MSI) onboard that can record 13 wide-swath bands. Sentinel-2's main goal is to provide high-resolution satellite data for land cover/use monitoring, climate change monitoring, and catastrophe monitoring (Malenovsky *et al.*, 2012). The Sentinel-2 is used to supplement existing global satellite programmes like Landsat and SPOT by providing continuity in monitoring Earth's surface dynamics (Korhonen *et al.*, 2017).

Sentinel-2 data has been used by the scientific community, government organisations, and the corporate sector for a variety of purposes, including agriculture, urban development, and forest monitoring (Pesaresi *et al.*, 2016). One of the most important applications for Sentinel-2 data, according to Bruzzone *et al.* (2017) is land cover/use monitoring. The construction of a high spatial resolution (20 m) map for Africa for 2016, the Copernicus Land Cover Services high spatial resolution maps, and the new pan-European high spatial resolution land cover/use maps are all examples of key Sentinel-2 applications (Xu *et al.*, 2019). Sentinel-2 data was also used to create country-wide high spatial resolution maps for Germany, Belgium, Bulgaria, and Greece (Gromny *et al.*, 2019).

Agricultural information are important indicators to monitor agriculture policies and developments, so, they need to be up-to-date, accurate, and reliable (Ji,1996). Mapping the spatio-temporal distribution and the characteristics of agricultural fields is of paramount importance for their effective and sound management.

Materials and methods

3. MATERIALS AND METHODS

The study on “Estimation of crop water requirement in rice using satellite data and GIS” was done in Palakkad district during *mundakan* season 2020-21. The materials used and methods followed are presented in this chapter.

3.1. Description of study area

The Palakkad district is one among 14 districts of the state of Kerala which extends over an area of 4,48,200 ha. The district is located at 10° 95’ North latitude and 76° 54’ East longitude in central Kerala bordered on the northwest by Malappuram District, on the southwest by Thrissur District, on the northeast by Nilgiris district and on the east by Coimbatore District of Tamil Nadu (Fig. 1).

3.2. Rice area delineation

3.2.1. Satellite data

The Copernicus Sentinel-2 mission consists of a pair of polar-orbiting satellites: Sentinel-2A launched by European Space Agency on June 23, 2015 and Sentinel-2B launched on March 7, 2017 in a sun-synchronous orbit, phased at 180 degrees apart. Its vast sweep width (290 km) and long revisit time (10 days at the equator with one satellite, and 5 days with two satellites in cloud-free circumstances, resulting in 2-3 days at mid-latitudes) would aid in the monitoring of Earth's surface changes. Every 10 days interval, the multispectral instrument on the Sentinel-2 satellite delivers worldwide 10-meter resolution multispectral images (from 83 °N to 56 °S latitude). The Sentinel-2 Multi Spectral Instrument (MSI) is capable of acquiring images in 13 spectral bands ranging from Visible and Near-Infrared (VNIR) to Shortwave Infrared (SWIR) wavelengths.

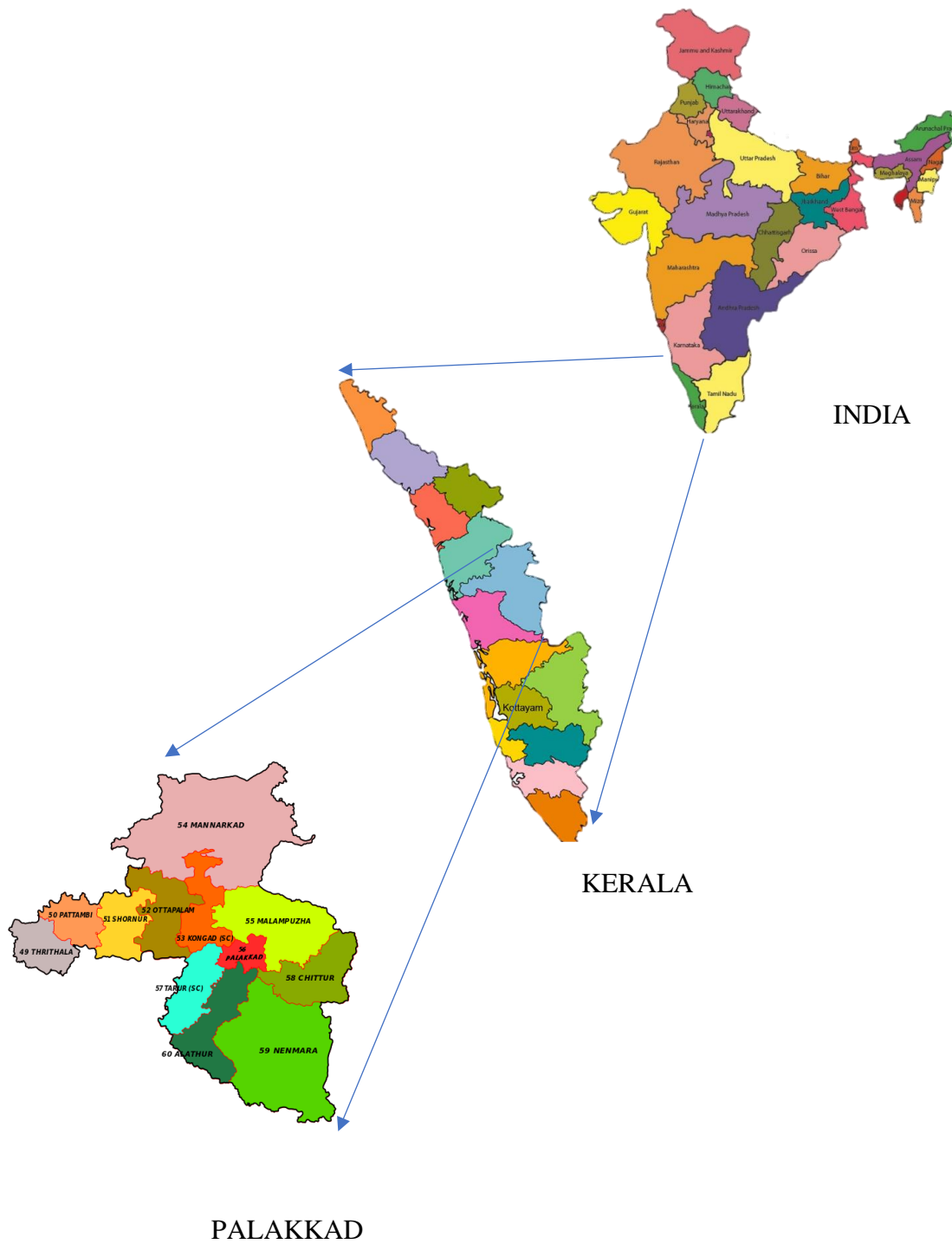


Fig 3.1. Location map of Palakkad district

In addition to direct user access from ESA portal, a coordinated effort between ESA and the USGS allows for free public access and redistribution of worldwide Sentinel-2 data acquisitions through secondary U.S. based portals. The USGS Earth Resources Observation and Science (EROS) Center repackages Sentinel-2 products per tile while maintaining the Sentinel Standard Archive Format for Europe (SAFE) format specification, which allows for the distribution of a 650 MB user-friendly file size. Each Level-1C product is a 100 km x 100 km tile with the UTM/WGS84 projection and datum (Universal Transverse Mercator/World Geodetic System 1984). The USGS provides a download package that includes one file for each of the 13 spectral bands as well as metadata. Image data, quality indicators, auxiliary data, and metadata are all included in the zip file that can be downloaded. Geographic Markup Language JPEG2000 (GMLJP2) format is used for Sentinel image data. The encoding required for georeferencing the image is provided by GML. Sentinel-2 data should be used in a Geographic Information System (GIS) or other special application software that supports the GMLJP2 format for research purposes. To search, preview and download Sentinel-2 data, sites like, Earth Explorer, USGS Global Visualization Viewer (GloVis) or the Sentinel-2 Look Viewer could be utilised. The collection can be found in Earth Explorer's Sentinel category.

3.2.2. Specification for Sentinel-2 standard products

- Product type: S2MSI1C
- Processing level: LEVEL-1C
- Output format: GMLP2/ GEOTIFF
- Pixel size: 10 meters/ 20 meters/ 60 meters
- Map projection: UTM
- Datum: WGS 84

3.2.3. Processing of Sentinel-2 images for area delineation

Sentinel-2 images at a spatial resolution of 10 m was used for area delineation. Three cloud free images were downloaded from the website <https://earthexplorer.usgs.gov> as the study area is covered by three scenes (Fig. 3.2).

Table 3.1. Sentinel-2 data acquisition schedule

Sentinel-2 data acquisition			
Date	Platform	Orbit No.	Product
26/01/2021	SENTINEL-2A	62	LIC_T43PFN_A029231_20210126T052106
28/01/2021	SENTINEL-2B	19	LIC_T43PFN_A020351_20210128T051756
28/01/2021	SENTINEL-2B	19	LIC_T43PFM_A020351_20210128T051756

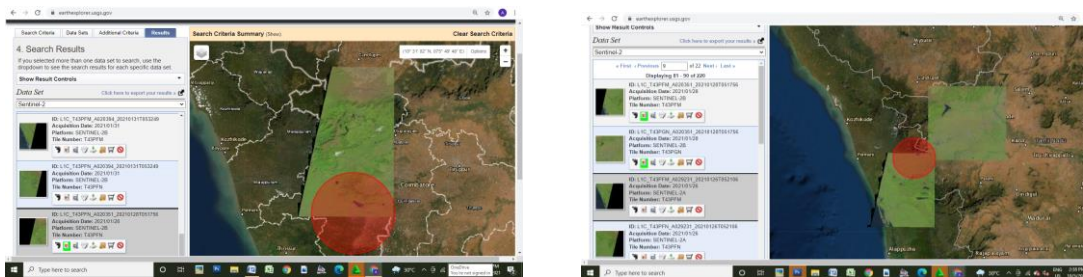


Fig. 3.2. Sentinel-2 image acquisition and coverage on Palakkad district from <https://earthexplorer.usgs.gov>.

3.2.3.1. Creating a composite from sentinel-2 imagery

Sentinel-2 images of four spectral bands having 10 m resolution was used for the study. Bands 2, 3, 4 and 8 were combined together to highlight vegetation features in the image (Table 3.2). Natural color combination is used in the red (B4), green (B3) and blue (B2) channels. This combination represents the objects in the image in the same way as we see the world with our eyes. The vegetation appears green, urban features in white or grey colour and water bodies in dark blue. The colour infrared combination are helps to distinguish between healthy and unhealthy vegetation. The near infrared (NIR) band (B8) is highly reflected by chlorophyll pigment in leaves.

Hence, denser vegetation appears in red colour in infrared images, whereas urban areas are represented by white colour.

Table 3.2. Band designation for Sentinel-2

Bands	Wavelength (nanometres)	Resolution (meters)
Band 2 - Blue	490 nm	10 m
Band 3 - Green	560 nm	10 m
Band 4 - Red	665 nm	10 m
Band 8 – Near Infrared	842 nm	10 m

Using provisions in ARCGIS, a new composite image was prepared by combining Band 2 (Blue), Band 3(Green), Band 4 (Red) and Band 8 (NIR) and it was changed to False Color Composite (FCC).

3.2.3.2. Mosaicking composite images

Mosaicking is a technique for combining two or more raster datasets into a single, unified raster dataset. To acquire a complete coverage of the study area, the three nearby composite raster datasets were mosaicked together into a single raster dataset.

3.2.3.3. Iso-cluster classification and rice area estimation

Unsupervised iso-cluster classification is a technique for recognizing, grouping, and classifying features in an image based on their spectral values. Pixels are clustered together in unsupervised classification based on spectral homogeneity and spectral distance. The rice area was delineated by identifying and removing classes such as water bodies, forests, other vegetation, agricultural crops and settlements from the mosaicked composite image. The study was determined to be suitable for an iso-cluster classification method with six classes.

3.2.4. Validation of rice area estimation

A sample of land cover data generated by remote sensing analysis representing rice (classified data) is compared with validation data indicating non-rice area

(reference data) to assess the accuracy of classification. The error matrix, which is a cross tabulation of categorised data versus reference data, is also known as the confusion, contingency or validation matrix in the literature. The error matrix's cross tabulation allows a number of standard reporting metrics to be calculated, including overall accuracy, as well as the accuracy of users and producers. These accuracy statistics indicate the degree to which the classified data is correct and how reliable it is. The validation in this study was done to estimate the accuracy of rice area estimation.

3.2.4.1. Ground survey data

The major rice growing tract of Palakkad district is spread over 5 blocks *viz.* Alathur, Nenmara, Kollengode, Chittur and Kuzhalmannam, each block having more than 10,000 hectares of land under rice cultivation. A total of 30 points were selected from 29 panchayats through random sampling technique in order to represent the whole rice area. The ground truth data was collected from these points using Global Positioning System (GPS) as well as camera during *mundakan* rice season (2020-21). The Table 3.3 represents the ground truth data collected.

Table 3.3. Rice area validation points

Sl. No.	Geographic co-ordinates (Degree decimals)		Location
	Latitude (°N)	Longitude (°E)	
1	10.6439	76.5352	Alathur I
2	10.6471	76.5495	Alathur II
3	10.6439	76.5105	Kavasseri
4	10.5758	76.5026	Kizhakkenchery
5	10.6316	76.4323	Pudukkode
6	10.6752	76.4667	Tarur
7	10.6194	76.5286	Vadakkenchery
8	10.6382	76.5955	Erimayur
9	10.5666	76.5827	Aliyur
10	10.6077	76.5533	Melarkode
11	0.5937	76.5057	Vandazy
12	10.5714	76.6125	Nenmara
13	10.5979	76.6378	Elevenchery
14	10.6208	76.6255	Pallassana



Plate I. Land based observations in rice fields at Palakkad



Plate II. Collection of information regarding plant height and leaf area index



Block : Alathur
Location: Alathur



Block : Nenmara
Location: Aliyur



Block : Kollengode
Location: Pudunagaram



Block : Chittur
Location: Polpully



Block : Kuzhalmannam
Location: Kuzhalmannam

Plate III. Rice fields located by GPS and Google earth in five blocks of Palakkad district

15	10.6310	76.7735	Pattanchery
16	10.6316	76.7453	Muthalamada
17	10.6344	76.6964	Vadavannur
18	10.6598	76.6607	Koduvayur
19	10.6533	76.6817	Pudunagaram
20	10.7095	76.6653	Peruvemb
21	10.6516	76.7653	Perumatty
22	10.7230	76.7728	Nallepilly
23	10.7177	76.7188	Polpully
24	10.6844	76.6960	Chittur-Thathamangalam
25	10.6566	76.6284	Thenkurissi
26	10.7161	76.5373	Kuthanoor
27	10.6994	76.5699	Kuzhalmannam
28	10.7061	76.4703	Peringottukurissi
29	10.7415	76.5608	Mathur
30	10.7396	76.5510	Kottayi

In general, locations with a homogeneous land cover within a 15-meter radius of the GPS points were chosen for the study. The ground truth data was obtained from the field during the active tillering or flowering stage of the crop. To ensure that the classification was accurate, the entire study region was classified into rice and non-rice areas. The ground truth data was compared with the designated rice areas to determine accuracy. In order to obtain the accuracy, a confusion matrix and kappa coefficient were developed based on rice and non-rice areas (Table 3.4) by comparing predicted and actual land coverage.

Table 3.4. Non rice area validation points in Palakkad district

Sl. No.	Latitude (°N)	Longitude (°E)
1	10.6185	76.5034
2	10.6343	76.5178
3	10.7089	76.5949
4	10.6951	76.5265
5	10.5943	76.5953
6	10.6870	76.6587

7	10.6912	76.6576
8	10.6627	76.6387
9	10.6862	76.6521
10	10.7484	76.6515
11	10.4918	76.4590
12	10.7724	76.6489
13	10.5678	76.6586
14	10.6771	76.5796
15	10.6827	76.5812
16	10.6845	76.5797
17	10.6486	76.5478
18	10.6377	76.5234
19	10.6324	76.5195
20	10.5796	76.4903
21	10.6150	76.5299
22	10.6359	76.5749
23	10.6853	76.5266
24	10.7173	76.5772
25	10.7128	76.6014
26	10.7033	76.5428
27	10.6430	76.6565
28	10.6012	76.6176
29	10.5998	76.6078
30	10.6038	76.4927

3.2.4.2. Confusion matrix

A confusion matrix contains information about a classification system's actual and expected classifications. The data in the matrix is widely used to evaluate the performance of such systems. While evaluating the thematic accuracy of a land-cover map, an error matrix is widely used to organise and present data (Stephen, 1997). The confusion matrix used for rice area classification validation is presented in Table 3.5. In the context of our investigation, the meaning of the entries in the confusion matrix are as follows.

Table 3.5. Confusion matrix for validation of rice area

	Predicted class from the map			
	Class	Rice	Non-rice	Accuracy
Actual class from survey	Rice	a	b	%
	Non-rice	c	d	%
	Average accuracy			

Where,

a is True positive, *ie.*, rice area was predicted and it turned out to be rice area

b is False negative, *ie.*, rice area was anticipated but it turned out to be non-rice area

c is False positive, *ie.*, non-rice area was anticipated but it turned out to be rice area

d is True negative, *ie.*, non-rice area was predicted and it turned out to be non-rice area

The average accuracy and percentage of accuracy for classification of rice and non-rice areas were computed using the confusion matrix. The computation formula is depicted below.

$$\text{Percentage accuracy of classification of rice area (R)} = \frac{a}{(a+b)} \times 100$$

$$\text{Percentage accuracy of classification of non-rice area (NR)} = \frac{d}{(c+d)} \times 100$$

$$\text{Average accuracy} = \frac{R+NR}{2}$$

3.2.4.3. Kappa coefficient

The Cohen's kappa coefficient, often known as the kappa coefficient, is a statistical method for determining inter-rater agreement for qualitative (categorical) items. It is typically considered to be a more reliable statistic than a simple percent agreement estimates since it considers the probability of the agreement occurring by chance (Cohen, 1960). The steps for calculating the Kappa coefficient are represented below.

$$\text{Observed agreement (OA)} = \frac{a+d}{a+b+c+d}$$

$$\text{Agreement of chance (AC)} = \frac{a+c}{a+b+c+d} \times \frac{a+b}{a+b+c+d} + \frac{b+d}{a+b+c+d} \times \frac{c+d}{a+b+c+d}$$

$$\text{Kappa coefficient} = \frac{(\text{OA}-\text{AC})}{(1-\text{AC})}$$

The numerator is the difference between the observed probability of success and the probability of success if the worst-case situation is assumed. Kappa coefficient is never greater than or equal to one. A value of 1 indicates perfect agreement, while values less than 1 indicate less than perfect agreement. The Table 3.6 represents one possible interpretation of the Kappa coefficient.

Table 3.6. Interpretation of Kappa coefficient

Interpretation levels	Kappa coefficient
Poor agreement	< 0.20
Fair agreement	0.20 to 0.40
Moderate agreement	0.40 to 0.60
Good agreement	0.60 to 0.80
Very good agreement	0.80 to 1.00

3.3. Crop water requirement estimation

3.3.1. Evapotranspiration

3.3.1.1. Reference crop evapotranspiration (ET_o)

Reference crop evapotranspiration/ reference evapotranspiration is the rate of evapotranspiration from a hypothetical reference crop with an assumed crop height (12 cm), a fixed crop surface resistance (70 S m⁻¹) and albedo (0.23), closely resembling the evapotranspiration from an extensive surface of green grass-cover of uniform height, actively growing, completely shading the ground and with adequate water (Allen *et al.*, 1997). FAO Penman-Monteith equation was used to estimate the reference evapotranspiration using daily or monthly mean weather data (Allen *et al.*, 1998). The equation is:

$$ET_0 = \frac{0.408\Delta(R_n - G) + \gamma \frac{900}{T+273} U_2 (e_a - e_d)}{\Delta + \gamma(1+0.34U_2)}$$

Where,

ET_0 = reference crop evapotranspiration (mm d^{-1})

R_n = net radiation at the crop surface ($\text{MJ m}^{-2} \text{d}^{-1}$)

G = soil heat flux ($\text{MJ m}^{-2} \text{d}^{-1}$)

T = average air temperature ($^{\circ}\text{C}$)

U_2 = wind speed measured at 2 m height (m s^{-1})

$(e_a - e_d)$ = vapour pressure deficit (kPa)

Δ = slope of the vapour pressure curve ($\text{kPa } ^{\circ}\text{C}^{-1}$)

γ = psychrometric constant ($\text{kPa } ^{\circ}\text{C}^{-1}$) and 900 is the conversion factor

3.3.1.2. Crop coefficient approach to estimate crop evapotranspiration

Crop evapotranspiration refers to the amount of water lost from the field through evapotranspiration, when the crop is grown under standard conditions (crops which are grown in large fields under ideal agronomic and soil conditions). In the crop coefficient approach the crop evapotranspiration (ET_c) is calculated by multiplying the reference crop evapotranspiration (ET_0) by a crop coefficient, K_c

$$ET_c = K_c \times ET_0$$

Where,

ET_c = crop evapotranspiration [mm d^{-1}]

K_c = crop coefficient [dimensionless]

ET_0 = reference crop evapotranspiration [mm d^{-1}]

3.3.2. Remote sensing to estimate crop water requirement

Satellite-based remote sensing is an alternative to estimate crop water requirement and its spatial and temporal distribution on a field-by-field basis at a

regional scale (Reyes- Gonzalez *et al.*, 2018). Estimation of crop evapotranspiration (ET_c) through remote sensing on a regional scale is less time consuming and cost effective as compared to other methods (Allen *et al.*, 2007). Crop coefficients are estimated based on spectral reflectance of vegetation indices (VIs) (Allen *et al.*, 1998). The Normalized Difference Vegetation Index (NDVI) is the most common vegetation index which takes into account the reflectance of red and near-infrared wavebands (Rouse *et al.*, 1973). The red waveband is strongly absorbed by the chlorophyll present in leaves, whereas the near infrared wave band is strongly reflected by the chlorophyll pigments present in the leaves (Glenn *et al.*, 2010). NDVI is the difference between the near infrared (NIR) and red wave band reflectance divided by their sum.

$$NDVI = \frac{(NIRband - Red\ band)}{(NIRband + Red\ band)}$$

These values usually range from -1 to +1. High positive values represent dense canopies with healthy vegetation (Toureiro *et al.*, 2017). Crop coefficients generated based on NDVI values were found to estimate ET_c more accurately as compared to tabulated ET_c because, it represents actual crop growth conditions and capture the spatial variability among different fields (Kulberg *et al.*, 2017). Crop coefficients derived from remotely sensed vegetation index were used to generate local and regional ET_c maps for corn crop in northern Mexico (Reyes- Gonzalez *et al.*, 2018).

3.3.2.1. MODIS Images

The MODIS is an imaging sensor developed by Santa Barbara Remote Sensing, which was launched to sun-synchronous orbit by NASA on board the Terra (EOS AM) satellite and the Aqua (EOS PM) satellite in 1999 and 2002 respectively. MODIS acquires the image of entire earth surface every 1 to 2 days and the data is collected in 36 spectral bands ranging in wavelength from 0.4 μm to 14.4 μm and at varying spatial resolutions (2 bands at 250 m, 5 bands at 500 m and 29 bands at 1 km). The data are useful for vegetation health monitoring using vegetation indices, track land use and land cover changes, global snow cover, monitor floods *etc.* Among the standard MODIS data products available to the users, the 16-day composite MODIS NDVI (MOD13Q1006) was used for the study. The spatial resolution of the MODIS product is 250 m and a total of 8 scene images coinciding with the *mundakan* rice season were downloaded

from <http://lpdaac.usgs.gov> (Fig. 3.3). The satellite images were downloaded during the period 15th October 2020 to 28th February 2021. The acquisition and coverage of MODIS NDVI product on Palakkad district from the website is presented in Table 3.7.

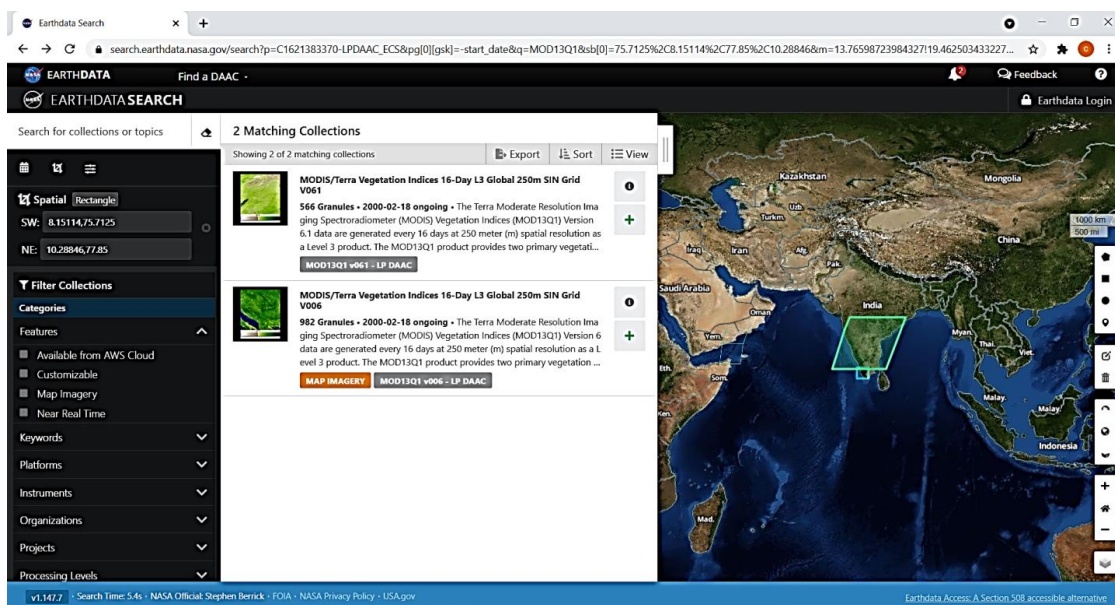


Fig. 3.3 MOD13Q1 NDVI acquisition and coverage on Palakkad district from <http://lpdaac.usgs.gov>.

Table 3.7. MOD13Q1 NDVI data acquisition schedule

MOD13Q1 NDVI data acquisition			
Date	Path	Row	Product
01/11/2020	25	7	MOD13Q1.A2020305.h25v07.006
17/11/2020	25	7	MOD13Q1.A2020321.h25v07.006
03/12/2020	25	7	MOD13Q1.A2020337.h25v07.006
19/12/2020	25	7	MOD13Q1.A2020353.h25v07.006
01/01/2021	25	7	MOD13Q1.A2021001.h25v07.006
17/01/2021	25	7	MOD13Q1.A2021017.h25v07.006
02/02/2021	25	7	MOD13Q1.A2021033.h25v07.006
18/02/2021	25	7	MOD13Q1.A2021049.h25v07.006

3.3.2.2. Data Analysis

Data analysis includes pre-processing of images, gathering rice spectral information from the MODIS images and statistical analysis. Pre-processing involves collection of MODIS images, image cropping, geographic coordinate transformation and several other procedures. HEQ Tool (Modis Reprojection Tool) is used to convert NDVI imageries downloaded in Sinusoidal Projection (Fig. 3.4) to Universal Transverse Mercator co-ordinate system (Fig. 3.5). The pre-processed images which were in the hierarchical data format (hdf) originally were converted to “img” format through “Export raster data” provision in ArcGIS. Using the “img” raster, NDVI for each pixel was calculated using raster calculator in map algebra by dividing it with a constant (10000). From the output raster NDVI values for 30 locations in Palakkad district were retrieved using the “Extract multivalues to points” provision in ArcGIS (Fig. 3.6).

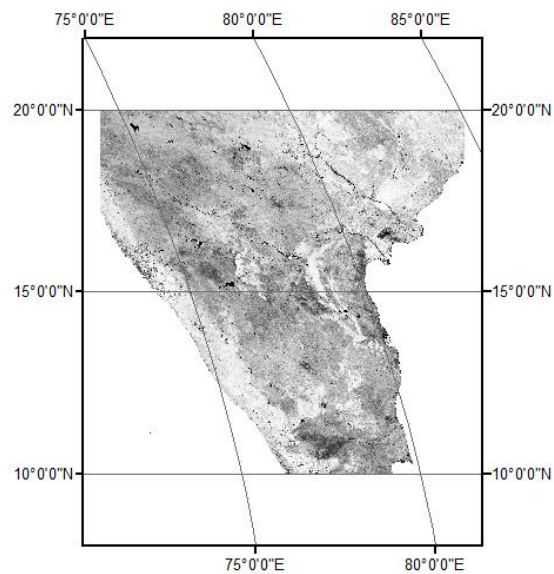


Fig. 3.4. MODIS downloaded image in sinusoidal projection

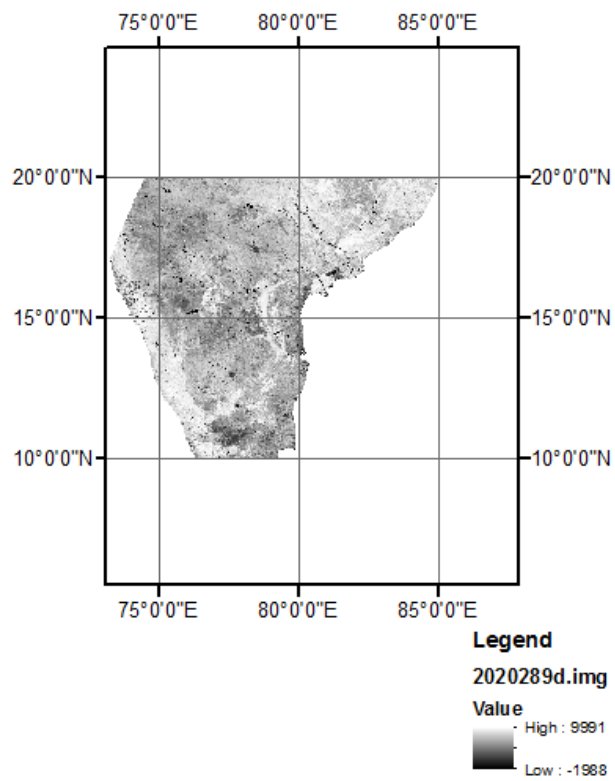


Fig. 3.5. MODIS reprojected image

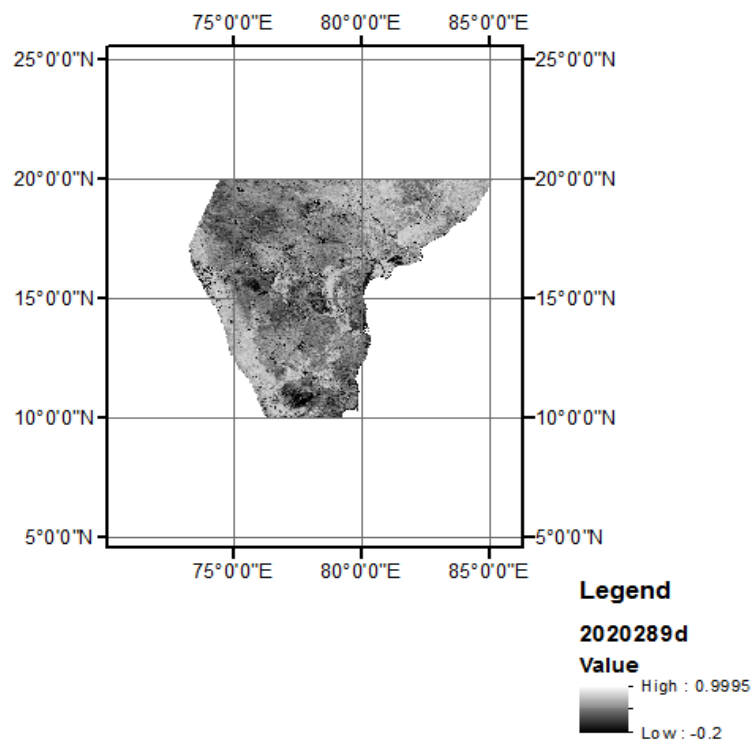


Fig. 3.6. MODIS-NDVI retrieved

3.3.2.3. NDVI and K_c

The relationship between NDVI and age of rice plant is such that (i) it will be low at the transplantation stage, (ii) increases over the vegetative-to-reproductive stage and (iii) gradually decreases with the progression of the ripening stage (IRRI, 2014). In the Fig. 3.7 red curve shows temporal dynamics of vegetation index.

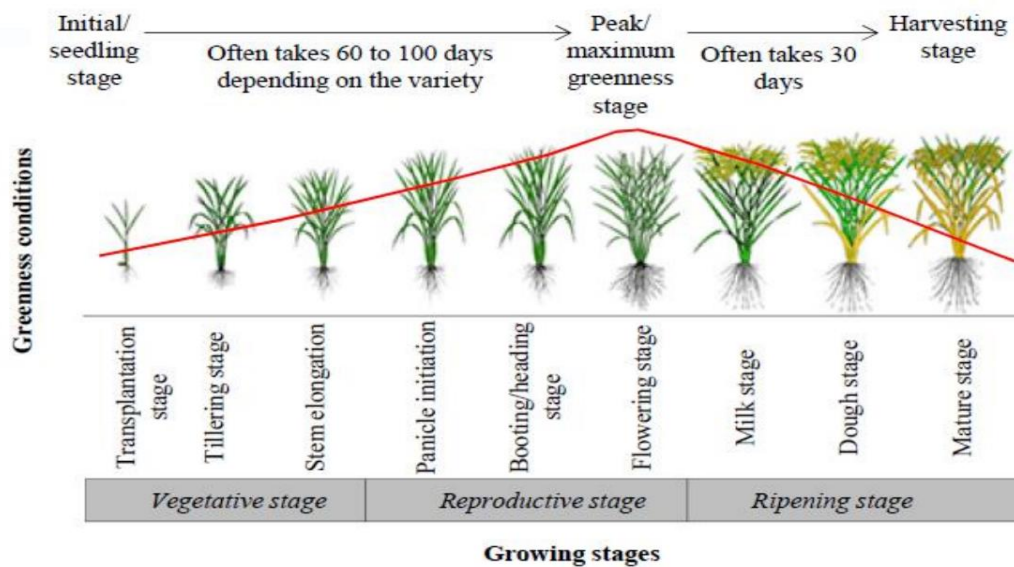


Fig. 3.7. Temporal variation of NDVI with crop stages in rice

The crop coefficient (K_c) value also shows a similar relationship with the age of the plant. The K_c value is low in the initial stage, maximum value is achieved when plant attains full vegetative growth, and further K_c value decreases as the crop approaches harvesting stage. The table K_c values were obtained from literature and these values are used to establish a relationship between NDVI and was expressed in the form of a linear equation.

3.3.2.4. Weather data

The daily weather data of the study area during the period October 2020 to February 2021 was collected from India Meteorological Department (IMD). Weather cock software was used to convert daily weather data into weekly and monthly formats. The weekly and monthly reference evapotranspiration was calculated using a software named PET calculator. The weather parameters like maximum and minimum

temperature, sunshine hours, forenoon and afternoon relative humidity, evaporation and windspeed are given as input in PET calculator.

3.3.2.5. Calculation of effective rainfall

Potential evapotranspiration/ Precipitation ratio method is a semi-empirical method suggested by FAO to calculate effective rainfall of a region (FAO, 2021). The ratio when expressed as percentage, the maximum value attained is 100. If the rainfall of a region is zero, the corresponding percentage value will be zero. If rainfall is less than PET, the percentage value is taken as 100 assuming that total rainfall received in the region was effectively utilised. The above mentioned percentage of actual rainfall of a region is considered as effective rainfall in millimetres.

3.3.2.6. Estimation of Irrigation requirement

Crop evapotranspiration (ET_c) was obtained by multiplying Crop coefficient (K_c) with ET_o . A part of the water requirement of the crop is acquired through rainfall and remaining water is supplied through irrigation. Water required to compensate crop evapotranspiration through irrigation was calculated by subtracting effective rainfall from crop evapotranspiration (ET_c). In rice fields additional water has to be supplied to maintain standing water in the fields, so it is also added up with irrigation water to be supplied to compensate crop evapotranspiration, in order to estimate the net irrigation requirement in rice. The stage wise irrigation requirement and total irrigation requirement for the crop season were hence estimated.

3.3.2.7. Preparation of K_c maps and crop water demand maps

The MODIS-NDVI retrieved images were used to generate K_c maps of the study area using provisions in ARCGIS software. The K_c value for each pixel was retrieved using raster calculator in map algebra, based on the relationship established between NDVI and K_c values. The crop water demand maps corresponding to the rice pixels during early vegetative stage, late vegetative stage, reproductive stage and maturity stage were developed using ARCGIS software.

Results

RESULT

A study on the 'Estimation of crop water requirement in rice using satellite data and GIS' was conducted in Palakkad district of Kerala during *mundakan* season 2020-21. Crop water requirement was estimated using crop coefficient values predicted through remote sensing techniques and reference crop evapotranspiration (ET_o) calculated based on weather variables. Rice area delineation for the district was done using satellite images. The results of the study are presented in this chapter.

4.1. Rice area delineation

Three multi temporal cloud free Sentinel-2 imageries at a spatial resolution of 10 m was obtained during *mundakan* season 2020-21 covering the study area consisting of 5 blocks in Palakkad district. The composite images consisting of 4 bands (B2, B3, B4 and B8) were downloaded from the website <https://earthexplorer.usgs.gov>. ArcGIS software was used to mosaick three composite raster datasets to obtain a single image covering the study area. Through mosaicking gaps and spaces in the image were removed resulting in a single smooth and continuous raster image which facilitated easy classification. The administrative boundaries of the district were superimposed over the image using ArcGIS software to extract all pixels corresponding to the study area. The pixels corresponding to the study area is clipped using the provisions present in the software. Clipping is done to project out a particular area from an image. The mosaicked and clipped image showing the study area in Palakkad district is shown in the Fig. 4.1.

The land use classification was done using iso cluster unsupervised classification technique and maps were generated representing the land use pattern in five blocks of Palakkad district based on six classes as represented in Fig. 4.2. Rice area maps were generated for five blocks of Palakkad district and is presented in Fig. 4.3. The total rice area estimated for the five blocks was 24742.76 ha which is slightly less than the actual area reported during *mundakan* season during 2018-19 period *ie*; 26952.2 ha as per Agricultural statistics report (2018-19).

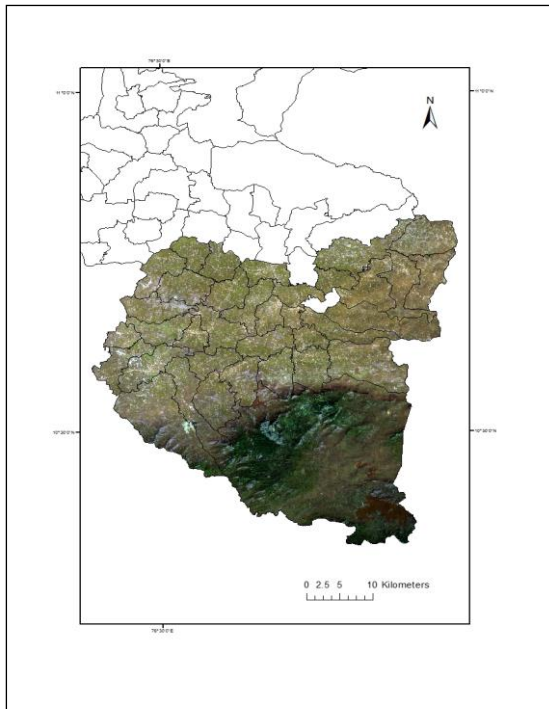


Fig. 4.1. Mosaicked composite image of the study area

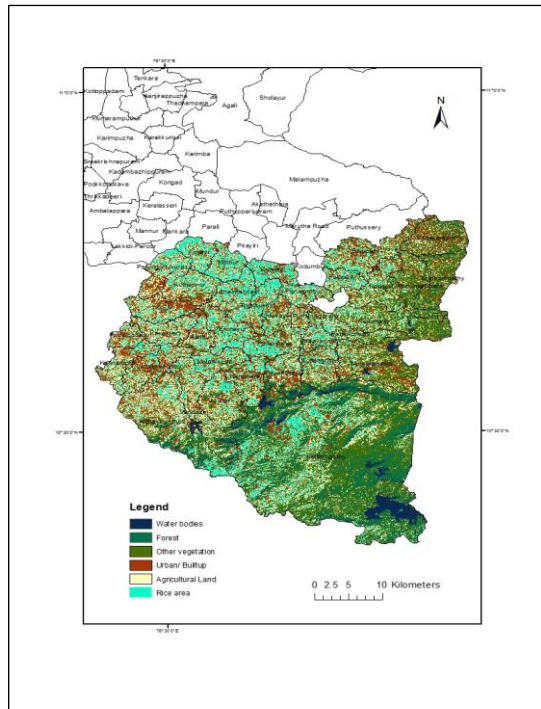


Fig. 4.2. Land use classification of study area

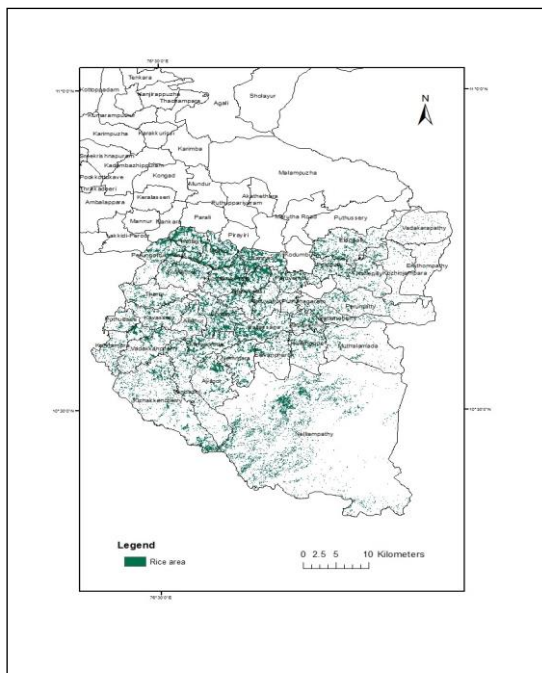


Fig. 4.3. Rice area map of the study area in Palakkad district

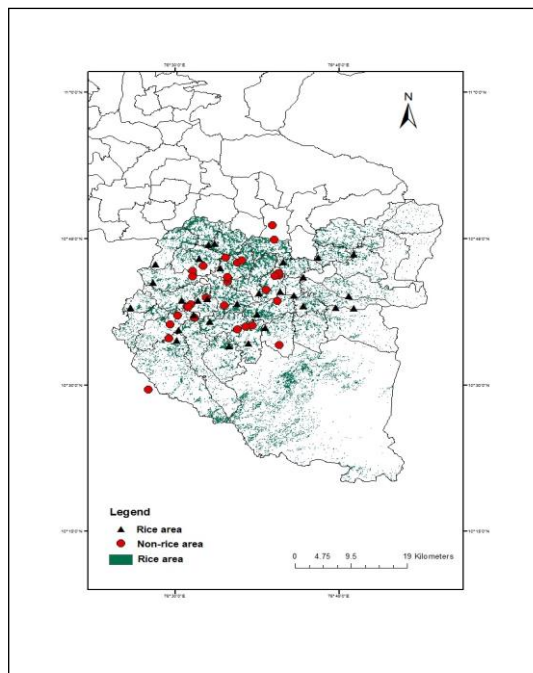


Fig. 4.4. Rice area map validation points for rice and non-rice classes across the study area in Palakkad district

The area under other classes were estimated as follows; water bodies (5513.65 ha), forest (24806.33 ha), other vegetation (48390.49 ha), urban area or build up structures (27506.51 ha) and agricultural land where crops other than rice is grown (48208.16 ha). The rice area was estimated to be 13.8 % of the study area. The rice acreage estimation was validated by grouping the entire study area into rice and non-rice areas. For the purposes of assessing accuracy, all the remaining classes except rice area were grouped into a single non-rice class. A total of 60 validation points were found throughout the study area spread across five blocks of the district, with 30 rice and 30 non-rice points (Fig 4.4). By comparing predicted and actual land coverage, confusion matrix and kappa coefficient were developed based on rice and non-rice areas in order to assess the accuracy. Table 4.1. shows an overview of the validation data, rice areas, non-rice areas, and classification accuracy. The overall classification accuracy was 88.33 % with a Kappa coefficient of 0.77. Small fragmented heterogeneous rice areas and large homogeneous rice areas were classified equally well.

Table 4.1. Confusion matrix for accuracy assessment of rice classification

	Predicted class from the map			Accuracy
	Class	Rice	Non-rice	
Actual class from survey	Rice	24	6	80 %
	Non-rice	1	29	96.66 %
	Reliability	96 %	82.85 %	
	Average accuracy	88.33 %		
	Average reliability	89.4 %		
	Kappa coefficient	0.77		

4.2. Normalized Difference Vegetation Index (NDVI), rice crop growth and yield

Ground truth verification of rice area during *mundakan* season 2020-21 was done at 30 locations in the district having rice fields of sufficiently bigger size and the geographical coordinates of the locations were obtained using GPS (Table 4.2). The coordinates of the sampling points and the shape file of Palakkad district were superimposed on the MODIS-NDVI map. Age of the rice plant at each location corresponding to the image acquisition date was calculated by considering sowing date as the reference.

NDVI values corresponding to the age of the rice plant were obtained for 30 ground truth locations (or training sites) from MOD13Q1 images. Among the 8 images of MOD13Q1 obtained during the crop period, some images showed very low NDVI values due to cloud interferences. The NDVI time series was smoothed using standard statistical procedures to overcome this problem. The NDVI values during early vegetative stage (*ie*; 0-21 Days After Sowing (DAS)) was in the range of 0.4-0.6 in different training sites of Alathur (Table 4.4), Chittur (Table 4.7) and Kuzhalmannam (Table 4.8) blocks, whereas, in some training sites of Nenmara (Table 4.5) and Kollengode (Table 4.6) blocks, slightly higher NDVI value of 0.7 was observed. During the late vegetative stage of the crop (*ie*; 21-60 DAS), NDVI of 0.6-0.8 was observed in all the blocks. The NDVI value decreased from 0.8 to 0.7 during reproductive phase of crop growth (60-90 DAS) and this trend was observed in all the training sites considered in the study. When the crop reached maturity stage (*ie*; 90-120 DAS), NDVI value further decreased to 0.4 in some training sites of Alathur and Nenmara block, 0.5 in Kollengode block and 0.6 in Chittur and Kuzhalmannam blocks. The block wise average rice yield obtained by crop cutting experiments was analysed in relation to the maximum NDVI values during the peak vegetative stage of the crop (Table 4.3). A strong relationship (correlation coefficient-0.88) was observed between maximum NDVI during the crop growth period and rice yield. The highest average yield was reported in Alathur block (6243.28 kg/ha) where maximum NDVI value of 0.8273 was observed, and the least yield (5625 kg/ha) in Chittur block where maximum NDVI was low *ie*; 0.7830.

Table 4.2. Ground truth locations in the study area

Sl. No.	Location	Block	Geographic co-ordinates (Degree decimals)		Rice observation age (DAS)	
			Latitude (N)	Longitude (E)	Start	End
1	Alathur I	Alathur	10.6439	76.5352	2	114
2	Alathur II	Alathur	10.6471	76.5495	0	112
3	Kavasseri	Alathur	10.6439	76.5105	8	120
4	Kizhakkenchery	Alathur	10.5758	76.5026	11	107
5	Pudukkode	Alathur	10.6316	76.4323	7	103
6	Tarur	Alathur	10.6752	76.4667	8	120
7	Vadakkenchery	Alathur	10.6194	76.5286	15	111
8	Erimayur	Alathur	10.6382	76.5955	4	116
9	Aliyur	Nenmara	10.5666	76.5827	2	114
10	Melarkode	Nenmara	10.6077	76.5533	7	119
11	Vandazy	Nenmara	0.5937	76.5057	15	111
12	Nenmara	Nenmara	10.5714	76.6125	5	117
13	Elevenchery	Nenmara	10.5979	76.6378	14	110
14	Pallassana	Nenmara	10.6208	76.6255	1	113
15	Pattanchery	Kollengode	10.6310	76.7735	10	106
16	Muthalamada	Kollengode	10.6316	76.7453	26	106
17	Vadavannur	Kollengode	10.6344	76.6964	6	118
18	Koduvayur	Kollengode	10.6598	76.6607	2	114
19	Pudunagaram	Kollengode	10.6533	76.6817	3	115
20	Peruvemb	Kollengode	10.7095	76.6653	5	117
21	Perumatty	Chittur	10.6516	76.7653	2	114
22	Nallepilly	Chittur	10.7230	76.7728	8	120
23	Polpully	Chittur	10.7177	76.7188	4	116
24	Chittur-Thathamangalam	Chittur	10.6844	76.6960	10	106
25	Thenkurissi	Kuzhalmannam	10.6566	76.6284	6	118

26	Kuthanoor	Kuzhalmannam	10.7161	76.5373	10	106
27	Kuzhalmannam	Kuzhalmannam	10.6994	76.5699	14	126
28	Peringottukurissi	Kuzhalmannam	10.7061	76.4703	1	113
29	Mathur	Kuzhalmannam	10.7415	76.5608	5	117
30	Kottayi	Kuzhalmannam	10.7396	76.5510	1	113

Table 4.3. Relationship between maximum NDVI and rice yield

Blocks	Average Yield (kg ha⁻¹)	Average Max NDVI
Alathur	6243.38	0.8273
Nenmara	6187.50	0.8359
Kollengode	6095.83	0.8268
Chittur	5625.00	0.7830
Kuzhalmannam	6208.33	0.8121



Plate IV. Crop cutting experiment at Palakkad

Table 4.4. NDVI values corresponding to the age of the plant extracted for each location in Alathur block from MOD13Q1 images

Alathur I		Alathur II		Kavasseri		Kizhakkenchery		Pudukkode		Tarur		Vadakkenchery		Erimayur	
DAS	NDVI	DAS	NDVI	DAS	NDVI	DAS	NDVI	DAS	NDVI	DAS	NDVI	DAS	NDVI	DAS	NDVI
2	0.4606	0	0.4585	8	0.4018	11	0.4393	7	0.4534	8	0.467	15	0.4432	4	0.425
18	0.6433	16	0.6343	24	0.5718	27	0.6704	23	0.7096	24	0.658	31	0.7211	20	0.5229
34	0.7599	32	0.7502	40	0.7351	43	0.7561	39	0.8264	40	0.7525	47	0.8511	32	0.5444
50	0.8219	48	0.8137	56	0.8035	59	0.8561	55	0.8618	56	0.8317	63	0.842	56	0.692
66	0.8134	64	0.8055	72	0.7883	75	0.8634	71	0.7913	72	0.8509	79	0.7619	68	0.7248
82	0.773	80	0.787	88	0.751	91	0.7494	87	0.7522	88	0.809	95	0.719	84	0.7429
98	0.6812	96	0.6736	104	0.6294	107	0.5646	103	0.6241	104	0.7263	111	0.629	100	0.752
114	0.4681	112	0.4531	120	0.4805					120	0.5514			116	0.5569

NDVI : Normalized Difference Vegetation Index

DAS : Days After Sowing

Table 4.5. NDVI values corresponding to the age of the plant extracted for each location in Nenmara block from MOD13Q1 images

Aliyur		Melarkode		Vandazy		Nenmara		Elevenchery		Pallassana	
DAS	NDVI	DAS	NDVI	DAS	NDVI	DAS	NDVI	DAS	NDVI	DAS	NDVI
2	0.4606	0	0.4585	8	0.4018	11	0.4393	7	0.4534	8	0.467
18	0.6433	16	0.6343	24	0.5718	27	0.6704	23	0.7096	24	0.658
34	0.7599	32	0.7502	40	0.7351	43	0.7561	39	0.8264	40	0.7525
50	0.8219	48	0.8137	56	0.8035	59	0.8561	55	0.8618	56	0.8317
66	0.8134	64	0.8055	72	0.7883	75	0.8634	71	0.7913	72	0.8509
82	0.773	80	0.787	88	0.751	91	0.7494	87	0.7522	88	0.809
98	0.6812	96	0.6736	104	0.6294	107	0.5646	103	0.6241	104	0.7263
114	0.4681	112	0.4531	120	0.4805					120	0.5514

NDVI : Normalized Difference Vegetation Index

DAS : Days After Sowing

Table 4.6. NDVI values corresponding to the age of the plant extracted for each location in Kollengode block from MOD13Q1 images

Pattanchery		Muthalamada		Vadavannur		Koduvayur		Pudunagaram		Peruvemb	
DAS	NDVI	DAS	NDVI	DAS	NDVI	DAS	NDVI	DAS	NDVI	DAS	NDVI
10	0.4571	26	0.5705	6	0.4468	2	0.4912	3	0.47595	5	0.4862
26	0.7538	42	0.7627	22	0.5977	18	0.6494	19	0.7133	21	0.6993
42	0.8538	58	0.8117	38	0.7562	34	0.6757	35	0.7888	37	0.751
58	0.8828	74	0.8255	54	0.8122	50	0.7815	51	0.8239	53	0.792
74	0.8427	90	0.7507	70	0.8253	66	0.8107	67	0.8121	69	0.7925
90	0.7193	106	0.5381	86	0.7813	82	0.7926	83	0.756	85	0.7543
106	0.5367			102	0.7041	98	0.7768	99	0.6344	101	0.6853
				118	0.5412	114	0.5918	115	0.5176	117	0.5278

NDVI : Normalized Difference Vegetation Index

DAS : Days After Sowing

Table 4.7. NDVI values corresponding to the age of the plant extracted for each location in Chittur block from MOD13Q1 images

Perumatty		Nallepilly		Polpully		Chittur-Thathamangalam	
DAS	NDVI	DAS	NDVI	DAS	NDVI	DAS	NDVI
2	0.4908	8	0.4809	4	0.47531	10	0.492
18	0.6651	24	0.6849	20	0.5434	26	0.5976
34	0.7041	40	0.7648	32	0.6805	42	0.694
50	0.7507	56	0.7829	56	0.75835	58	0.7533
66	0.7537	72	0.7844	68	0.8362	74	0.7391
82	0.7567	88	0.7859	84	0.7807	90	0.721
98	0.7288	104	0.7569	100	0.7449	106	0.651
114	0.6358	120	0.6851	116	0.6609		

NDVI : Normalized Difference Vegetation Index

DAS : Days After Sowing

Table 4.8. NDVI values corresponding to the age of the plant extracted for each location in Kuzhalmannam block from MOD13Q1 images

Thenkurissi		Kuthanoor		Kuzhalmannam		Peringottukurissi		Mathur		Kottayi	
DAS	NDVI	DAS	NDVI	DAS	NDVI	DAS	NDVI	DAS	NDVI	DAS	NDVI
6	0.4837	10	0.6363	14	0.558	1	0.446	5	0.4642	1	0.4934
22	0.6724	26	0.7323	30	0.698	17	0.5946	21	0.6432	17	0.5808
38	0.7554	42	0.7672	46	0.7721	33	0.6818	37	0.7188	33	0.6636
54	0.7724	58	0.791	62	0.8113	49	0.7679	53	0.7865	49	0.789
70	0.7598	74	0.817	78	0.762	65	0.7977	69	0.8234	65	0.8424
86	0.7472	90	0.7723	94	0.647	81	0.791	85	0.7968	81	0.809
102	0.761	106	0.626	110	0.598	97	0.8061	101	0.7223	97	0.7567
118	0.6461			126	0.512	113	0.64	117	0.6853	113	0.6975

NDVI : Normalized Difference Vegetation Index

DAS : Days After Sowing

4.3. Relationship of crop coefficient (K_c value) with the age of the plant

Lee and Huang (2014) studied the impact of climate change on irrigation water requirement in northern Taiwan and found out K_c values corresponding to the age of the rice plant as presented in Table 4.9. The K_c values obtained from the above study was used as reference value for establishing a relationship between satellite derived NDVI and is referred to as K_c table value in this study. The trends in variation of K_c table value in ground truth locations of Alathur (Table 4.10), Nenmara (Table 4.11), Kollengode (Table 4.12), Chittur (Table 4.13) and Kuzhalmannam (Table 4.14) blocks depicted that, during initial stages the K_c value was 0.5, then it gradually increased to 1.3 as the crop approached late vegetative stage. Further K_c value showed a decreasing trend towards reproductive and maturity stage. The K_c table value was 1.1 during reproductive stage and 0.7 towards maturity stage in all the locations considered in this study.

Table 4.9. K_c table value corresponding to the age of the rice plant

Days After Sowing (DAS)	K_c table value
0-15	0.5
15-35	0.8
35-45	1.2
45-75	1.3
75-90	1.2
90-105	1.1
105-120	0.7

Table 4.10. K_c table values corresponding to age of the crop for Alathur block

Alathur I		Alathur II		Kavasseri		Kizhakkenchery		Pudukkode		Tarur		Vadakkenchery		Erimayur	
DAS	K_c (Table value)	DAS	K_c (Table value)	DAS	K_c (Table value)	DAS	K_c (Table value)	DAS	K_c (Table value)	DAS	K_c (Table value)	DAS	K_c (Table value)	DAS	K_c (Table value)
2	0.5	0	0.5	8	0.5	11	0.5	7	0.5	8	0.5	15	0.5	4	0.5
18	0.8	16	0.8	24	0.8	27	0.8	23	0.8	24	0.8	31	0.8	20	0.8
34	1.2	32	1.2	40	1.2	43	1.2	39	1.2	40	1.2	47	1.3	32	0.8
50	1.3	48	1.3	56	1.3	59	1.3	55	1.3	56	1.3	63	1.3	56	1.3
66	1.3	64	1.3	72	1.3	75	1.3	71	1.3	72	1.3	79	1.2	68	1.3
82	1.2	80	1.2	88	1.2	91	1.1	87	1.2	88	1.2	95	1.1	84	1.2
98	1.1	96	1.1	104	1.1	107	0.7	103	1.1	104	1.1	111	0.7	100	1.1
114	0.7	112	0.7	120	0.7					120	0.7			116	0.7

K_c : Crop coefficient

DAS: Days After Sowing

Table 4.11. K_c table values corresponding to age of the crop for Nenmara block

Aliyur		Melarkode		Vandazy		Nenmara		Elevenchery		Pallassana	
DAS	K_c (Table value)	DAS	K_c (Table value)	DAS	K_c (Table value)	DAS	K_c (Table value)	DAS	K_c (Table value)	DAS	K_c (Table value)
2	0.5	7	0.5	15	0.5	5	0.5	14	0.5	1	0.5
18	0.8	23	0.8	31	0.8	21	0.8	30	0.8	17	0.8
34	0.8	39	1.2	47	1.2	37	1.2	46	1.2	33	0.8
50	1.3	55	1.3	63	1.3	53	1.3	62	1.3	49	1.3
66	1.3	71	1.3	79	1.2	69	1.3	78	1.2	65	1.3
82	1.2	87	1.2	95	1.1	85	1.2	94	1.1	81	1.2
98	1.1	103	1.1	111	0.7	101	1.1	110	0.7	97	1.1
114	0.7	119	0.7			117	0.7			113	0.7

K_c : Crop coefficient

DAS: Days After Sowing

Table 4.12. K_c table values corresponding to age of the crop for Kollengode block

Pattanchery		Muthalamada		Vadavannur		Koduvayur		Pudunagaram		Peruvemb	
DAS	K_c (Table value)	DAS	K_c (Table value)	DAS	K_c (Table value)	DAS	K_c (Table value)	DAS	K_c (Table value)	DAS	K_c (Table value)
10	0.5	26	0.8	6	0.5	2	0.5	3	0.5	5	0.5
26	0.8	42	1.2	22	0.8	18	0.8	19	0.8	21	0.8
42	1.2	58	1.3	38	1.2	34	0.8	35	1.2	37	1.2
58	1.3	74	1.3	54	1.3	50	1.3	51	1.3	53	1.3
74	1.3	90	1.2	70	1.3	66	1.3	67	1.3	69	1.3
90	1.2	106	0.7	86	1.2	82	1.2	83	1.2	85	1.2
106	0.7			102	1.1	98	1.1	99	1.1	101	1.1
				118	0.7	114	0.7	115	0.7	117	0.7

K_c : Crop coefficient

DAS: Days After Sowing

Table 4.13. K_c table values corresponding to age of the crop for Chittur block

Perumatty		Nallepilly		Polpully		Chittur-Thathamangalam	
DAS	K_c (Table value)	DAS	K_c (Table value)	DAS	K_c (Table value)	DAS	K_c (Table value)
2	0.5	8	0.5	4	0.5	10	0.5
18	0.8	24	0.8	20	0.8	26	0.8
34	0.8	40	1.2	32	0.8	42	1.2
50	1.3	56	1.3	56	1.3	58	1.3
66	1.3	72	1.3	68	1.3	74	1.3
82	1.2	88	1.2	84	1.2	90	1.2
98	1.1	104	1.1	100	1.1	106	0.7
114	0.7	120	0.7	116	0.7		

K_c : Crop coefficient

DAS: Days After Sowing

Table 4.14. K_c table values corresponding to age of the crop for Kuzhalmannam block

Thenkurissi		Kuthanoor		Kuzhalmannam		Peringottukurissi		Mathur		Kottayi	
DAS	K_c (Table value)	DAS	K_c (Table value)	DAS	K_c (Table value)	DAS	K_c (Table value)	DAS	K_c (Table value)	DAS	K_c (Table value)
6	0.5	10	0.8	14	0.8	1	0.5	5	0.5	1	0.5
22	0.8	26	0.8	30	1.2	17	0.8	21	0.8	17	0.8
38	1.2	42	1.2	46	1.3	33	0.8	37	1.2	33	0.8
54	1.3	58	1.3	62	1.3	49	1.3	53	1.3	49	1.3
70	1.3	74	1.3	78	1.2	65	1.3	69	1.3	65	1.3
86	1.2	90	1.2	94	1.2	81	1.2	85	1.2	81	1.2
102	1.1	106	0.7	110	0.7	97	1.1	101	1.1	97	1.1
118	0.7			126	0.7	113	0.7	117	0.7	113	0.7

K_c : Crop coefficient

DAS: Days After Sowing

4.4. Estimation of crop water demand in rice using remote sensing

4.4.1. Establishing NDVI - K_c relationship and validation of K_c predicted value

Analysis was done to establish a relationship between Normalized Difference Vegetation Index and K_c table values for the 30 locations under the study. A linear equation was set, between NDVI values obtained from MOD13Q1 and K_c table values, and the equation showed a strong relation with an R^2 value of 0.8156 (Fig. 4.5). The NDVI and K_c table values of 15 locations were used to develop the equation and it was validated for remaining 15 locations. During validation, a fairly high R^2 value of 0.80-0.93 was observed. The K_c values for 30 locations corresponding to the age of the plant was predicted using the equation developed.

The K_c predicted values were compared with K_c table values for each ground truth location and it was observed that during early vegetative stage K_c table values were in the range of 0.5-0.8, but, the predicted K_c values in Alathur block was in the range of 0.5-1.08 (Table 4.15), in Nenmara block the values ranged between 0.5-1.0 (Table 4.16), in Kollengode block 0.5-1.15 (Table 4.17), in Chittur 0.5-1.02 (Table 4.18) and in Kuzhalmannam 0.5-1.11 (Table 4.19). Towards the late vegetative stage, the predicted K_c value showed an increasing trend from 0.8 to 1.2 and then to 1.3, a similar trend was observed in almost all the blocks. During the reproductive stage, K_c predicted value decreased from 1.3 to 1.1 in the majority of the locations. Both the late vegetative and reproductive stages showed a similar trend as that of K_c table value. Towards the maturity of the crop, in some locations K_c predicted value was as low as 0.58 compared to the table value 0.7 (Table 4.15), whereas, in some other locations predicted value was higher *ie*; 1.02 when compared to table value (Table 4.18).

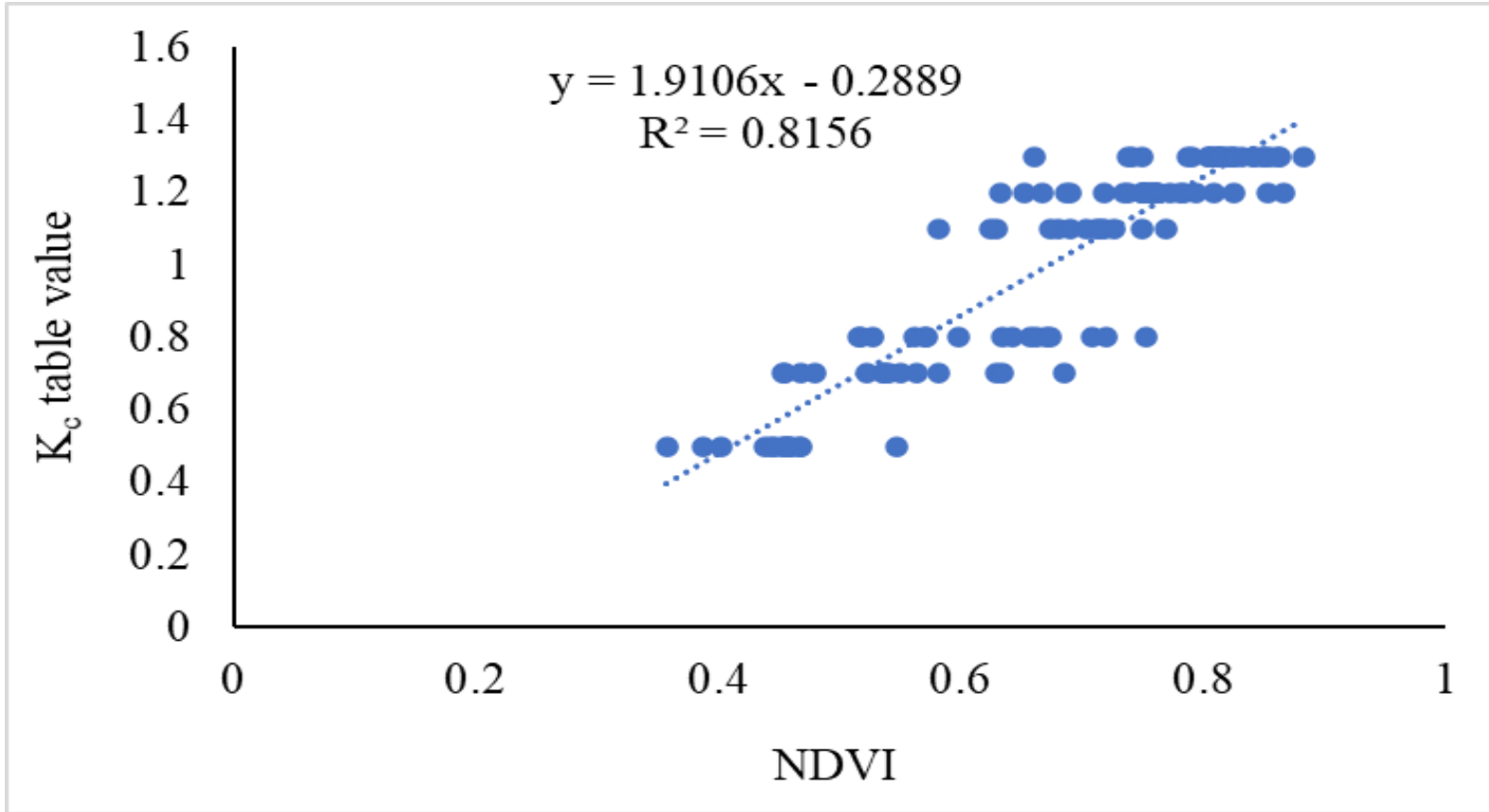


Fig. 4.5. NDVI - K_c relationship

Table 4.15. K_c (Table value) and K_c (Predicted) value for Alathur block

Alathur I		Alathur II		Kavasseri		Kizhakkenchery	
K_c (Table value)	K_c (Predicted)	K_c (Table value)	K_c (Predicted)	K_c (Table value)	K_c (Predicted)	K_c (Table value)	K_c (Predicted)
0.5	0.591	0.5	0.587	0.5	0.48	0.5	0.551
0.8	0.94	0.8	0.923	0.8	0.804	0.8	0.993
1.2	1.163	1.2	1.144	1.2	1.116	1.2	1.157
1.3	1.281	1.3	1.266	1.3	1.247	1.3	1.348
1.3	1.265	1.3	1.25	1.3	1.218	1.3	1.362
1.2	1.188	1.2	1.215	1.2	1.147	1.1	1.144
1.1	1.013	1.1	0.998	1.1	0.914	0.7	0.791
0.7	0.606	0.7	0.577	0.7	0.63		

K_c : Crop coefficient

Table 4.15. K_c (Table value) and K_c (Predicted) value for Alathur block (Contd.)

Pudukkode		Tarur		Vadakkenchery		Erimayur	
K_c (Table value)	K_c (Predicted)	K_c (Table value)	K_c (Predicted)	K_c (Table value)	K_c (Predicted)	K_c (Table value)	K_c (Predicted)
0.5	0.578	0.5	0.603	0.5	0.558	0.5	0.523
0.8	1.068	0.8	0.968	0.8	1.089	0.8	0.71
1.2	1.291	1.2	1.149	1.3	1.337	0.8	0.751
1.3	1.358	1.3	1.3	1.3	1.32	1.3	1.033
1.3	1.224	1.3	1.337	1.2	1.167	1.3	1.096
1.2	1.149	1.2	1.257	1.1	1.085	1.2	1.131
1.1	0.904	1.1	1.099	0.7	0.913	1.1	1.148
		0.7	0.765			0.7	0.775

K_c : Crop coefficient

Table 4.16. K_c (Table value) and K_c (Predicted) value for Nenmara block

Aliyur		Melarkode		Vandazy		Nenmara		Elevenchery		Pallassana	
K_c (Table value)	K_c (Predicted)	K_c (Table value)	K_c (Predicted)	K_c (Table value)	K_c (Predicted)	K_c (Table value)	K_c (Predicted)	K_c (Table value)	K_c (Predicted)	K_c (Table value)	K_c (Predicted)
0.5	0.581	0.5	0.452	0.5	0.607	0.5	0.395	0.5	0.758	0.5	0.568
0.8	0.701	0.8	0.696	0.8	0.977	0.8	0.721	0.8	1	0.8	0.649
0.8	0.786	1.2	1.031	1.2	1.123	1.2	0.922	1.2	0.987	0.8	0.878
1.3	1.128	1.3	1.277	1.3	1.269	1.3	1.144	1.3	0.974	1.3	1.166
1.3	1.251	1.3	1.255	1.2	1.23	1.3	1.121	1.2	1.024	1.3	1.265
1.2	1.367	1.2	1.211	1.1	1.077	1.2	0.959	1.1	1.03	1.2	1.373
1.1	1.182	1.1	1.072	0.7	0.71	1.1	0.822	0.7	1.023	1.1	1.132
0.7	0.923	0.7	0.823			0.7	0.58			0.7	0.893

K_c : Crop coefficient

Table 4.17. K_c (Table value) and K_c (Predicted) value for Kollengode block

Pattanchery		Muthalamada		Vadavannur		Koduvayur		Pudunagaram		Peruvemb	
K_c (Table value)	K_c (Predicted)	K_c (Table value)	K_c (Predicted)	K_c (Table value)	K_c (Predicted)	K_c (Table value)	K_c (Predicted)	K_c (Table value)	K_c (Predicted)	K_c (Table value)	K_c (Predicted)
0.5	0.584	0.8	0.801	0.5	0.565	0.5	0.65	0.5	0.621	0.5	0.64
0.8	1.151	1.2	1.168	0.8	0.853	0.8	0.952	0.8	1.074	0.8	1.047
1.2	1.342	1.3	1.262	1.2	1.156	0.8	1.002	1.2	1.218	1.2	1.146
1.3	1.398	1.3	1.288	1.3	1.263	1.3	1.204	1.3	1.285	1.3	1.224
1.3	1.321	1.2	1.145	1.3	1.288	1.3	1.26	1.3	1.263	1.3	1.225
1.2	1.085	0.7	0.739	1.2	1.204	1.2	1.225	1.2	1.156	1.2	1.152
0.7	0.737			1.1	1.056	1.1	1.195	1.1	0.923	1.1	1.02
				0.7	0.745	0.7	0.842	0.7	0.7	0.7	0.72

K_c : Crop coefficient

Table 4.18. K_c (Table value) and K_c (Predicted) value for Chittur block

Perumatty		Nallepilly		Polpully		Chittur-Thathamangalam	
K_c (Table value)	K_c (Predicted)	K_c (Table value)	K_c (Predicted)	K_c (Table value)	K_c (Predicted)	K_c (Table value)	K_c (Predicted)
0.5	0.649	0.5	0.63	0.5	0.619	0.5	0.651
0.8	0.982	0.8	1.02	0.8	0.749	0.8	0.853
0.8	1.056	1.2	1.172	0.8	1.011	1.2	1.037
1.3	1.145	1.3	1.207	1.3	1.16	1.3	1.15
1.3	1.151	1.3	1.21	1.3	1.309	1.3	1.123
1.2	1.157	1.2	1.213	1.2	1.203	1.2	1.089
1.1	1.104	1.1	1.157	1.1	1.134	0.7	0.955
0.7	0.926	0.7	1.02	0.7	0.974		

K_c : Crop coefficient

Table 4.19. K_c (Table value) and K_c (Predicted) value for Kuzhalmannam block

Thenkurissi		Kuthanoor		Kuzhalmannam		Peringottukurissi		Mathur		Kottayi	
K_c (Table value)	K_c (Predicted)	K_c (Table value)	K_c (Predicted)	K_c (Table value)	K_c (Predicted)	K_c (Table value)	K_c (Predicted)	K_c (Table value)	K_c (Predicted)	K_c (Table value)	K_c (Predicted)
0.5	0.635	0.8	0.927	0.8	0.777	0.5	0.564	0.5	0.599	0.5	0.654
0.8	0.996	0.8	1.11	1.2	1.045	0.8	0.848	0.8	0.941	0.8	0.821
1.2	1.154	1.2	1.177	1.3	1.186	0.8	1.015	1.2	1.085	0.8	0.979
1.3	1.187	1.3	1.222	1.3	1.261	1.3	1.179	1.3	1.215	1.3	1.219
1.3	1.163	1.3	1.272	1.2	1.167	1.3	1.236	1.3	1.285	1.3	1.321
1.2	1.139	1.2	1.187	1.2	0.947	1.2	1.223	1.2	1.234	1.2	1.257
1.1	1.165	0.7	0.907	0.7	0.854	1.1	1.252	1.1	1.092	1.1	1.157
0.7	0.946			0.7	0.689	0.7	0.935	0.7	1.021	0.7	1.044

K_c : Crop coefficient

4.4.2. Reference evapotranspiration (ET_o) during the crop period

Modified Penman, Hargreaves, Turc, Blaney-Criddle, Christiansen, Open pan and FAO Penman-Montieth methods were used in PET calculator software to estimate potential evapotranspiration based on the weather data of study area. Among the different methods FAO Penman-Montieth method was found to be more reliable because maximum number of weather variables were considered in this method to estimate ET_o. The weekly and monthly ET_o was estimated for Alathur, Chittur, Kollengode, Kuzhalmannam and Nenmara blocks in Palakkad district. ET_o calculated by Open pan method gave the lowest value as compared to other methods. The highest ET_o was obtained in Modified Penman method.

4.4.4.2.1. ET_o of Alathur block

Crop period considered for this study ranged from 42nd meteorological week of 2020 to 9th meteorological week of 2021. During this period weekly ET_o estimated through open pan method was in the range of 7.58-24.91 mm/week and Christiansen method was 8.87-33.43 mm/week (Table 4.20). Hargreaves and Turc methods gave similar values throughout the period. ET_o estimated by Blaney-Criddle method ranged from 19.07-46.53 mm/week. High value of ET_o in the range of 25.6-60.37 mm/week was obtained though Modified Penman method. FAO Penman-Montieth method is said to be more accurate in estimating ET_o and by this method ET_o estimated was in the range 22.17-52.65 mm/week during the crop period.

The crop was in the field during the months of October, November, December in the year 2020 and January and February 2021. During this period the ET_o estimated was lowest in Open pan method (54.36-86.3 mm/month) and highest in Modified Penman method (134.38-200.24 mm/month). ET_o estimated by FAO Penman-Montieth method ranged from 123.19-174.94 mm/ month (Table 4.21).

Table 4.20. Weekly ET_o of Alathur block during the crop period

Year	SMW	Modified Penman (mm)	Hargreaves (mm)	Turc (mm)	Blanley-Criddle (mm)	Christiansen (mm)	Open pan (mm)	FAO Penman-Montieth (mm)
2020	42	28.41	28.6	27.69	21.56	8.87	7.58	26.06
2020	43	30.71	29.74	29.02	25.82	14.2	12.02	27.78
2020	44	29.23	29.53	27.65	25.23	12.71	10.91	26.2
2020	45	36.64	28.81	29.33	30.84	16.89	13.45	31.6
2020	46	34.59	26.69	28.09	26.9	16.13	12.9	29.56
2020	47	33.58	24.53	29.6	30.71	17.43	14.66	28.35
2020	48	33.21	27.42	28.53	27.25	17.83	14.35	28.66
2020	49	25.6	29.76	21.23	19.48	10.52	8.96	22.17
2020	50	36.09	28.91	30.15	32.49	21.66	17.05	31.28
2020	51	45.04	31.14	28.6	34.12	20.2	13.82	38.86
2020	52	41.15	32	29.23	33.57	29.85	21.77	36.01
2021	1	39.27	25.31	26.28	27.56	17.8	12.97	32.32
2021	2	26.17	30.17	20.48	19.07	14.69	12.24	22.59
2021	3	39.18	28.11	28.03	29.12	23.56	17.87	33.05
2021	4	36.95	29.32	30.71	32.55	20.38	16.26	31.98
2021	5	50.12	33.45	31.7	38.09	30.57	22.71	42.79
2021	6	60.37	37.06	33.98	46.53	31.81	21.92	52.65
2021	7	47.62	33.65	35.08	43.85	33.43	24.91	41.61
2021	8	44.31	39.14	33.71	37.91	22.02	17.03	38.85
2021	9	47.77	34.66	33.37	41.98	26.55	20.7	41.64

SMW : Standard meteorological week

Table 4.21. Monthly ET_o of Alathur block during the crop period

Year	Month	Modified Penman (mm)	Hargreaves (mm)	Turc (mm)	Thornthwaite (mm)	Blanley-Criddle (mm)	Christiansen (mm)	Open pan (mm)	Penman Montieth (mm)
2020	October	134.38	128.31	129.54	194.73	101.45	64.95	54.36	123.88
2020	November	142.71	117.15	122.17	144.14	118.99	70.09	57.46	123.19
2020	December	164.18	134.42	122.03	174.68	132.39	86.52	66.04	142.47
2021	January	159.41	126.43	117.98	132.86	122.91	87.41	68.55	136.49
2021	February	200.24	144.42	134.95	196.19	164.01	118.03	86.3	174.94

Table 4.22. Monthly ET_o of Nenmara block during the crop period

Year	Month	Modified Penman (mm)	Hargreaves (mm)	Turc (mm)	Thornthwaite (mm)	Blanley-Criddle (mm)	Christiansen (mm)	Open pan (mm)	Penman Montieth (mm)
2020	October	134.29	130.94	129.51	193.6	101.3	64.92	54.36	123.85
2020	November	141.63	114.15	121.67	138.02	117.68	69.81	57.46	122.03
2020	December	163.48	135.25	121.82	170.66	131.63	86.31	66.04	141.99
2021	January	159.61	126	118.13	133.73	123.13	87.46	68.55	136.68
2021	February	199.79	145.46	134.85	193.95	163.57	117.87	86.3	174.83

4.4.2.2. ET_o of Nenmara block

The weekly ET_o calculated through Modified Penman method was in the range of 25.42-49.31 mm/ week in Nenmara block (Table 4.23). At the same time, Open pan method estimated 7.58-24.91 mm/ week. Weekly ET_o estimated in crop growing period by other methods like Hargreaves, Turc, Blaney-Criddle and Christiansen methods gave intermediate values. FAO Penman Montieth estimated weekly ET_o in the range of 22.04-51.94 mm/ week in Nenmara block.

The monthly ET_o estimated by FAO Penman-Montieth method ranged from 122.03-174.83 mm/ month. Among the different methods used to estimate ET_o, lowest value was estimated by Open pan method and highest value by Modified Penman method (Table 4.22).

4.4.2.3. ET_o of Kollengode block

The weekly ET_o of Kollengode block estimated through different methods are presented in Table 4.24. Open pan and Christiansen methods underestimated ET_o and was in the range of 7.58-24.91 mm/week and 8.88-33.45 mm/week. Modified Penman method estimated high values for ET_o. Among Hargreaves, Turc and Blaney-Criddle methods, Blaney-Criddle method gave slightly lower values for ET_o, but the other two methods estimated almost similar values. FAO Penman-Montieth method estimated PET in the range of 21.93–52.61 mm/week during the crop period.

The monthly ET_o (Table 4.25) showed similar trend as that of weekly ET_o. The monthly ET_o estimated by FAO Penman-Montieth method for October 2020 was 124.2 mm/month, November 2020 was 121.8 mm/ month, December 2020 was 141.21 mm/ month, January 2021 was 135.98 mm/ month and for February 2021 was 175.49 mm/ month.

Table 4.23. Weekly ET_o of Nenmara block during the crop period

Year	SMW	Modified Penman (mm)	Hargreaves (mm)	Turc (mm)	Blanley-Criddle (mm)	Christiansen (mm)	Open pan (mm)	Penman Montieth (mm)
2020	42	28.37	29.32	27.67	21.49	8.86	7.58	26.03
2020	43	30.34	28.83	28.86	25.39	14.13	12.02	27.41
2020	44	28.91	28.86	27.51	24.86	12.65	10.91	25.89
2020	45	36.97	29.07	29.48	31.21	16.97	13.45	31.94
2020	46	34.4	27.41	28.02	26.69	16.08	12.9	29.44
2020	47	33.36	22.4	29.48	30.4	17.37	14.66	28.03
2020	48	32.75	27.64	28.31	26.71	17.7	14.35	28.27
2020	49	25.42	30.25	21.15	19.26	10.48	8.96	22.04
2020	50	35.39	26.77	29.84	31.64	21.45	17.05	30.45
2020	51	45.08	32.59	28.64	34.18	20.22	13.82	39.18
2020	52	40.93	31.72	29.16	33.33	29.75	21.77	35.78
2021	1	40.16	26.23	26.64	28.47	18.07	12.97	33.34
2021	2	25.93	30.34	20.38	18.79	14.62	12.24	22.39
2021	3	39.05	27.88	27.99	28.99	23.51	17.87	32.91
2021	4	36.79	30.14	30.65	32.36	20.34	16.26	31.93
2021	5	49.31	31.94	31.39	37.22	30.25	22.71	41.75
2021	6	59.8	36.29	33.82	45.96	31.6	21.92	51.94
2021	7	47.57	34.87	35.07	43.8	33.41	24.91	41.75
2021	8	44.4	39.24	33.76	38.02	22.04	17.03	38.96
2021	9	47.52	34.65	33.27	41.68	26.47	20.7	41.44

SMW : Standard meteorological week

Table 4.24. Weekly ET_o of Kollengode block during the crop period

Year	SMW	Modified Penman (mm)	Hargreaves (mm)	Turc (mm)	Blanley-Criddle (mm)	Christiansen (mm)	Open pan (mm)	Penman Montieth (mm)
2020	42	28.46	29.59	27.72	21.6	8.88	7.58	26.13
2020	43	30.55	30.17	28.95	25.62	14.17	12.02	27.64
2020	44	28.97	28.92	27.54	24.93	12.66	10.91	25.95
2020	45	36.97	29.07	29.47	31.21	16.97	13.45	31.93
2020	46	34.39	27.06	28.01	26.68	16.08	12.9	29.41
2020	47	33.23	22.14	29.4	30.24	17.35	14.66	27.91
2020	48	32.62	27.39	28.24	26.57	17.67	14.35	28.13
2020	49	25.3	30.11	21.09	19.13	10.45	8.96	21.93
2020	50	35.17	26.46	29.73	31.38	21.39	17.05	30.22
2020	51	44.88	32.44	28.57	33.98	20.16	13.82	38.96
2020	52	40.83	31.64	29.12	33.23	29.72	21.77	35.67
2021	1	39.13	25.4	26.23	27.43	17.76	12.97	32.21
2021	2	26.06	30.35	20.44	18.95	14.66	12.24	22.51
2021	3	39	28.29	27.96	28.94	23.49	17.87	32.92
2021	4	36.7	29.14	30.6	32.25	20.31	16.26	31.75
2021	5	49.88	33.87	31.63	37.86	30.49	22.71	42.71
2021	6	60.16	37.4	33.93	46.34	31.74	21.92	52.61
2021	7	47.66	34.59	35.1	43.91	33.45	24.91	41.79
2021	8	44.35	39.98	33.74	37.97	22.03	17.03	39.01
2021	9	47.85	35.73	33.41	42.1	26.59	20.7	41.94

SMW : Standard meteorological week

Table 4.25. Monthly ET_o of Kollengode block during the crop period

Year	Month	Modified Penman (mm)	Hargreaves (mm)	Turc (mm)	Thornthwaite (mm)	Blanley-Criddle (mm)	Christiansen (mm)	Open pan (mm)	Penman Montieth (mm)
2020	October	134.59	132.98	129.64	196.41	101.62	64.98	54.36	124.2
2020	November	141.43	113.26	121.57	137.09	117.48	69.78	57.46	121.8
2020	December	162.71	134.63	121.5	166.97	130.81	86.1	66.04	141.21
2021	January	158.68	127.24	117.7	129.43	122.13	87.18	68.55	135.98
2021	February	200.18	147	134.98	196.78	164.03	118.02	86.3	175.49

4.4.2.4. ET_o of Chittur block

The weekly ET_o of Chittur block during the crop period as per Open pan method ranged from 7.58-22.71 mm/ week (Table 4.26). ET_o estimated by Hargreaves, Turc and Blaney-Criddle method were almost similar. Modified Penman method estimated ET_o in the range of 25.41-60.18 mm/ week. FAO Penman Montieth method was more accurate in estimating ET_o and the values were in the range of 22.06-42.79 mm/week.

The monthly ET_o estimated through different methods are presented in Table 4.28. Open pan and Christiansen method estimated very low value of ET_o, whereas, Modified Penman method overestimated ET_o, during the crop period. ET_o estimated by other three methods *ie*; Hargreaves, Turc and Blaney-Criddle methods were on par. ET_o estimated by FAO Penman Montieth method was used in this study and the in the range of 122.99-176.48 mm/month.

4.4.2.5. ET_o of Kuzhalmannam block

The weekly ET_o of Kuzhalmannam block (Table 4.27) was in the range of 7.58-24.91 mm/week as per Open pan method, while 25.35-60.08 mm/week according to Modified Penman method. All other methods estimated ET_o values in between the values estimated by Open Pan method and Modified penman method.

The monthly ET_o values estimated are presented in Table 4.29. Lowest value of ET_o was estimated by Open pan method and highest by Modified Penman method. FAO Penman-Montieth method gave the accurate ET_o in the range of 121.34-174.69 mm/ month during the crop period in Kuzhalmannam block.

Table 4.26. Weekly ET_o of Chittur block during the crop period

Year	SMW	Modified Penman (mm)	Hargreaves (mm)	Turc (mm)	Blanley-Criddle (mm)	Christiansen (mm)	Open pan (mm)	Penman Montieth (mm)
2020	42	28.45	29.2	27.7	21.59	8.88	7.58	26.11
2020	43	30.47	28.93	28.91	25.54	14.15	12.02	27.53
2020	44	29.09	29.02	27.59	25.08	12.69	10.91	26.07
2020	45	37.17	29.23	29.56	31.48	17.03	13.45	32.16
2020	46	34.67	27.62	28.14	27.02	16.16	12.9	29.73
2020	47	33.59	22.73	29.61	30.76	17.44	14.66	28.28
2020	48	32.87	28.02	28.36	26.88	17.75	14.35	28.43
2020	49	25.41	30.38	21.14	19.29	10.48	8.96	22.06
2020	50	35.34	27.04	29.81	31.62	21.45	17.05	30.45
2020	51	44.96	32.66	28.59	34.12	20.2	13.82	39.13
2020	52	40.86	31.67	29.13	33.32	29.76	21.77	35.75
2021	1	39.08	25.37	26.21	27.43	17.76	12.97	32.2
2021	2	26.04	30.32	20.42	18.94	14.66	12.24	22.5
2021	3	38.95	28.56	27.94	28.93	23.5	17.87	32.95
2021	4	36.66	29.42	30.58	32.25	20.31	16.26	31.77
2021	5	49.87	34.02	31.63	37.91	30.51	22.71	42.79
2021	6	60.18	37.74	33.95	46.46	31.79	21.92	52.82
2021	7	47.71	34.99	35.12	44.03	33.49	24.91	41.93
2021	8	44.4	40.35	33.76	38.07	22.06	17.03	39.14
2021	9	47.95	36.32	33.46	42.28	26.64	20.7	42.18

SMW : Standard meteorological week

Table 4.27. Weekly ET_o of Kuzhalmannam block during the crop period

Year	SMW	Modified Penman (mm)	Hargreaves (mm)	Turc (mm)	Blanley-Criddle (mm)	Christiansen (mm)	Open pan (mm)	Penman-Montieth (mm)
2020	42	28.3	29.07	27.63	21.45	8.86	7.58	25.96
2020	43	30.2	28.51	28.79	25.27	14.11	12.02	27.27
2020	44	28.81	28.39	27.45	24.77	12.64	10.91	25.79
2020	45	36.77	28.55	29.38	31.02	16.93	13.45	31.71
2020	46	34.24	26.77	27.93	26.54	16.05	12.9	29.25
2020	47	33.16	21.91	29.35	30.18	17.34	14.66	27.82
2020	48	32.58	27.35	28.21	26.56	17.67	14.35	28.09
2020	49	25.35	29.96	21.07	19.15	10.46	8.96	21.91
2020	50	35.21	26.48	29.74	31.47	21.41	17.05	30.26
2020	51	44.99	32.64	28.58	34.11	20.2	13.82	39.11
2020	52	40.79	31.59	29.09	33.22	29.72	21.77	35.63
2021	1	39.05	25.17	26.18	27.38	17.75	12.97	32.11
2021	2	25.95	30.06	20.38	18.84	14.63	12.24	22.39
2021	3	38.79	28.12	27.85	28.74	23.43	17.87	32.7
2021	4	36.62	29.22	30.55	32.19	20.3	16.26	31.69
2021	5	49.81	33.65	31.57	37.79	30.47	22.71	42.59
2021	6	60.08	37.17	33.88	46.27	31.72	21.92	52.46
2021	7	47.59	33.98	35.06	43.84	33.43	24.91	41.64
2021	8	44.23	39.55	33.68	37.85	22.01	17.03	38.85
2021	9	47.69	35.1	33.33	41.92	26.54	20.7	41.67

SMW : Standard meteorological week

Table 4.28. Monthly ET_o of Chittur block during the crop period

Year	Month	Modified Penman (mm)	Hargreaves (mm)	Turc (mm)	Thorntwaite (mm)	Blanley-Criddle (mm)	Christiansen (mm)	Open pan (mm)	Penman Montieth (mm)
2020	October	134.41	130.1	129.52	195.41	101.45	64.95	54.36	123.93
2020	November	142.45	116.25	122.05	143.24	118.78	70.05	57.46	122.99
2020	December	163.05	135.57	121.63	170.01	131.37	86.26	66.04	141.79
2021	January	158.49	127.13	117.63	129.37	122.1	87.18	68.55	135.93
2021	February	200.55	149.25	135.15	200.32	164.69	118.26	86.3	176.48

Table 4.29. Monthly ET_o of Kuzhalmannam block during the crop period

Year	Month	Modified Penman (mm)	Hargreaves (mm)	Turc (mm)	Thorntwaite (mm)	Blanley-Criddle (mm)	Christiansen (mm)	Open pan (mm)	Penman Montieth (mm)
2020	October	133.7	129.51	129.19	190.73	100.8	64.82	54.36	123.25
2020	November	140.97	112.85	121.28	135.32	117.05	69.7	57.46	121.34
2020	December	162.73	133.91	121.42	167.85	130.95	86.15	66.04	141.14
2021	January	158.18	126.76	117.41	127.73	121.68	87.07	68.55	135.47
2021	February	199.67	145.28	134.73	194.42	163.53	117.88	86.3	174.69

4.4.3. Effective rainfall

The monthly effective rainfall was calculated for five blocks of Palakkad district viz, Alathur, Chittur, Kollengode, Kuzhalmannam and Nenmara from October 2020 to February 2021. The rice crop duration is almost four months but the sowing date in some locations was in October and in some other locations was November. So, the effective rainfall was considered from October 2020 to February 2021. In Alathur block, rainfall was 100% effectively utilized and the cumulative monthly rainfall received during the crop period ranged from 1.1-117.5 mm (Table 4.30). The effective rainfall observed in Nenmara block ranged from 8-88 mm (Table 4.31). The effective cumulative rainfall of Kollengode block ranged from 0.6-124 mm (Table 4.32). In Chittur Block, effective rainfall was 0 mm in February 2021 (Table 4.33), but in other months cumulative rainfall of 15-96 mm was obtained. The rainfall reported was 0 mm in February 2021 in Kuzhalmannam block, but in the rest of the months effective cumulative rainfall of 29.7-123 mm was observed (Table 4.34).

Table 4.30. Effective rainfall in Alathur block during the crop period

Month	ET _o (mm)	Rainfall (mm)	Effective rainfall (%)	Effective rainfall (mm)
Oct-2020	123.88	117.5	100	117.5
Nov-2020	123.19	31.8	100	31.8
Dec-2020	142.47	7.7	100	7.7
Jan-2021	136.49	47.7	100	47.7
Feb-2021	174.94	1.1	100	1.1

Table 4.31. Effective rainfall in Nenmara block during the crop period

Month	ET _o (mm)	Rainfall (mm)	Effective rainfall (%)	Effective rainfall (mm)
Oct-2020	123.85	75	100	75
Nov-2020	122.03	88	100	88
Dec-2020	141.99	30	100	30
Jan-2021	136.68	28	100	28
Feb-2021	174.83	8	100	8

Table 4.32. Effective rainfall in Kollengode block during the crop period

Month	ET_o (mm)	Rainfall (mm)	Effective rainfall (%)	Effective rainfall (mm)
Oct-2020	124.2	163.2	76	124
Nov-2020	121.8	41	100	41
Dec-2020	141.21	26	100	26
Jan-2021	135.98	11.4	100	11.4
Feb-2021	175.49	0.6	100	0.6

Table 4.33. Effective rainfall in Chittur block during the crop period

Month	ET_o (mm)	Rainfall (mm)	Effective rainfall (%)	Effective rainfall (mm)
Oct-2020	123.93	95.7	100	96
Nov-2020	122.99	29	100	29
Dec-2020	141.79	37	100	37
Jan-2021	135.93	15	100	15
Feb-2021	176.48	0	0	0

Table 4.34. Effective rainfall in Kuzhalmannam block during the crop period

Month	ET_o (mm)	Rainfall (mm)	Effective rainfall (%)	Effective rainfall (mm)
Oct-2020	123.25	122.5	100	123
Nov-2020	121.34	71.1	100	71.1
Dec-2020	141.14	29.7	100	29.7
Jan-2021	135.47	54.4	100	54.4
Feb-2021	174.69	0	0	0

4.4.4. Irrigation requirement during the crop growth period

The total irrigation requirement and water needed to be supplied in each crop growth stage for selected training sites were estimated based on crop evapotranspiration, effective rainfall received and additional volume of water to be supplied to maintain standing water in the rice field. Water lost through crop evapotranspiration is compensated by effective rainfall and water supplied through irrigation. As per Package of practice recommendations, (KAU, 2016) water level of 1.5 cm should be maintained in rice fields during the time of transplanting. Further, it should be gradually increased to 5 cm as the crop reaches active tillering stage. A

water level of 5 cm should be maintained in the fields during the crop period. Complete drainage of the field could be done 13 days before harvest. Irrigation could be provided 2 days after the disappearance of ponded water. The time taken for disappearance of ponded water was observed to be around one week in rice field located in slightly slopy land whereas, water disappears after 15 days in plain topography. This interval of successive irrigation to maintain standing water in the field was fixed based on farmer practices followed in the study area.

4.4.4.1. Irrigation requirement in Alathur block

In Alathur block, 8 training sites were selected for the study. The four crop stages considered are early vegetative/seedling stage with a duration of nearly 21 days, late vegetative stage with 40 days duration, reproductive stage with 30-35 days duration and maturity stage with 30 days duration. In the first training site, Alathur I, the irrigation requirement during early vegetative stage was estimated to be 92.53 mm, in late vegetative stage 266.43 mm, in reproductive stage 219.72 mm and in ripening stage 190.44 mm. Hence, the total irrigation requirement during the crop period was 769.11 mm. Similarly, in other training sites the total irrigation estimated was 912.39 mm in Alathur II, 885.64 mm in Kavasseri, 761.56 mm in Kizhakkenchery, 782.9 mm in Pudukkode, 802.96 mm in Tarur, 775.96 mm in Vadakkenchery, 864.94 mm in Erimayur (Table 4.35).

4.4.4.2. Irrigation requirement in Nenmara block

In Nenmara block, 6 training sites were considered for the study. The total irrigation requirement during the crop period in different locations were estimated as 703.07 mm in Aliyur, 694.11 mm in Melarkode, 674.34 mm in Vandazy, 647.59 mm in Nenmara, 723.2 mm in Elevenchery and 702.68 mm in Pallassana (Table 4.36).

4.4.4.3. Irrigation requirement in Kollengode block

In Kollengode block, there are 6 training sites. In the first training site Pattanchery, the irrigation requirement during early vegetative stage was 94.71 mm, 267.47 mm in late vegetative stage, 252.22 mm in reproductive stage and 178.66 mm in ripening stage. The total irrigation requirement during the crop period was 793.07

mm. Similarly, in other training sites the total irrigation estimated was 915.37 mm in Muthalamada, 611.18 mm in Vadavannur, 802.05 mm in Koduvayur, 937.80 mm in Pudunagaram, 935.44 mm Peruvemb (Table 4.37).

4.4.4.4. Irrigation requirement in Chittur block

The Chittur block consists of 4 training sites. In the first training site *ie*; Perumatty the irrigation requirement during early vegetative stage was 101.28 mm, in late vegetative stage 319.10 mm, in reproductive stage 291.86 mm and in ripening stage 229.08 mm. Hence, the total irrigation requirement during the crop period was 941.32 mm. Similarly, in other training sites the total irrigation estimated was 975.90 mm in Nallepilly, 943.82 mm in Polpully, 767.64 mm in Chittur-Thathamangalam (Table 4.38).

4.4.4.5. Irrigation requirement in Kuzhalmannam block

Kuzhalmannam block contains 6 training sites. The total water requirement in Thenkurissi was 700 mm, Kuthanoor was 743 mm, Kuzhalmannam was 667 mm, Peringottukurissi was 723 mm, Kottayi was 886 mm and Mathur was 885.75 mm (Table 4.39).

Table 4.35. Irrigation requirement in Alathur block

Location	Sowing date	Crop stage	Duration (Days)	K _c	ET _c	Effective rainfall (mm)	Water required to compensate crop evapotranspiration (mm)	Water required to maintain standing water in fields during each crop stage (mm)	Irrigation requirement during the crop period (mm)
Alathur I	16-11-2020	Early vegetative/ seedling stage	21	0.77	94.33	31.8	62.53	30	92.53
		Late vegetative stage	40	1.22	174.13	7.7	166.43	100	266.43
		Reproductive stage	30-35	1.23	167.42	47.7	119.72	100	219.72
		Ripening stage	30	0.81	141.54	1.1	140.44	50	190.44
		Total			577.41	88.3	489.11	280	769.11
Alathur II	18-11-2020	Early vegetative/ seedling stage	21	0.76	93.02	31.8	61.22	30	91.22
		Late vegetative stage	40	1.21	171.69	7.7	163.99	200	363.99
		Reproductive stage	30-35	1.23	168.22	47.7	120.52	150	270.52
		Ripening stage	30	0.79	137.76	1.1	136.66	50	186.66
		Total			570.69	88.3	482.39	430	912.39

K_c = Crop coefficient

ET_c = Crop evapotranspiration

Table 4.35. Irrigation requirement in Alathur block (Contd.)

Kavasseri	25-10-2020	Early vegetative/ seedling stage	21	0.64	79.09	31.8	47.29	30	77.29
		Late vegetative stage	40	1.18	168.36	7.7	160.66	200	360.66
		Reproductive stage	30-35	1.18	161.39	47.7	113.69	150	263.69
		Ripening stage	30	0.77	135.09	1.1	133.99	50	183.99
		Total			543.94	88.3	455.64	430	885.64
Kizhakkenchery	21-10-2020	Early vegetative/ seedling stage	21	0.77	95.64	118	0.00	30	30.00
		Late vegetative stage	40	1.25	154.24	31.8	122.44	200	322.44
		Reproductive stage	30-35	1.25	178.46	7.7	170.76	150	320.76
		Ripening stage	30	0.79	107.92	47.7	60.22	50	110.22
		Total			536.26	204.7	331.56	430	761.56
Pudukkode	19-09-2020	Early vegetative/ seedling stage	21	0.82	101.95	118	0.00	30	30.00
		Late vegetative stage	40	1.32	163.18	31.8	131.38	200	331.38
		Reproductive stage	30-35	1.19	169.03	7.7	161.33	150	311.33
		Ripening stage	30	0.90	123.43	47.7	75.73	50	125.73
		Total			557.60	204.7	352.90	430	782.90

Table 4.35. Irrigation requirement in Alathur block (Contd.)

Tarur	25-10-2020	Early vegetative/ seedling stage	21	0.79	96.81	31.8	65.01	30	95.01
		Late vegetative stage	40	1.22	174.46	7.7	166.76	100	266.76
		Reproductive stage	30-35	1.30	177.00	47.7	129.30	100	229.30
		Ripening stage	30	0.93	163.00	1.1	161.90	50	211.90
		Total			611.26	88.3	522.96	280	802.96
Vadakkenchery	01-10-2020	Early vegetative/ seedling stage	21	0.82	102.00	118	0.00	30	30.00
		Late vegetative stage	40	1.33	163.66	31.8	131.86	200	331.86
		Reproductive stage	30-35	1.13	160.40	7.7	152.70	150	302.70
		Ripening stage	30	0.91	124.60	47.7	76.90	50	126.90
		Total			550.66	204.7	345.96	430	775.96
Erimayur	29-10-2020	Early vegetative/ seedling stage	21	0.62	75.97	31.8	44.17	30	74.17
		Late vegetative stage	40	0.89	127.12	7.7	119.42	200	319.42
		Reproductive stage	30-35	1.11	151.94	47.7	104.24	150	254.24
		Ripening stage	30	0.96	168.21	1.1	167.11	50	217.11
		Total			523.24	88.3	434.94	430	864.94

Table 4.36. Irrigation requirement in Nenmara block

Location	Sowing date	Crop stage	Duration (Days)	K _c	ET _c	Effective rainfall (mm)	Water required to compensate crop evapotranspiration (mm)	Water required to maintain standing water in fields during each crop stage (mm)	Irrigation requirement during the crop period (mm)
Aliyur	02-11-2020	Early vegetative/ seedling stage	21	0.64	78.20	88	0.00	30	30.00
		Late vegetative stage	40	0.96	135.88	30	105.88	100	205.88
		Reproductive stage	30-35	1.31	178.95	28	150.95	100	250.95
		Ripening stage	30	1.05	184.05	8	176.05	50	226.05
		Total			577.07	154	423.07	280	703.07
Melarkode	08-11-2020	Early vegetative/ seedling stage	21	0.57	70.04	88	0.00	30	30.00
		Late vegetative stage	40	1.15	163.88	30	133.88	100	233.88
		Reproductive stage	30-35	1.23	168.51	28	140.51	100	240.51
		Ripening stage	30	0.95	165.67	8	157.67	50	207.67
		Total			568.11	154	414.11	280	694.11

K_c = Crop coefficient

ET_c = Crop evapotranspiration

Table 4.36. Irrigation requirement in Nenmara block (Contd.)

Vandazy	17-10-2020	Early vegetative/ seedling stage	21	0.79	96.66	88	8.66	30	38.66
		Late vegetative stage	40	1.20	169.81	30	139.81	100	239.81
		Reproductive stage	30-35	1.15	157.68	28	129.68	100	229.68
		Ripening stage	30	0.71	124.20	8	116.20	50	166.20
		Total			548.34	154.00	394.34	280	674.34
Nenmara	12-10-2020	Early vegetative/ seedling stage	21	0.56	69.06	75	0.00	30	30.00
		Late vegetative stage	40	1.03	126.01	88	38.01	200	238.01
		Reproductive stage	30-35	1.04	147.68	30	117.68	150	267.68
		Ripening stage	30	0.70	95.84	28	67.84	50	117.84
		Total			438.59	221	217.59	430	647.59
Elevenchery	02-10-2020	Early vegetative/ seedling stage	21	0.88	108.90	75	33.90	30	63.90
		Late vegetative stage	40	0.98	119.70	88	31.70	200	231.70
		Reproductive stage	30-35	1.03	145.85	30	115.85	150	265.85
		Ripening stage	30	1.02	139.76	28	111.76	50	161.76
		Total			514.20	221	293.20	430	723.20
Pallassana	01-11-2020	Early vegetative/ seedling stage	21	0.61	74.23	88	0.00	30	30.00
		Late vegetative stage	40	1.02	145.10	30	115.10	100	215.10
		Reproductive stage	30-35	1.32	180.28	28	152.28	100	252.28
		Ripening stage	30	1.01	177.07	8	169.07	50	219.07
		Total			576.68	154	422.68	280	702.68

Table 4.37. Irrigation requirement in Kollengode block

Location	Sowing date	Crop stage	Duration (Days)	K_c	ET_c	Effective rainfall (mm)	Water required to compensate crop evapotranspiration (mm)	Water required to maintain standing water in fields during each crop stage (mm)	Irrigation requirement during the crop period (mm)
Pattanchery	07-11-2020	Early vegetative/ seedling stage	21	0.87	105.71	41	64.71	30	94.71
		Late vegetative stage	40	1.37	193.47	26	167.47	100	267.47
		Reproductive stage	30-35	1.20	163.62	11.4	152.22	100	252.22
		Ripening stage	30	0.74	129.26	0.6	128.66	50	178.66
		Total			592.07	79	513.07	280	793.07
Muthalamada	22-10-2020	Early vegetative/ seedling stage	21	0.80	97.58	41	56.58	30	86.58
		Late vegetative stage	40	1.22	171.59	26	145.59	200	345.59
		Reproductive stage	30-35	1.22	165.47	11.4	154.07	150	304.07
		Ripening stage	30	0.74	129.73	0.6	129.13	50	179.13
		Total			564.37	79	485.37	430	915.37

K_c = Crop coefficient

ET_c = Crop evapotranspiration

Table 4.37. Irrigation requirement in Kollengode block (Contd.)

Vadavannur	10-10-2020	Early vegetative/ seedling stage	21	0.71	88.05	124	0.00	30	30.00
		Late vegetative stage	40	1.21	147.31	41	106.31	100	206.31
		Reproductive stage	30-35	1.25	175.93	26	149.93	100	249.93
		Ripening stage	30	0.90	122.49	11.4	111.09	50	161.09
		Total			533.78	203	331.18	280	611.18
Koduvayur	15-10-2020	Early vegetative/ seedling stage	21	0.80	97.53	41	56.53	30	86.53
		Late vegetative stage	40	1.10	155.78	26	129.78	100	229.78
		Reproductive stage	30-35	1.24	168.99	11.4	157.59	100	257.59
		Ripening stage	30	1.02	178.75	0.6	178.15	50	228.15
		Total			601.05	79	522.05	280	802.05
Pudunagaram	30-10-2020	Early vegetative/ seedling stage	21	0.85	103.19	41	62.19	30	92.19
		Late vegetative stage	40	1.25	176.76	26	150.76	200	350.76
		Reproductive stage	30-35	1.21	164.42	11.4	153.02	150	303.02
		Ripening stage	30	0.81	142.44	0.6	141.84	50	191.84
		Total			586.80	79	507.80	430	937.80
Peruvemb	12-11-2020	Early vegetative/ seedling stage	21	0.84	102.76	41	61.76	30	91.76
		Late vegetative stage	40	1.19	167.36	26	141.36	200	341.36
		Reproductive stage	30-35	1.19	161.65	11.4	150.25	150	300.25
		Ripening stage	30	0.87	152.68	0.6	152.08	50	202.08
		Total			584.44	79.00	505.44	430	935.44

Table 4.38. Irrigation requirement in Chittur block

Location	Sowing date	Crop stage	Duration (Days)	K _c	ET _c	Effective rainfall (mm)	Water required to compensate crop evapotranspiration (mm)	Water required to maintain standing water in fields during each crop stage (mm)	Irrigation requirement during the crop period (mm)
Perumatty	02-11-2020	Early vegetative/ seedling stage	21	0.82	100.28	29	71.28	30	101.28
		Late vegetative stage	40	1.10	156.10	37	119.10	200	319.10
		Reproductive stage	30-35	1.15	156.86	15	141.86	150	291.86
		Ripening stage	30	1.01	179.08	0	179.08	50	229.08
		Total			592.32	81.00	511.32	430	941.32
Nallepilly	25-10-2020	Early vegetative/ seedling stage	21	0.82	101.45	29	72.45	30	102.45
		Late vegetative stage	40	1.19	168.68	37	131.68	200	331.68
		Reproductive stage	30-35	1.21	164.64	15	149.64	150	299.64
		Ripening stage	30	1.09	192.13	0	192.13	50	242.13
		Total			626.90	81.00	545.90	430	975.90

K_c = Crop coefficient

ET_c = Crop evapotranspiration

Table 4.38. Irrigation requirement in Chittur block (contd.)

Polpully	29-10-2020	Early vegetative/ seedling stage	21	0.68	84.16	29	55.16	30	85.16
		Late vegetative stage	40	1.09	153.94	37	116.94	200	316.94
		Reproductive stage	30- 35	1.26	170.69	15	155.69	150	305.69
		Ripening stage	30	1.05	186.03	0	186.03	50	236.03
		Total			594.82	81	513.82	430	943.82
Chittur-Thathamangalam	06-10-2020	Early vegetative/ seedling stage	21	0.75	93.2	96	0	30	30
		Late vegetative stage	40	1.09	134.52	29	105.52	200	305.52
		Reproductive stage	30- 35	1.11	156.81	37	119.81	150	269.81
		Ripening stage	30	0.95	129.8	15	114.8	50	164.8
		Total			514.34	176.7	337.64	430	767.64

Table 4.39. Irrigation requirement in Kuzhalmannam block

Location	Sowing date	Crop stage	Duration (Days)	K _c	ET _c	Effective rainfall (mm)	Water required to compensate crop evapotranspiration (mm)	Water required to maintain standing water in fields during each crop stage (mm)	Irrigation requirement during the crop period (mm)
Thenkurissi	10-10-2020	Early vegetative/ seedling stage	21	0.82	100.52	123	0.00	30	30
		Late vegetative stage	40	1.17	142.04	71.1	70.94	200	271
		Reproductive stage	30-35	1.15	162.42	29.7	132.72	150	283
		Ripening stage	30	1.06	142.97	54.4	88.57	50	139
		Total			547.95	277.7	270.25	430	700
Kuthanoor	22-10-2020	Early vegetative/ seedling stage	21	1.02	123.59	71.1	52.49	30	82
		Late vegetative stage	40	1.20	169.32	29.7	139.62	100	240
		Reproductive stage	30-35	1.23	166.54	54.4	112.14	100	212
		Ripening stage	30	0.91	158.47	0	158.47	50	208
		Total			617.93	155.2	462.73	280	743

K_c = Crop coefficient

ET_c = Crop evapotranspiration

Table 4.39. Irrigation requirement in Kuzhalmannam block (Contd.)

Kuzhalmannam	02-10-2020	Early vegetative/ seedling stage	21	0.91	112.28	123	0.00	30	30
		Late vegetative stage	40	1.22	148.49	71.1	77.39	200	277
		Reproductive stage	30-35	1.06	149.21	29.7	119.51	150	270
		Ripening stage	30	0.77	104.52	54.4	50.12	50	100
		Total			514.49	277.70	236.79	430	667
Peringottukurissi	16-10-2020	Early vegetative/ seedling stage	21	0.71	85.67	71.1	14.57	30	45
		Late vegetative stage	40	1.10	154.81	29.7	125.11	100	225
		Reproductive stage	30-35	1.23	166.57	54.4	112.17	100	212
		Ripening stage	30	1.09	191.00	0	191.00	50	241
		Total			598.05	155.2	442.85	280	723
Kottayi	01-11-2020	Early vegetative/ seedling stage	21	0.74	89.47	71.1	18.37	30	48
		Late vegetative stage	40	1.10	155.08	29.7	125.38	200	325
		Reproductive stage	30-35	1.29	174.58	54.4	120.18	150	270
		Ripening stage	30	1.10	192.22	0	192.22	50	242
		Total			611.35	155.2	456.15	430	886
Mathur	27-10-2020	Early vegetative/ seedling stage	21	0.77	93.41	71.1	22.31	30	52.31
		Late vegetative stage	40	1.15	162.30	29.7	132.60	200	332.60
		Reproductive stage	30-35	1.26	170.65	54.4	116.25	150	266.25
		Ripening stage	30	1.06	184.58	0	184.58	50	234.58
		Total			610.95	155.2	455.75	430	885.75

4.4.5. Crop coefficient (K_c) maps and crop water demand maps

The crop coefficient (K_c) value for each pixel in the study area was calculated from NDVI value using the linear equation representing the relationship between NDVI and K_c values using the provisions in ArcGIS software and this was developed to K_c maps. The K_c map corresponding to early vegetative stage of the crop is presented in Fig 4.6 and 4.7. The K_c map of late vegetative stage is represented by Fig 4.8 and 4.9. The K_c map depicting reproductive stage of the crop is shown in Fig. 4.10 and 4.11. The K_c map towards the maturity stage of the crop is presented in Fig. 4.12 and 4.13. Similarly, crop water demand maps were generated for early vegetative stage, late vegetative stage, reproductive stage and maturity stage are shown in Fig. 4.14, 4.15, 4.16 and 4.17 respectively. These crop demand maps will be helpful in estimating irrigation requirement of any rice field in the study area where the coordinates are known.

Under warming climate projections, irrigation frequency may increase leading to increased irrigation water demands. Water resources planning and management in agriculture need spatially-explicit irrigated area information for different crops and different crop growing seasons. The delineated rice area will give a vivid picture of spatial coverage of irrigation requirement and the water demand maps provide the stage wise requirement of irrigation water. However, seasonal, high-resolution rice area and irrigation requirement maps for 5 blocks in Palakkad are developed and it can be used for water resources planning and management. This is also helpful to understand inter seasonal variability in irrigated area and water requirement at various spatial and temporal scales.

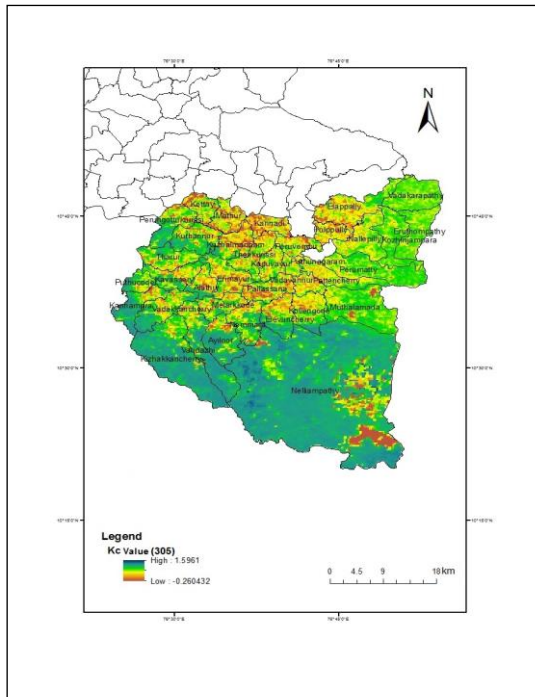


Fig. 4.6. K_c map of 305th Julian day 2020 representing the early vegetative stage of the crop

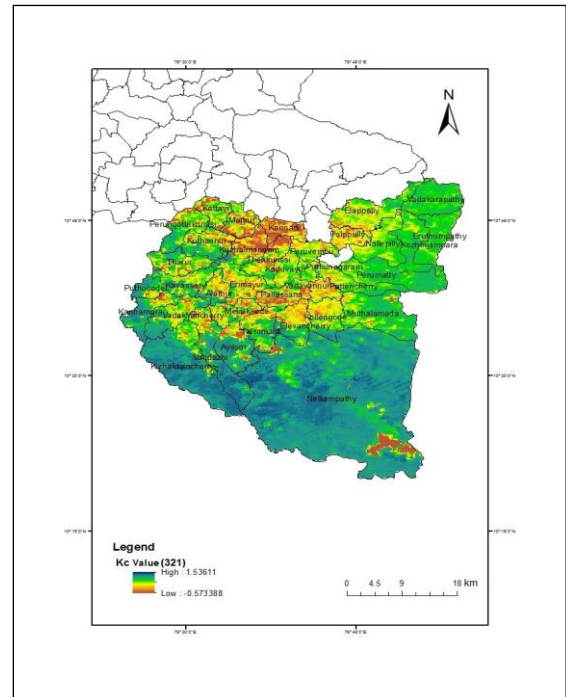


Fig. 4.7. K_c map of 321st Julian day 2020 representing the early vegetative stage of the crop

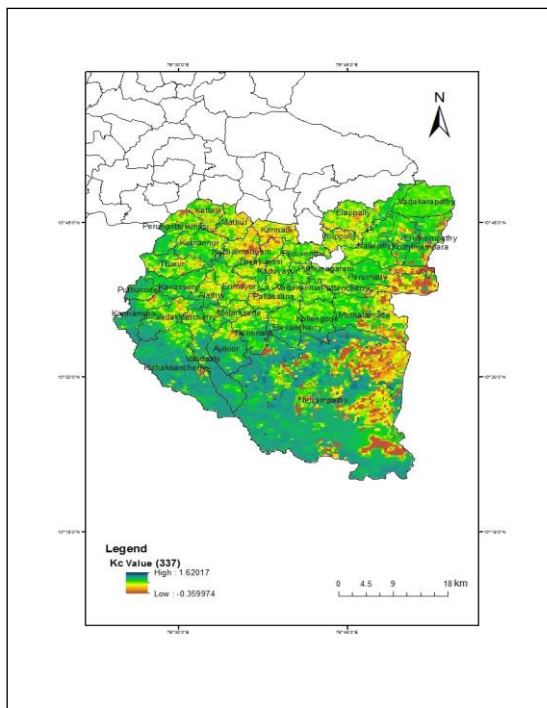


Fig. 4.8. K_c map of 337th Julian day 2020 representing the late vegetative stage of the crop

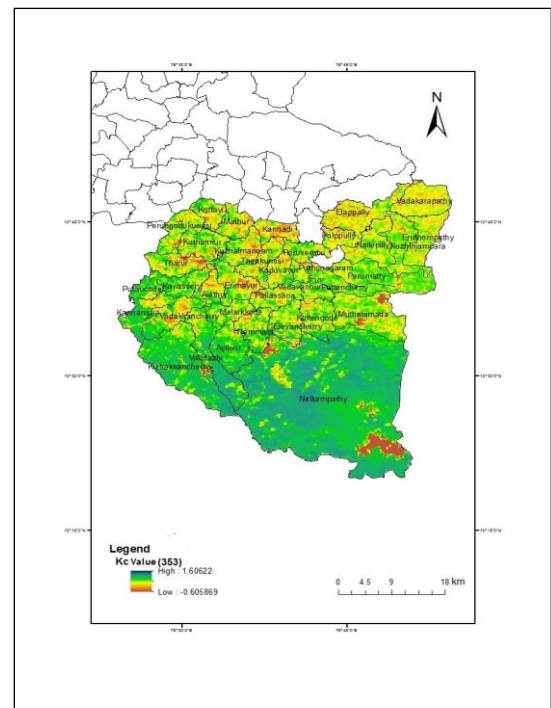


Fig. 4.9. K_c map of 363rd Julian day 2020 representing the late vegetative stage of the crop

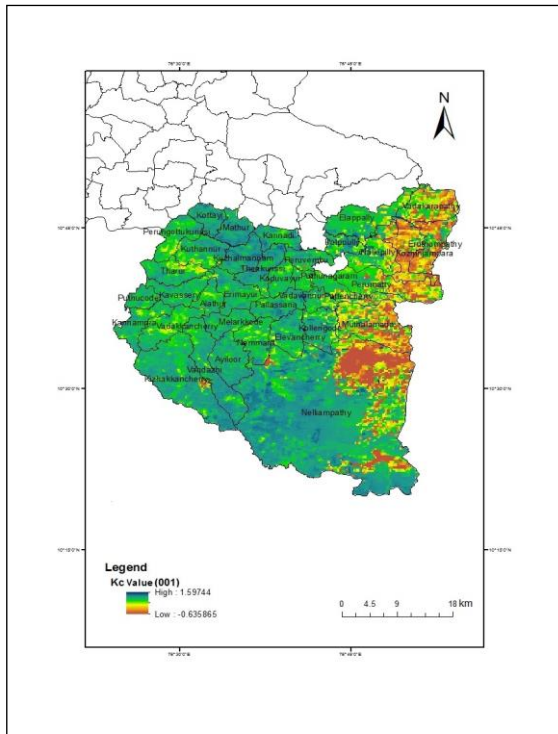


Fig. 4.10. K_c map of 1st Julian day 2021 representing the reproductive stage of the crop

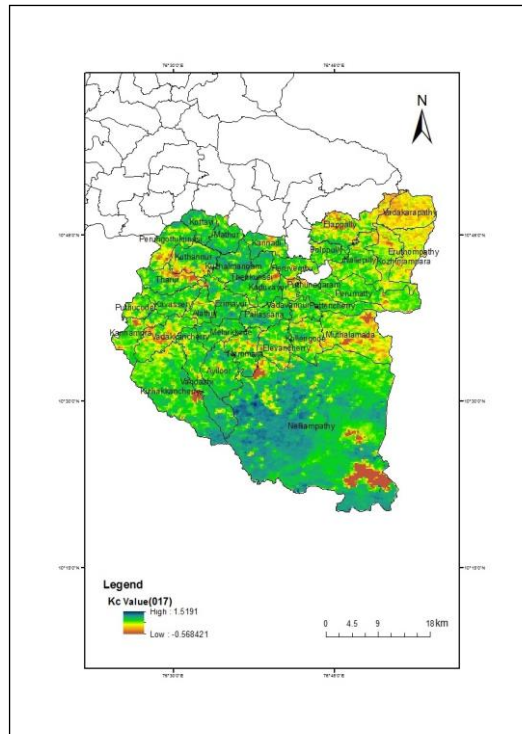


Fig. 4.11. K_c map of 17th Julian day 2021 representing the reproductive stage of the crop

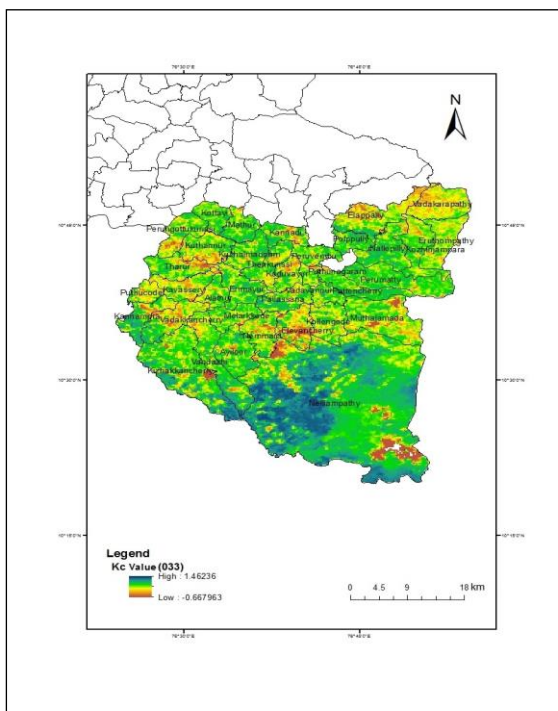


Fig. 4.12. K_c map of 33rd Julian day 2021 representing the maturity stage of the crop

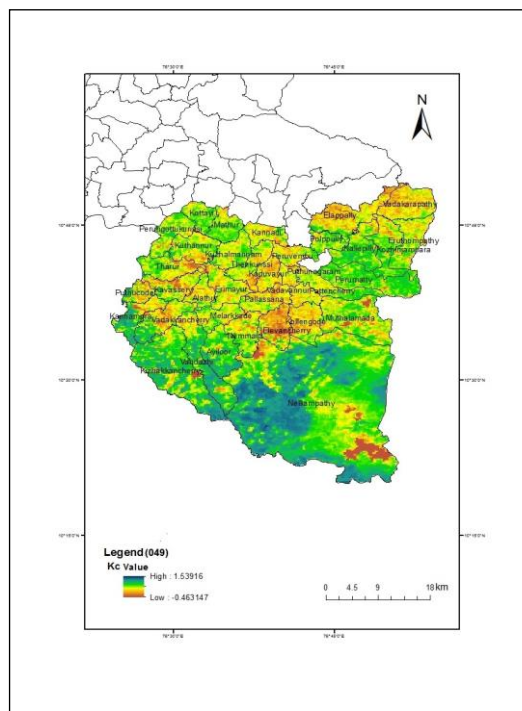


Fig. 4.13. K_c map of 49th Julian day 2021 representing the maturity stage of the crop

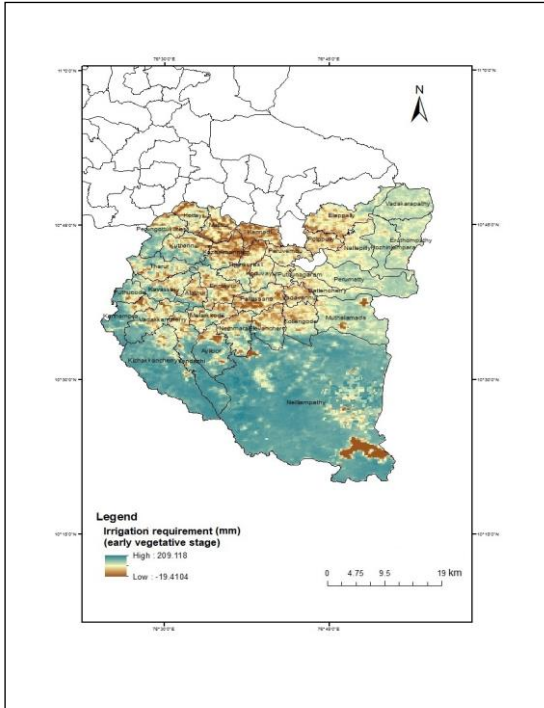


Fig. 4.14. Crop water demand map for early vegetative stage of the crop

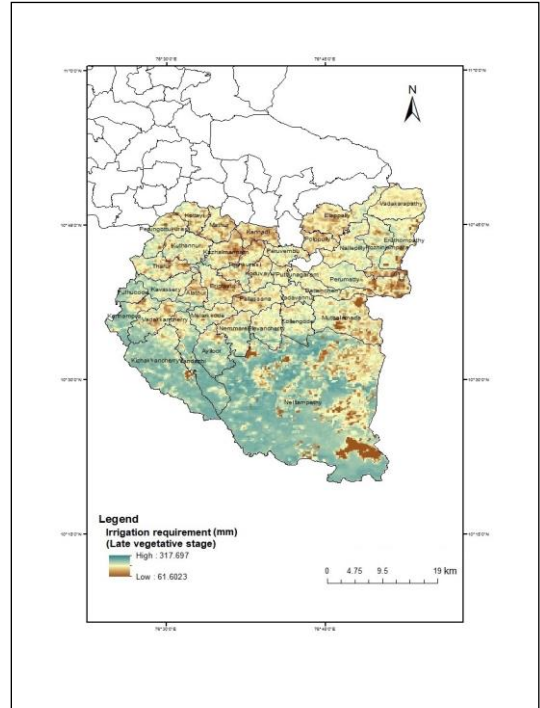


Fig. 4.15. Crop water demand map for late vegetative stage of the crop

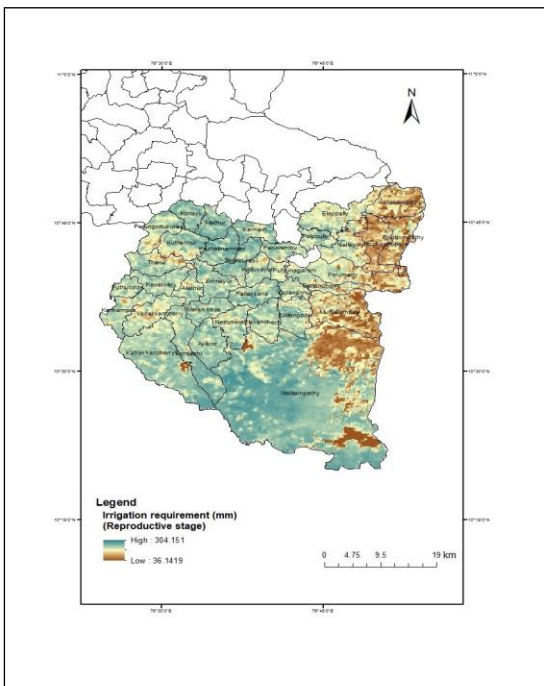


Fig. 4.16. Crop water demand map for reproductive stage of the crop

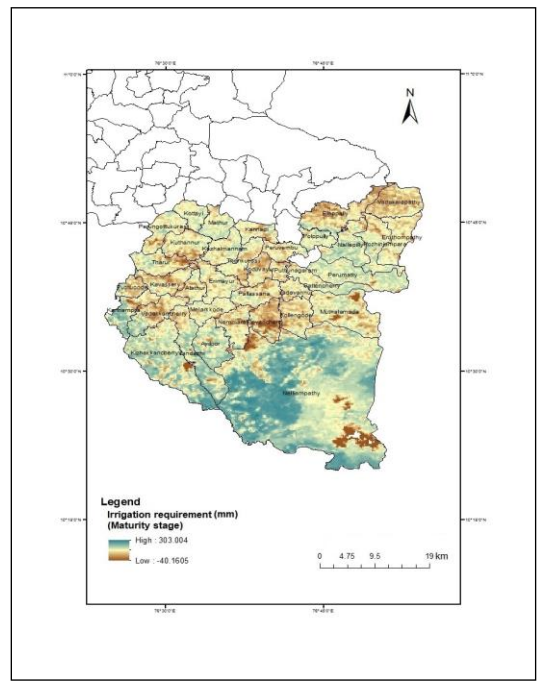


Fig. 4.17. Crop water demand map for maturity stage of the crop

Discussion

5. DISCUSSION

The crop water requirement of rice in Palakkad district during 2020-21 *mundakan* season was estimated based on remote sensing and GIS. The results of the study are discussed in this chapter.

5.1. Rice area delineation

The fact that each crop has a distinct spectral signature allows for crop identification and classification using optical remote sensing data. The typical spectral reflectance of a crop depends upon absorption of visible light (0.62- 0.68 m) due to the presence of various pigments. Because of the interior cellular structure of the leaves and the vigour of the crop, high reflectance is seen in the near infrared region (0.7 to 1 m), which is manifested by the ratio of red absorption and near infrared reflectance (Dadhwal and Ray, 2000). Digital iso-cluster unsupervised classification was used to identify and delineate existing rice areas, other agriculture forms, and other land cover using FCC of the Bands 2, 3, 4 and 8 of Sentinel-2 during the *mundakan* season. Sethi *et al.* (2014) estimated the rice area in the state of Haryana using Landsat ETM+ satellite images employing iso-cluster unsupervised classification. She opined that spatial variability of crop coverage and delineation of cropped area not only assist in yield estimation but also provides information of crop water demand at regional scales. Rice acreage estimation using optical satellite images often encounters challenges, owing to cloud interception. Hence, crop acreage estimation would be difficult during *viruppu* rice season as compared to *mundakan* and *punja* seasons in Kerala due to cloud interference. Though disturbances due to cloud interference were faced during the study period due to northeast monsoon it was overcome by using multitemporal cloud free satellite images of Sentinel -2 with 10 m resolution. The predicted area is approximately 2-8 percent less compared to previous years. However, such analysis with ground truthing information would be less cumbersome and accomplished with minimal cost and time. The protocol developed in this study pertaining to analysis of remote sensing image to delineate the rice area can be replicated to other regions. The rice area map developed may be useful to the planners and extension personals to get an idea about the irrigation water demand during the season. The classification clearly distinguishes

between areas with high and low levels of rice coverage. Similar results were observed in a study done by Ajith *et al.* (2017) in Thanjavur district of Tamil Nadu.

5.2. Normalized Difference Vegetation Index (NDVI), rice crop growth and yield

NDVI is an important parameter indicating the vegetation cover and vegetation growth conditions with obvious seasonal variations (Zhao *et al.*, 2004). A definite pattern was observed with regard to NDVI value and age of the rice plant, NDVI increases with the age of the plant, attains a peak value and then declines. The NDVI values varied between 0.40-0.80 during the crop period, the peak value was observed 50-70 days after sowing. A similar pattern of NDVI behaviour is observed in a study done in Thanjavur district of Tamil Nadu during *Samba* rice season by Ajith *et al.*, (2017). The NDVI values for rice in Thanjavur ranged from 0.45-0.81 with peak value during the third month. Niel and McVicar (2001) reported that high NDVI value is obtained when the plant reflects higher amount of Near Infrared Radiation (NIR) which is an indicator of greenness of plants. More greenness of a plant indicates high chlorophyll content which in turn results in higher yield (Ajith *et al.*, 2017). Nuarsa and Nishio (2007) reported that NDVI during maximum vegetative stage the highest exponential relationship with rice yield and suggested the potential of estimating yield using MODIS-NDVI. In this study, a positive correlation (correlation coefficient-0.88) was obtained when maximum NDVI of rice was compared with blockwise average yield during *mundakan* season 2020-21 (Fig. 5.1). The rice yield was found to increase when the maximum NDVI value increased, similarly, a reduction in yield was observed when maximum NDVI values was low. Hence, maximum NDVI showed a positive correlation with rice yield.

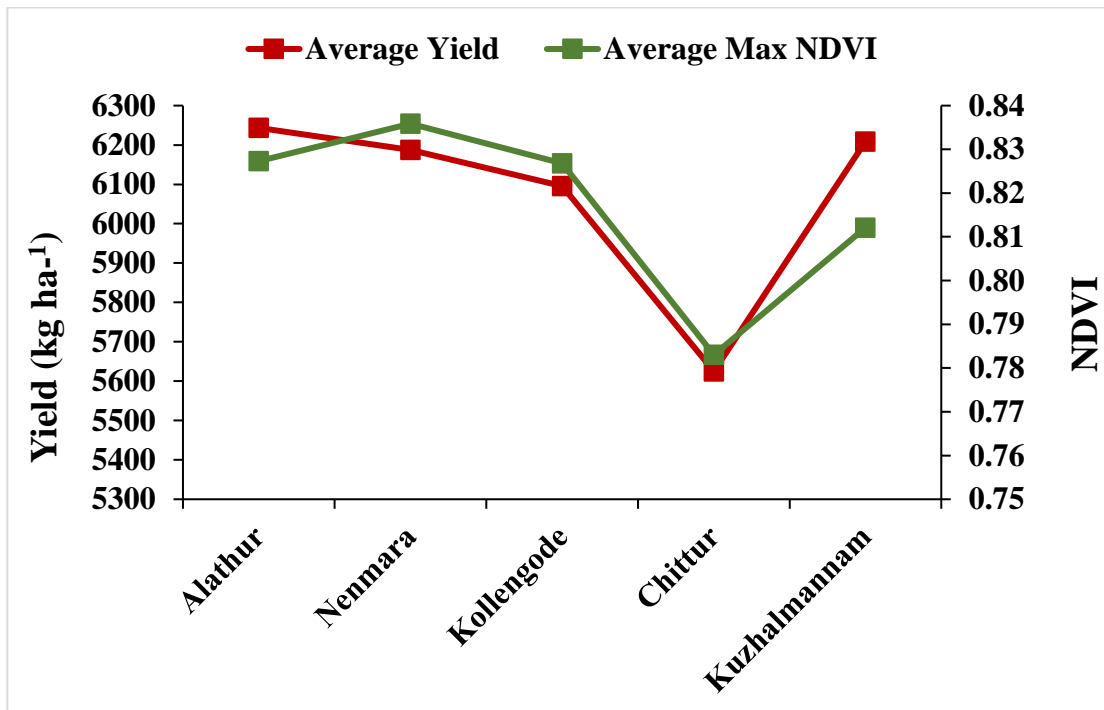


Fig. 5.1. Correlation between maximum NDVI and rice yield

5.3. Estimation of crop water demand in rice using remote sensing

5.3.1. Normalized Difference Vegetation Index (NDVI) and crop coefficient (K_c)

Multitemporal values of MODIS-NDVI corresponding to ground truth locations in Alathur (Fig. 5.2), Nenmara (Fig. 5.3), Kollengode (Fig. 5.4), Chittur (Fig. 5.5) and Kuzhalmannam (Fig. 5.6) blocks of Palakkad district was plotted against the age of the rice plant. The crop coefficient (K_c) curve showed a similar trend as that of satellite derived vegetation index (*ie*; NDVI) when plotted against the age of the plant. In this study a relationship was established between NDVI acquired through satellite images and K_c values of rice in the form of a linear regression equation with an R^2 value of 0.81. This equation was used to predict regional level K_c values for the five blocks of Palakkad district.

Gonzalez *et al.* (2018) established a relationship between NDVI derived from satellite images and K_c from literature. This relationship was used to create new K_c values for corn and alfalfa using additional overpass dates. Similarly, the potential of estimating crop coefficient (K_c) values as a function of remote sensing-based vegetation index has been studied by Kamble *et al.* (2013) in Maize fields of USA. A simple linear

regression model was developed to establish a relationship between a normalized difference vegetation index (NDVI) from a moderate resolution satellite data (MODIS) and crop coefficient (K_c) calculated from the flux data measured for different crops and cropping practices available as a product in Ameriflux sites. The relationship between the NDVI derived from Landsat images and K_c for different dates of the year (DOY) was established to estimate the crop coefficients of summer groundnut at field and regional scales for different growth stages for the Ozat-II canal command of Junagadh district of Gujarat State, India by Parmar and Gontia (2016). Thus, several research workers have proved that a strong positive relation exists between NDVI values and K_c and this can be used to derive K_c from known NDVI values.

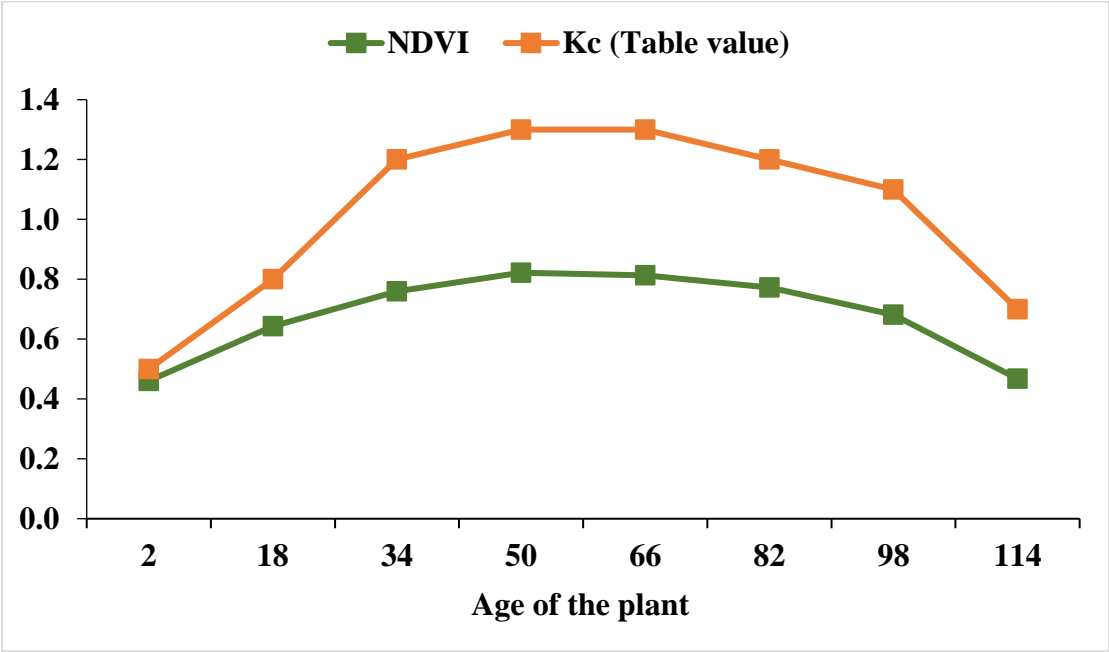


Fig. 5.2. Relationship of NDVI and K_c with age of the plant in Alathur block

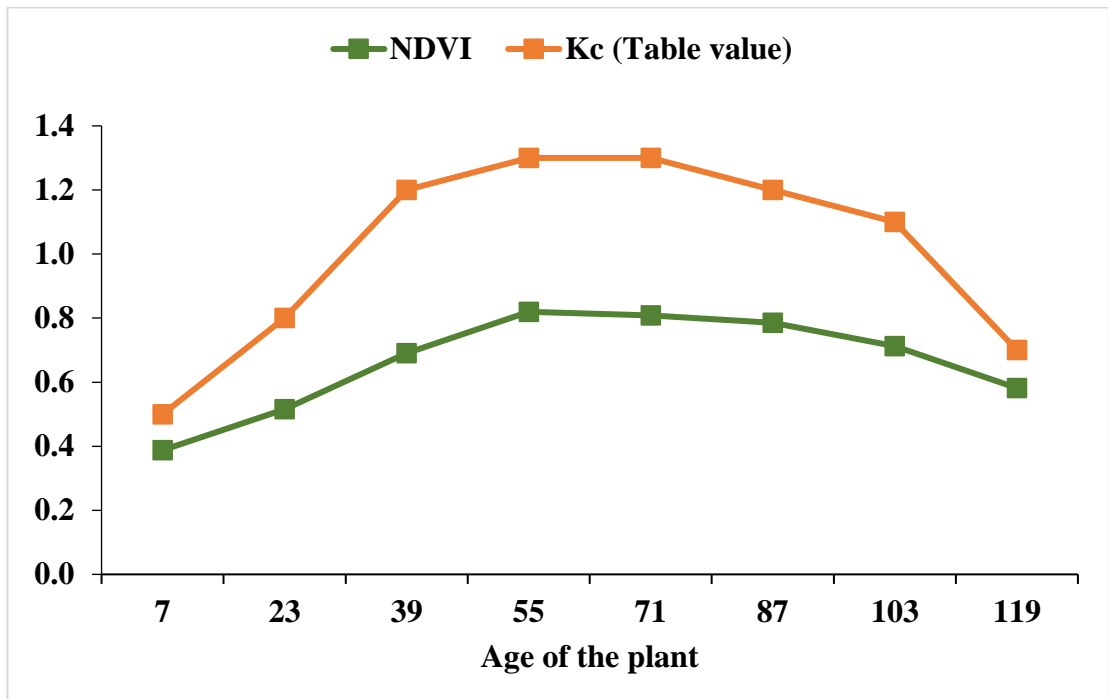


Fig. 5.3. Relationship of NDVI and K_c with age of the plant in Nenmara block

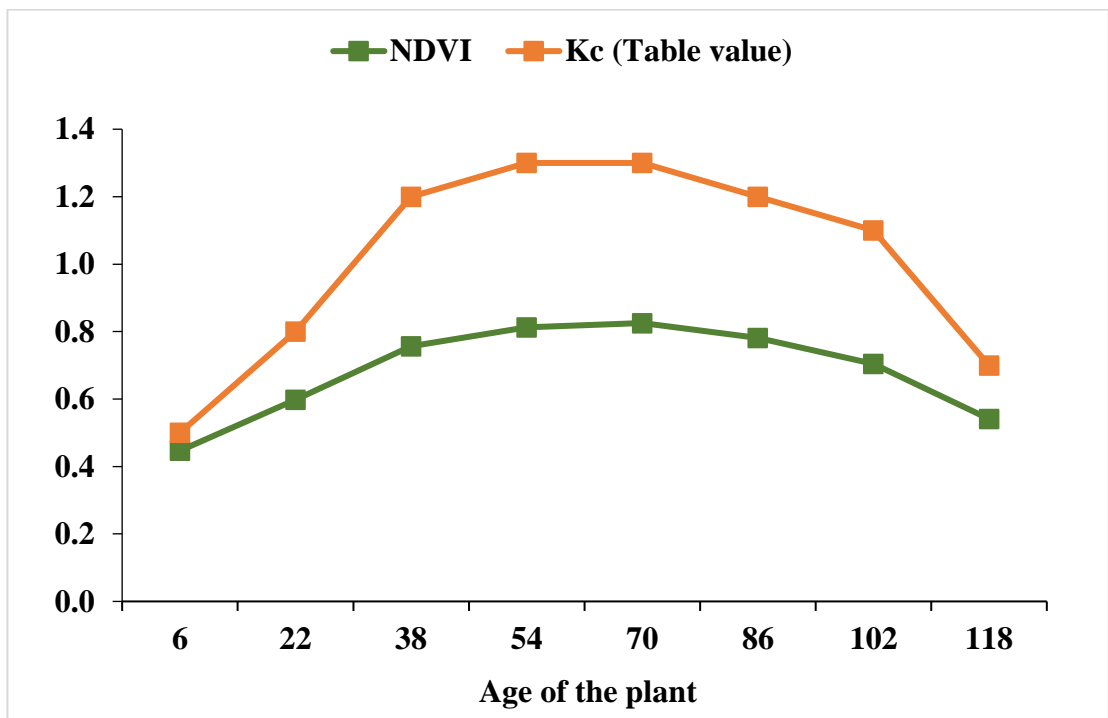


Fig. 5.4. Relationship of NDVI and K_c with age of the plant in Kollengode block

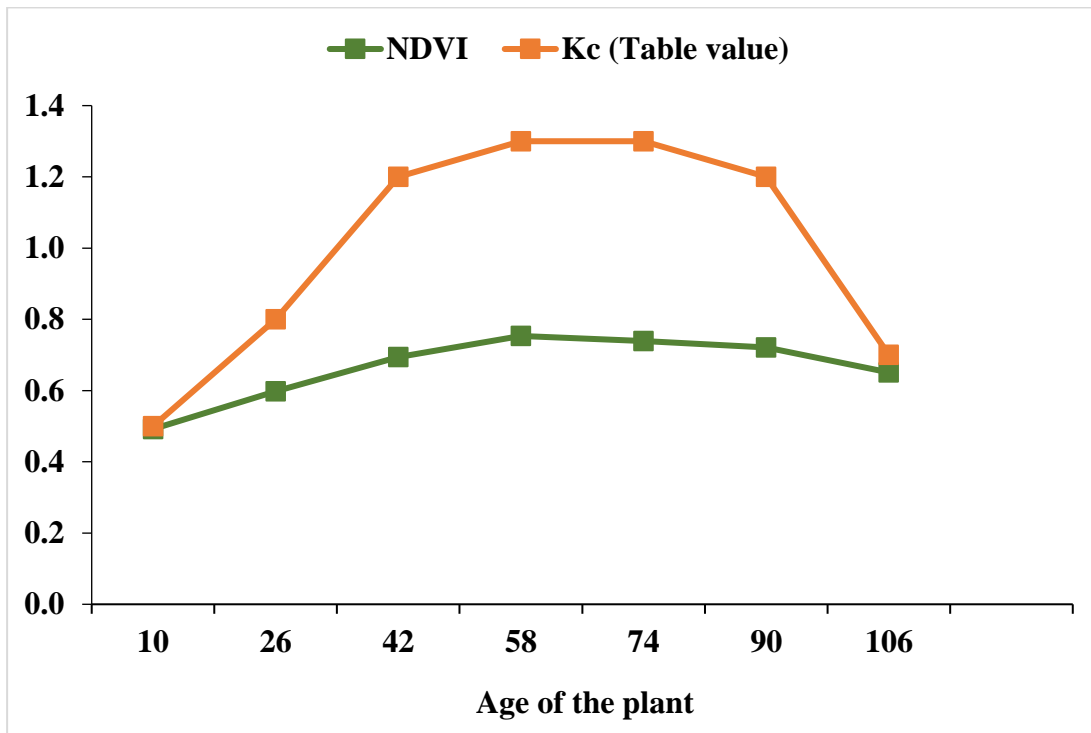


Fig. 5.5. Relationship of NDVI and K_c with age of the plant in Chittur block

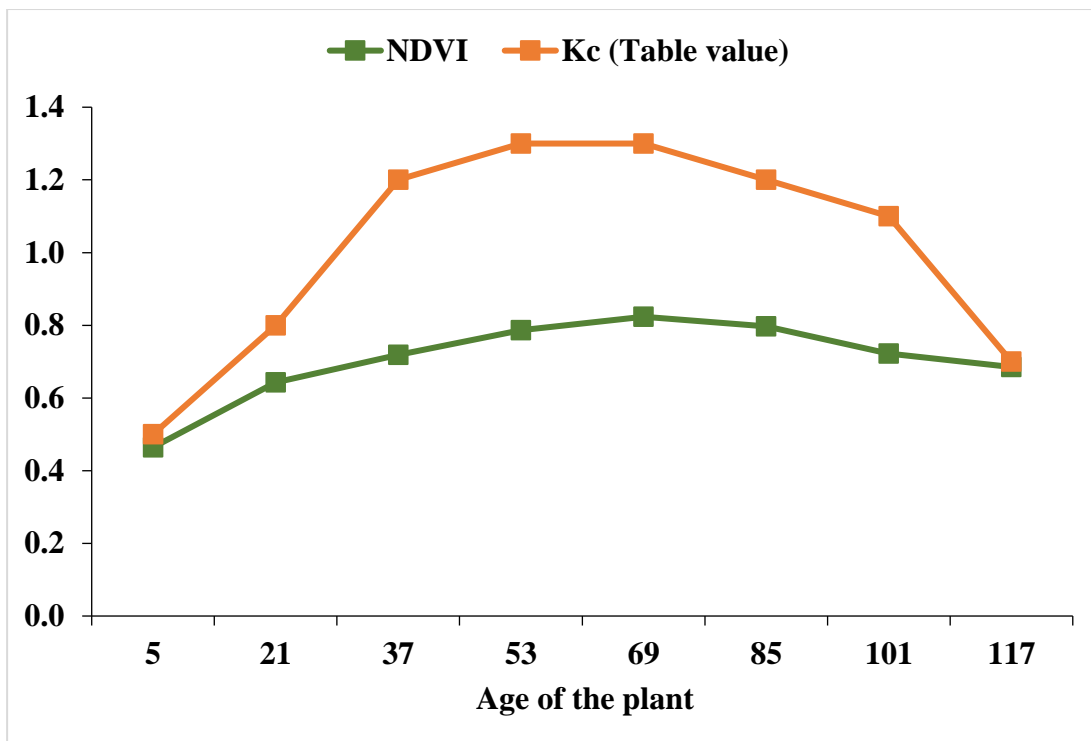


Fig. 5.6. Relationship of NDVI and K_c with age of the plant in Kuzhalmannam block

5.3.2. Validation of K_c predicted value

The K_c value predicted based on satellite derived NDVI values were validated for the training sites in 5 blocks of Palakkad district. The coefficient of determination (R^2) was 0.865 in Alathur block (Fig. 5.8), 0.823 in Nenmara block (Fig. 5.9), 0.840 in Kollengode block (Fig. 5.10), 0.868 in Chittur block (Fig. 5.11), 0.831 in Kuzhalmannam block (Fig. 5.12). This indicates a strong relationship between the predicted K_c values and the reference values. Generally, K_c value for rice will be low during the initial stage (0.5), the value increases as the crop grows, reaches maximum value stage (1.3) during peak vegetative and the value further decreases towards 0.7 during maturity stage of the crop (Lee and Huang, 2014). In this study, the predicted K_c values ranged between 0.5 to 1.3 in the study area with peak value during maximum vegetative stage. Moratiel and Martinez-Cob (2013) estimated crop coefficients (K_c) values for the initial, mid-season and late-season stages as 0.92, 1.06 and 1.03, respectively, with these stages lasting roughly 55, 45, and 25 days using remote sensing techniques in Spain. Another study done by Montazar *et al.* (2017) in California showed K_c values of 1.10, 1.00, and 0.80 for the initial-growth, midseason and late-season stages, respectively in rice.

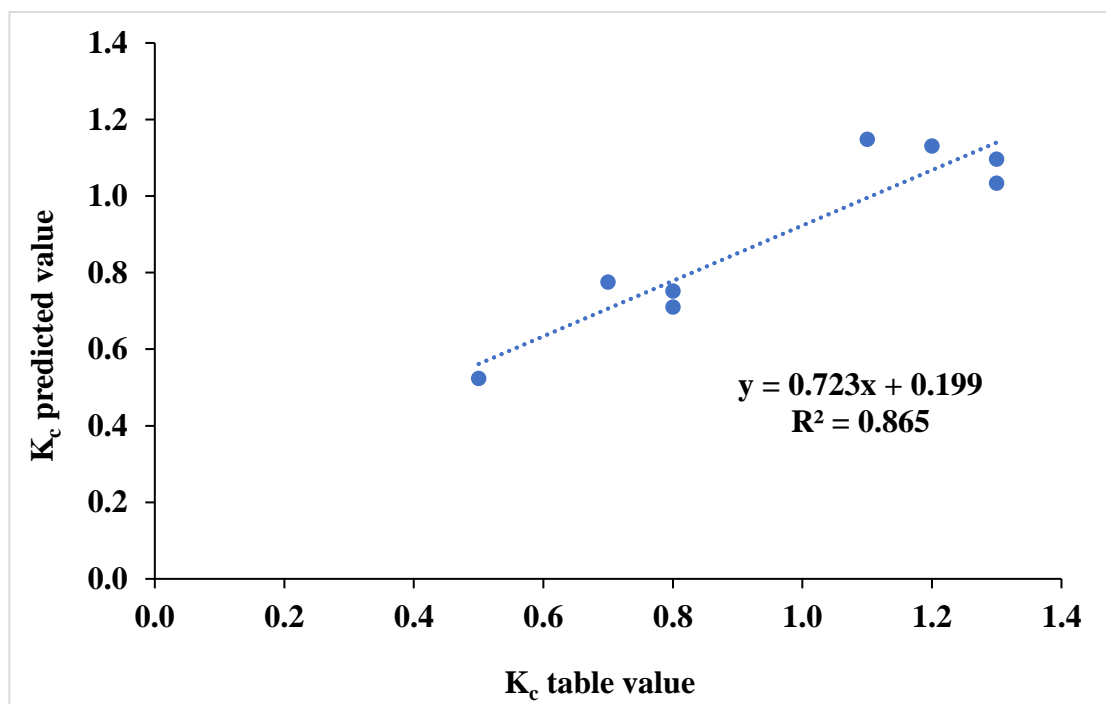


Fig. 5.7. Relationship of K_c table value and K_c predicted value in Alathur block

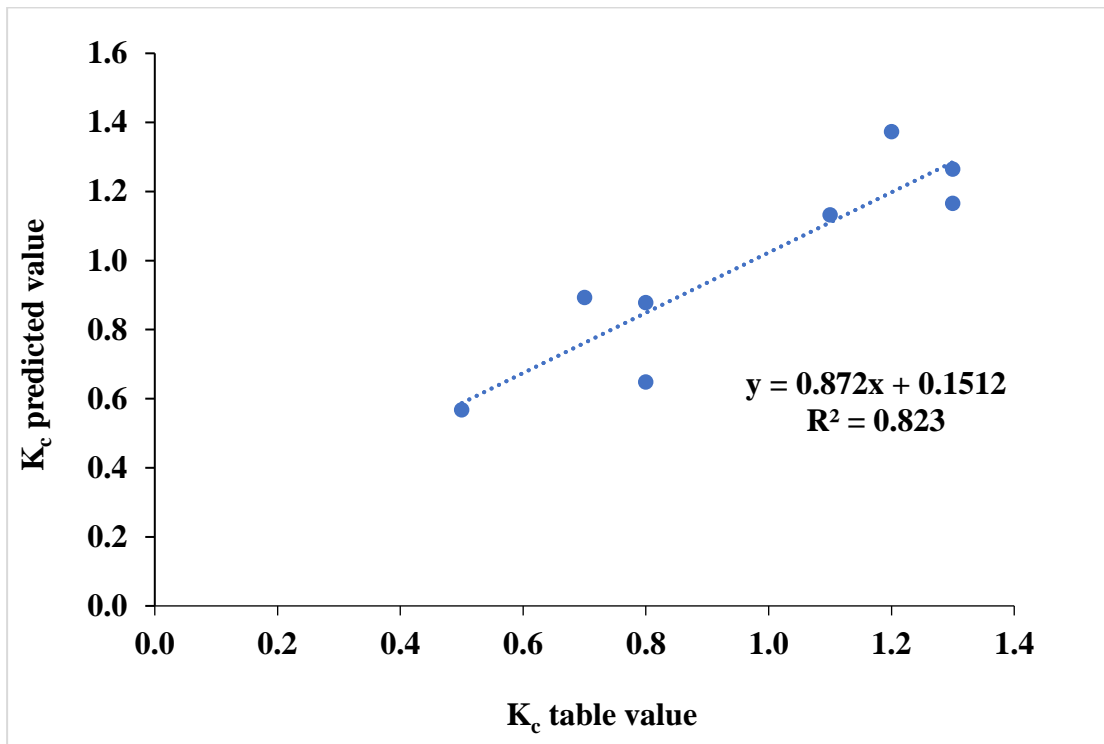


Fig. 5.8. Relationship of K_c table value and K_c predicted value in Nernmara block

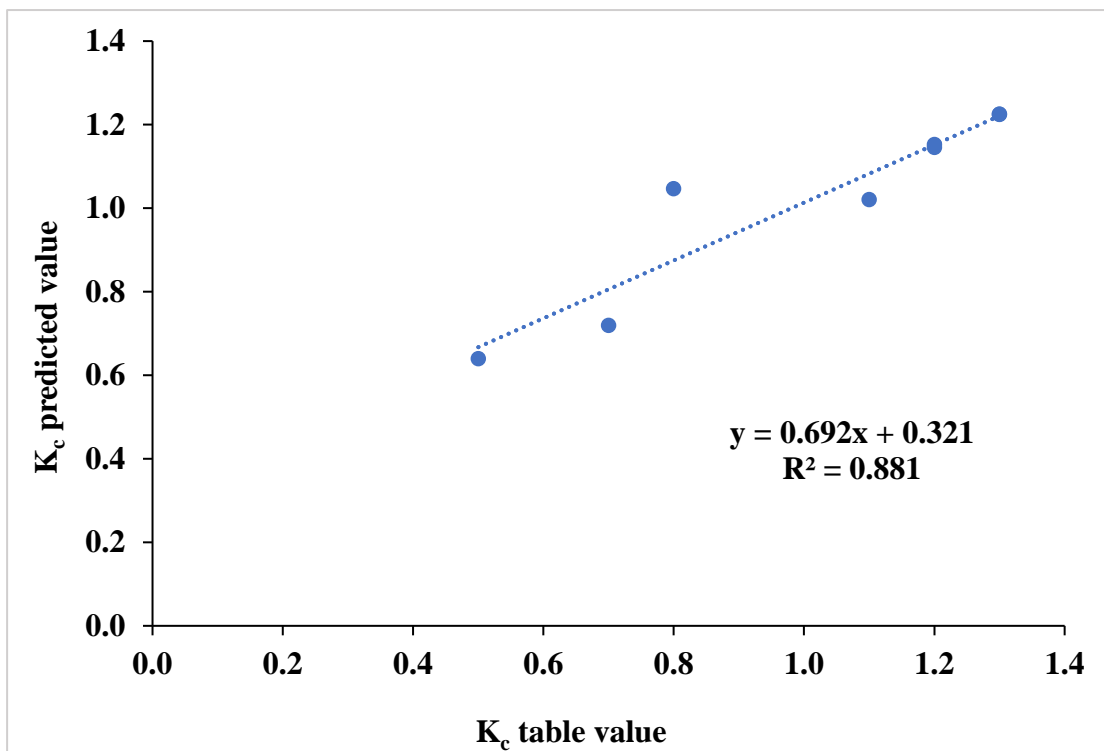


Fig. 5.9. Relationship of K_c table value and K_c predicted value in Kollengode block

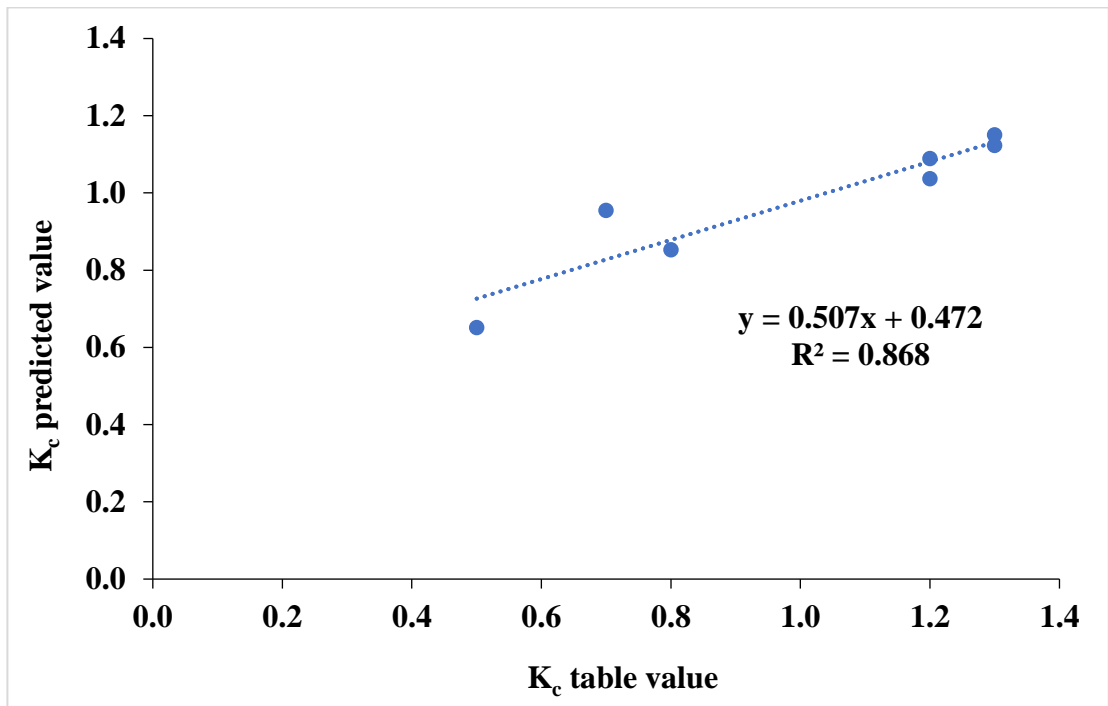


Fig. 5.10. Relationship of K_c table value and K_c predicted value in Chittur block

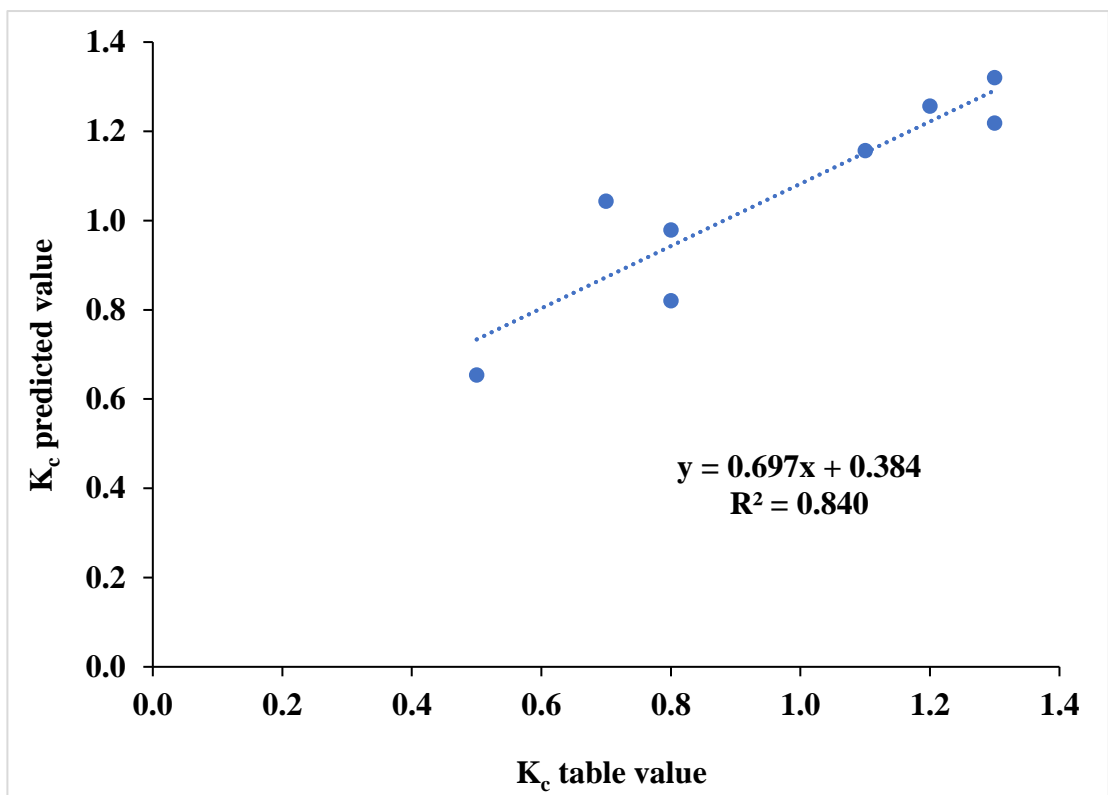


Fig. 5.11. Relationship of K_c table value and K_c predicted value in Kuzhalmannam block

5.3.3. Reference evapotranspiration (ET_o) during the crop period

A comparison was done regarding the potential evapotranspiration (ET_o) estimated during the crop growth period using different methods *viz.* Modified Penman, Hargreaves, Turc, Blaney-Criddle, Christiansen, Open pan and FAO Penman Montieth for Alathur (Fig. 5.12), Nenmara (Fig. 5.13), Kollengode (Fig. 5.14), Chittur (Fig. 5.15) and Kuzhalmannam (Fig. 5.16) blocks of Palakkad district. In this study, open pan and Christiansen methods underestimated ET_o during the overall crop growth period, whereas, Modified Penman method overestimated ET_o in all the 5 blocks of Palakkad district. Hargreaves, Turc and Blaney-Criddle were on par and estimated similar values throughout. In this study ET_o estimated through FAO Penman Montieth was found to be more realistic and reliable. According to a study done by FAO, Penman Montieth method was found to be more reliable in estimating ET_o as compared to other conventional methods (Yoo *et al.*, 2006). Further, maximum number of weather parameters are considered while estimating ET_o through FAO Penman Montieth method. The ET_o estimated through all the methods mentioned above showed an increasing trend from 2nd meteorological week 2021 to 9th meteorological week 2021, this can be reasoned by the rise in wind speed and reduced relative humidity during January and February months in the study area due to the presence of Palakkad gap.

According to a study conducted by Surendran *et al.* (2015), except for the month of June, July, August, September and October, the potential evaporation is more than the effective rainfall in majority of Agro-Ecological Units in Palakkad. Hence, irrigation is required in rest of the months. According to Saravanan (1994) the cumulative ET_o during December-February period was greater than 40 cm in all stations in Kerala. Both these references indicate that ET_o calculated through Penman Montieth method in this study shows resemblance with the actual value specific to Palakkad district.

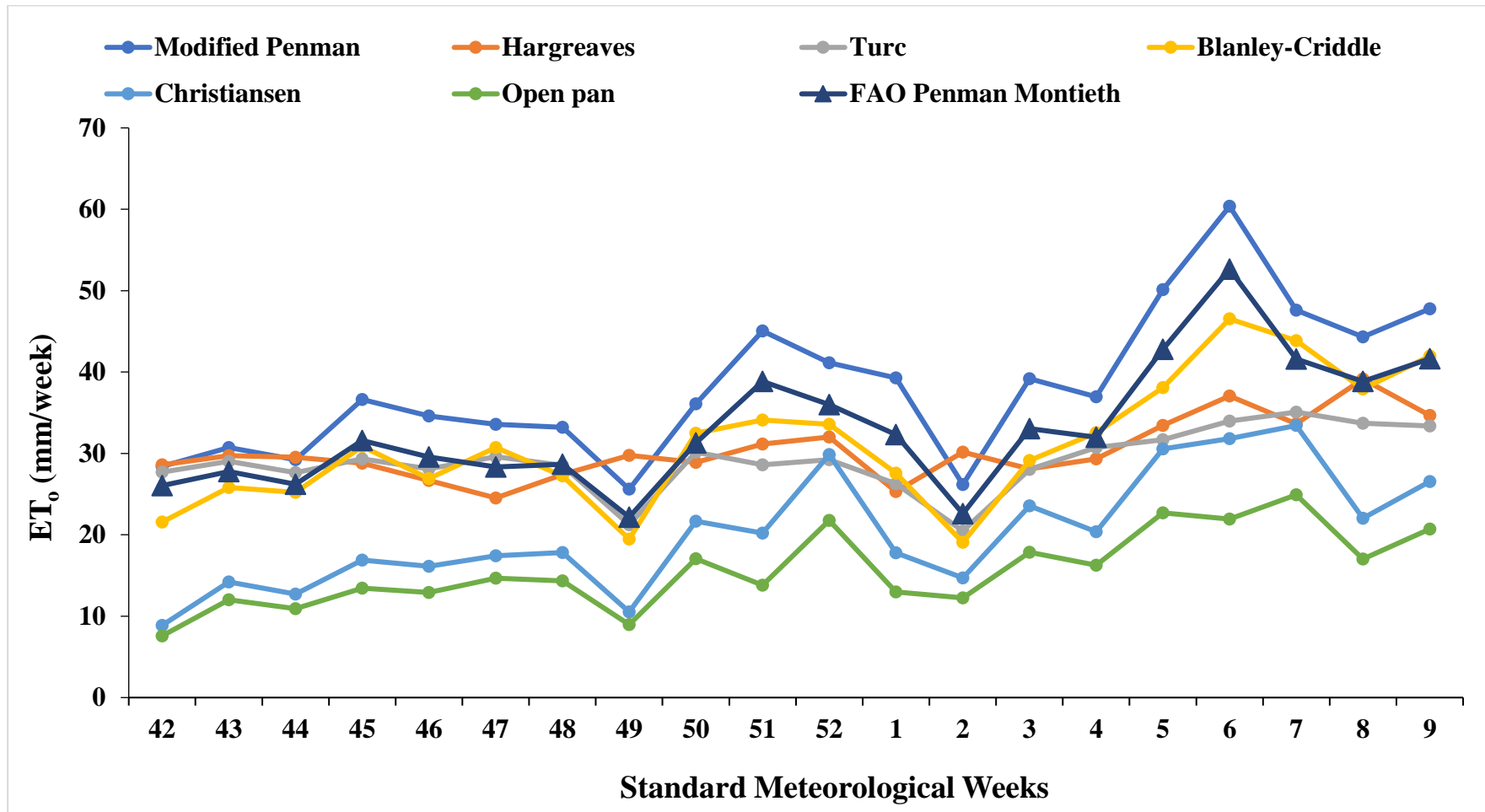


Fig. 5.12. Weekly reference evapotranspiration (ET₀) of Alathur block during the crop growth period

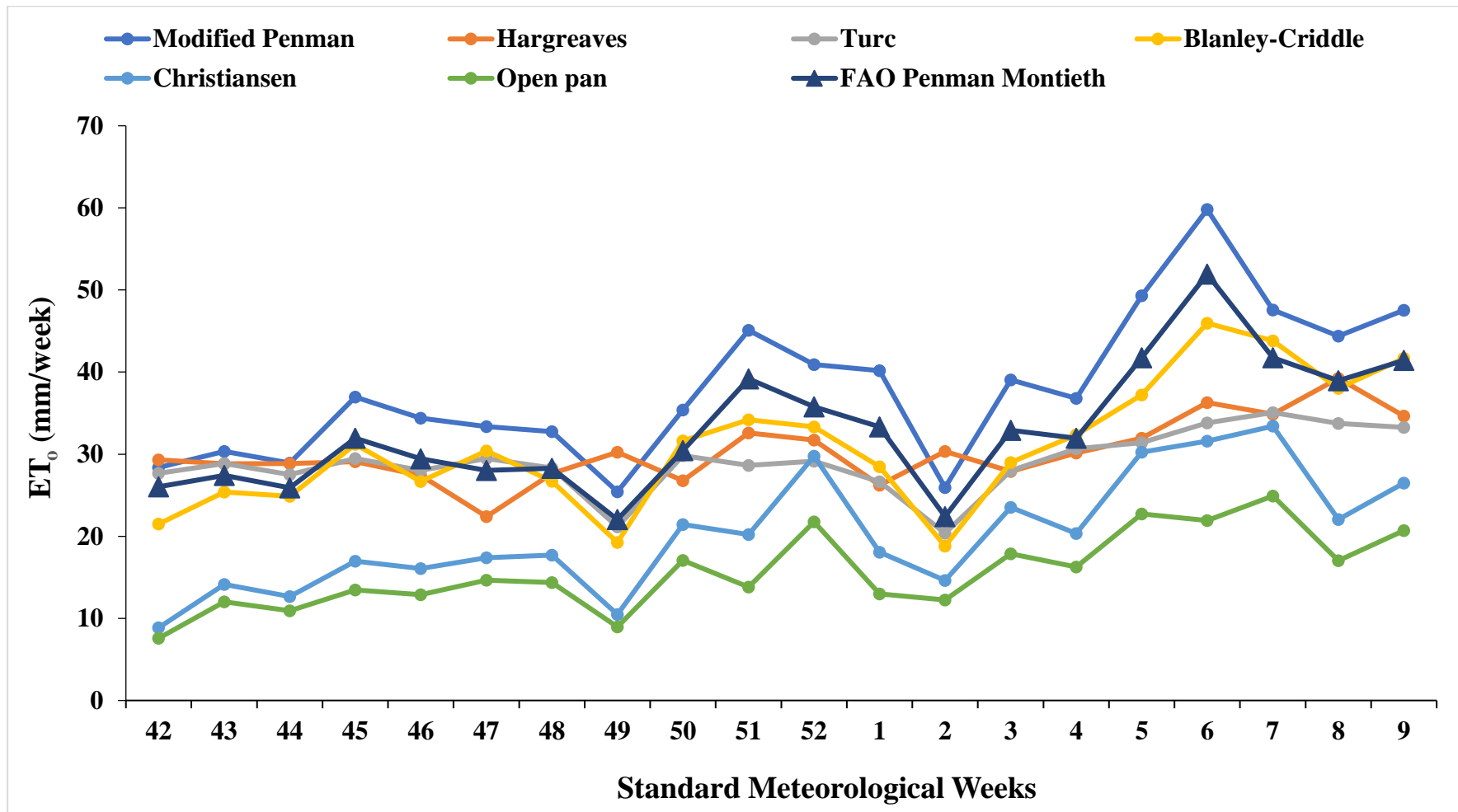


Fig. 5.13. Weekly reference evapotranspiration (ET_0) of Nenmara block during the crop growth period

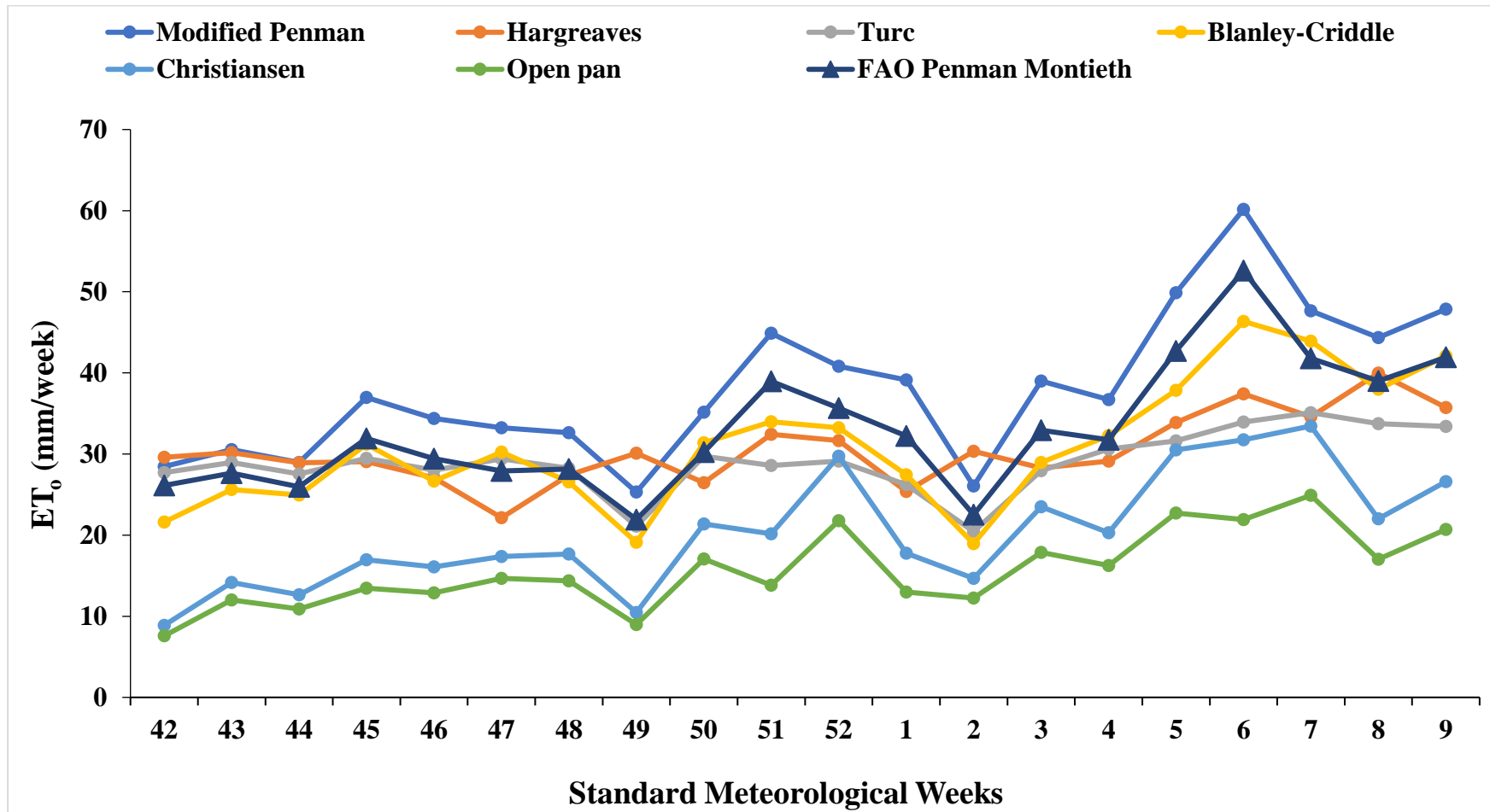


Fig. 5.14. Weekly reference evapotranspiration (ET₀) of Kollengode block during the crop growth period

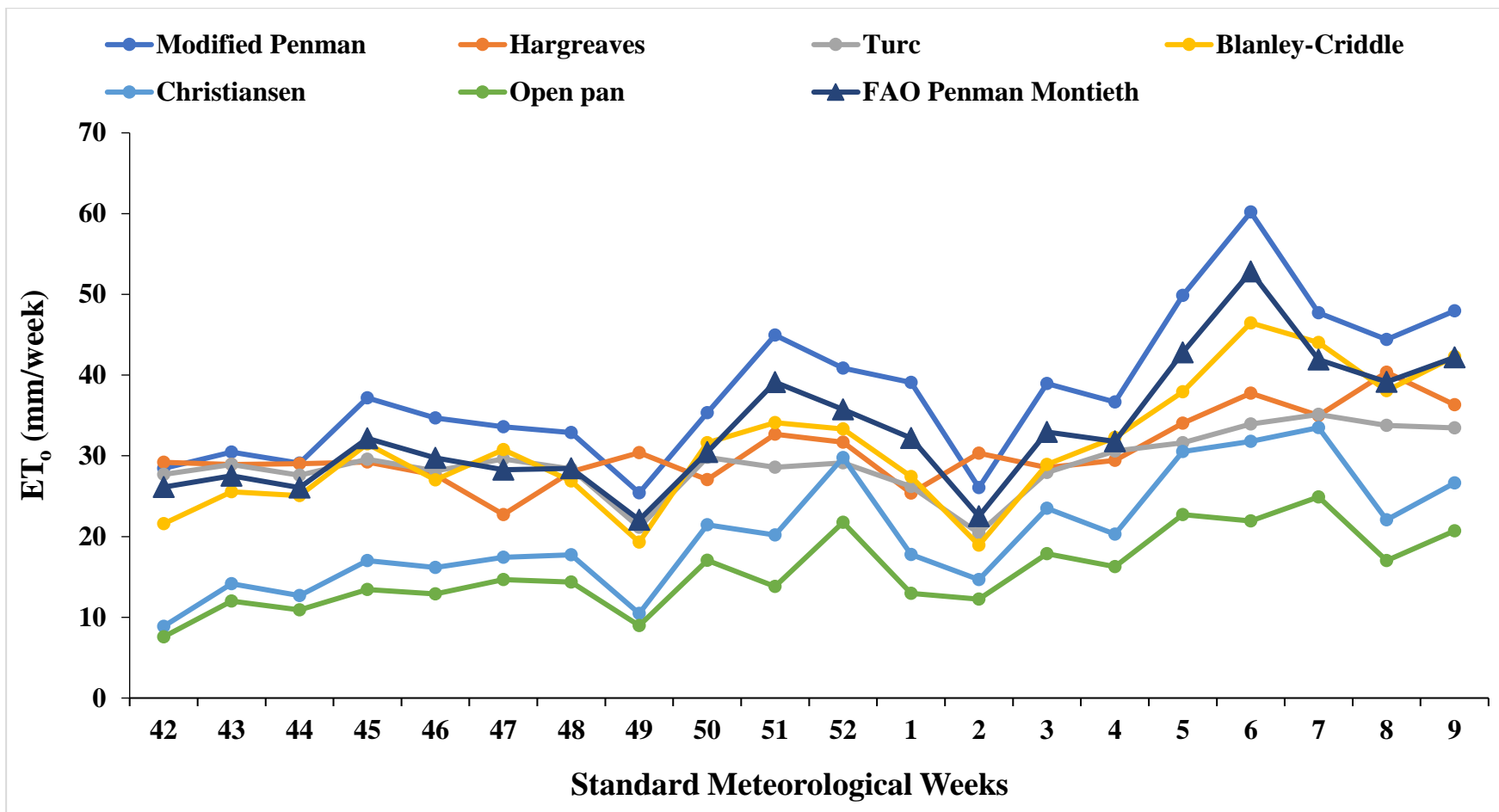


Fig. 5.15. Weekly reference evapotranspiration (ET_0) of Chittur block during the crop growth period

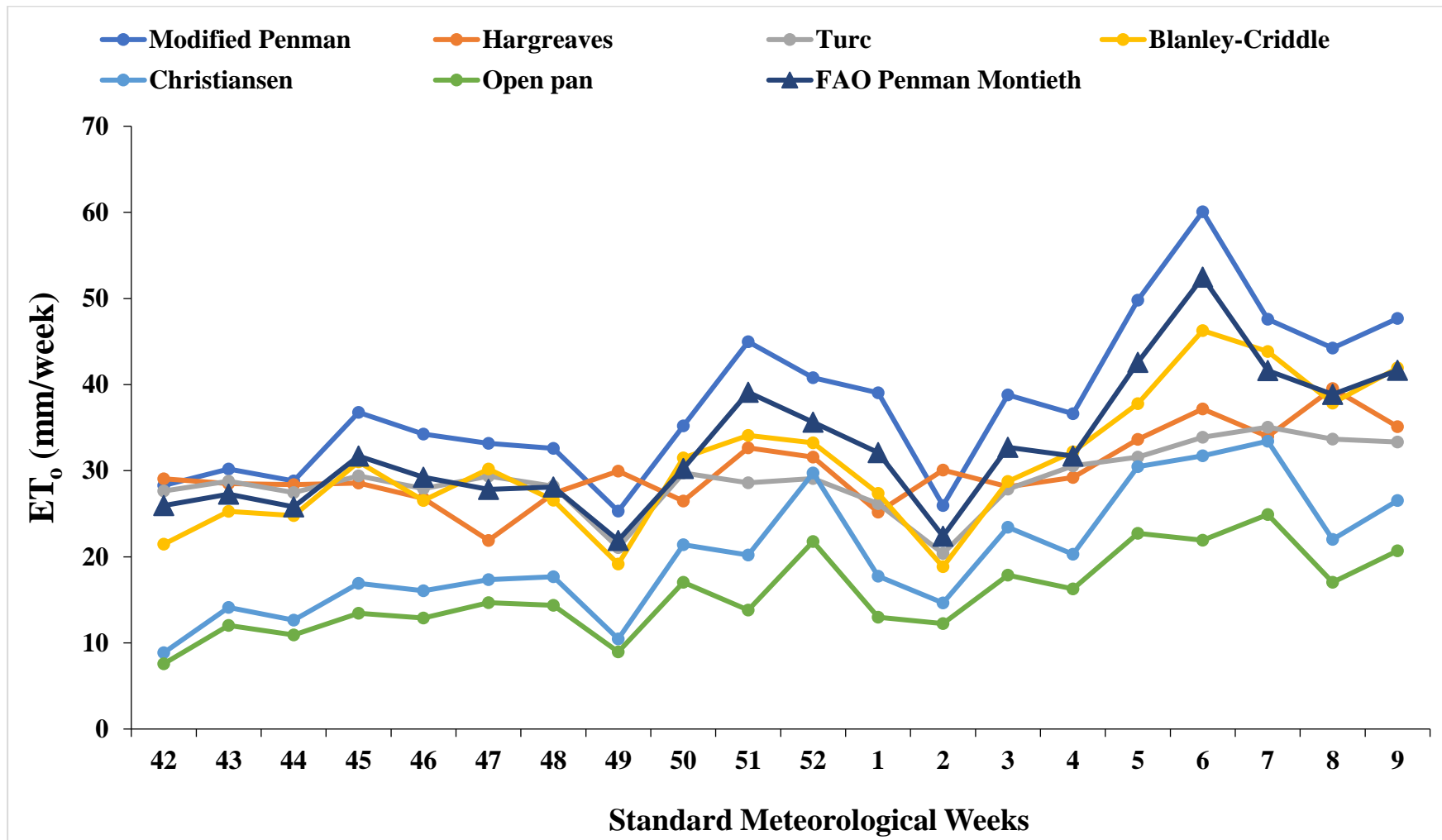


Fig. 5.16. Weekly reference evapotranspiration (ET₀) of Kuzhalmannam block during the crop growth period

5.3.4. Irrigation requirement based on effective rainfall and Crop evapotranspiration (ET_c)

The cumulative monthly rainfall, effective rainfall, reference evapotranspiration (ET_o) and crop evapotranspiration (ET_c) during the *mundakan* season of rice in Alathur block is illustrated in Fig 5.17. The total rainfall received during the crop period was 100 % effectively utilised in Alathur block. The maximum rainfall was observed during October 2020 (117.5 mm), followed by January 2021 (47.7 mm). During October 2020, the crop evapotranspiration (ET_c) in the ground truth location Kizhakkenchery was 95.64 mm, whereas, the effective rainfall received during this period was 118 mm. Similar situation was observed in another training site, Vadakkenchery where ET_c was 102 mm while effective rainfall was 118 mm. In both the cases, effective rainfall was higher than crop evapotranspiration. In such a situation irrigation requirement will be zero, for crops other than rice which does not require standing water need in the field. The total rainfall received during the crop period was not sufficient to meet the water requirement of the crop, so irrigation requirement during the crop period ranged between 761.56-912.39 mm in Alathur block.

The irrigation requirement during early vegetative stage ranged between 30-95 mm in the ground truth locations in Alathur block. During late vegetative stage 266-363 mm was the irrigation requirement, in reproductive stage 219-320 mm and in maturity stage 110-217 mm. Irrigation requirement was maximum in the late vegetative stage followed by reproductive stage of crop growth (Fig. 5.18).

The distribution of monthly rainfall, effective rainfall, reference evapotranspiration and crop evapotranspiration in Nenmara block are presented in Fig. 5.19. The crop was sown during October 2020 in two ground truth locations viz, Nenmara and Elevenchery and in rest of the locations sowing was done in November 2020. Similar to Alathur block, the rainfall received during the crop period in Nenmara block was also 100 % effectively utilised. Among the ground truth locations in the block, the effective rainfall (75 mm) received in Nenmara during the month of October was sufficient to compensate crop evapotranspiration (69.06 mm). A similar situation was also observed in training sites, Melarkode, Pallassana and Ayilur during November 2020. During these months water required for maintaining standing water in the fields has

to be provided through irrigation. In Nenmara block highest rainfall during the crop period was experienced in November 2020 (88 mm) followed by October 2020 (75 mm) and least in February 2021 (8 mm).

The irrigation requirement during early vegetative stage was 30-63 mm, late vegetative stage was 215-239 mm, reproductive stage was 229-265 mm, maturity stage was 117-226 mm in ground truth locations of Nenmara block. The reproductive stage of the crop showed maximum irrigation requirement in this block during the crop growth period (Fig. 5.20).

In Kollengode block, highest rainfall was received during October 2020 (163.2 mm) whereas, the ET_o during this period was 124.2 mm/month. Hence only, 76 % of the rainfall received in October 2020 was effectively utilised. Vadavannur was the only location in which the crop was sown during October, hence irrigation requirement during the initial stages of crop growth in this region was very less. During the rest of the crop period rainfall received was effectively utilised. The Fig 5.21 represents the distribution of monthly rainfall and effective rainfall during the crop period along with the reference evapotranspiration and crop evapotranspiration of the crop in Kollengode block.

In kollengode block, irrigation requirement of the crop in the early vegetative stage was 30-94 mm, during late vegetative stage was 206-350 mm, in reproductive stage 249-304 mm and in maturity stage was 161-228 mm. The maximum irrigation requirement was observed in late vegetative stage in this region (Fig. 5.22).

The cumulative monthly rainfall, effective rainfall, reference evapotranspiration (ET_o) and crop evapotranspiration of rice in Chittur block is presented in Fig 5.23. The maximum rainfall during the crop growth period was received in October 2020 (96 mm), whereas no rainfall was received in February 2021. The rainfall received during the crop period was 100 % effectively utilised. Among the ground truth locations, Chittur-Thathamangalam location received an effective rainfall of 96 mm in October month which corresponds to initial stage of crop growth, during this period the crop evapotranspiration was 92.30 mm. Hence, the irrigation requirement was only 30 mm to maintain standing water in the fields.

Irrigation was necessary to grow the crop during November, December, January and February months, since rainfall received was not sufficient to meet the crop water demands.

The irrigation requirement of rice during mundakan 2020-21 in various ground truth locations of Chittur block ranged between 30-102 mm in the early vegetative stage of the crop, 305-331 mm during late vegetative stage, 269-305 mm in the reproductive stage and 164-242 mm in the maturity. The late vegetative stage showed maximum irrigation requirement in this block when compared to other stages during the crop growth period (Fig. 5. 24).

The Fig 5.25 illustrates the distribution of monthly rainfall, effective rainfall, reference evapotranspiration and crop evapotranspiration in Kuzhalmannam block. The maximum rainfall during the crop period was received during October 2020 (123 mm) and no rainfall was received in February 2021. The effective rainfall received could compensate crop evapotranspiration in two ground truth locations *namely*, Kuzhalmammanm and Thenkurissi during October 2020. During the months of November, December, January and February supplemental irrigation water has to be supplied to meet the water demands of the crop.

In Kuzhalmannam block, the irrigation requirement during the early vegetative stage of the crop was 30-82 mm, in late vegetative stage 239-332 mm, in the reproductive stage 212-282 mm and in the maturity stage was 100-241 mm. The maximum irrigation requirement was observed in the late vegetative stage (Fig. 5.26).

Lee and Huang (2014) assessed the impact on irrigation water by climate change in Taoyuan in northern Taiwan. They estimated irrigation requirement in rice based on crop evapotranspiration and effective rainfall. Hossain *et al.* (2017) conducted a study to estimate irrigation water requirement in *Boro* rice in Bangladesh based on actual evapotranspiration of rice during the crop season and the effective rainfall received during the crop period.

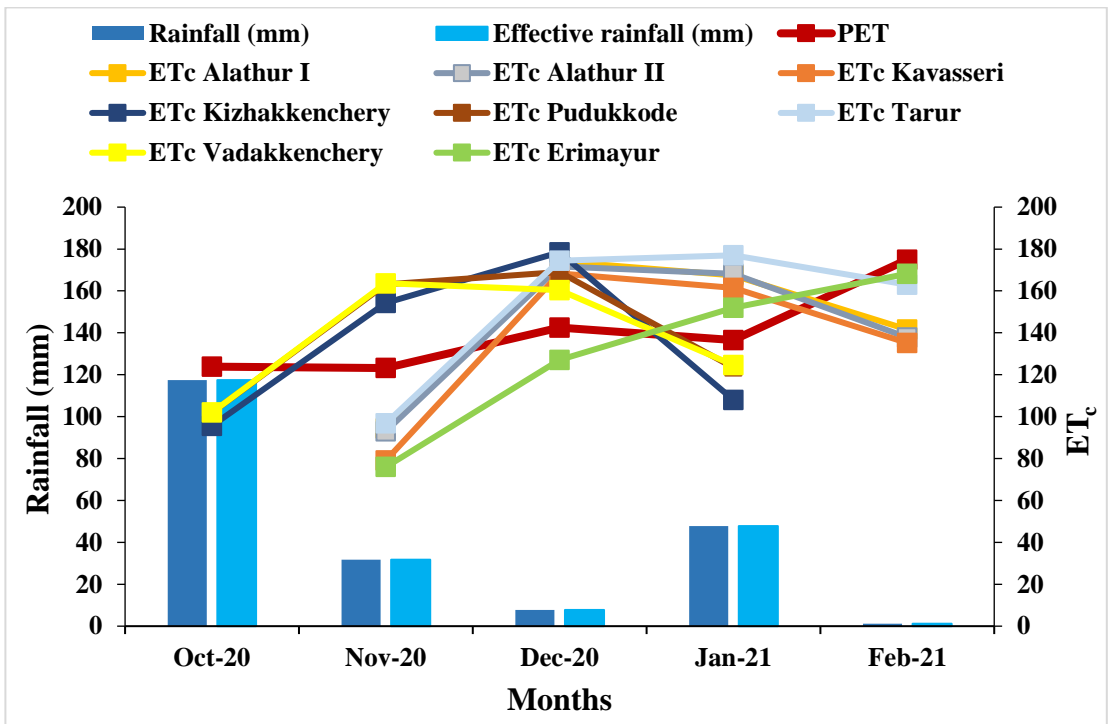


Fig. 5.17. Distribution of monthly rainfall, effective rainfall, reference evapotranspiration and crop evapotranspiration of rice in Alathur block

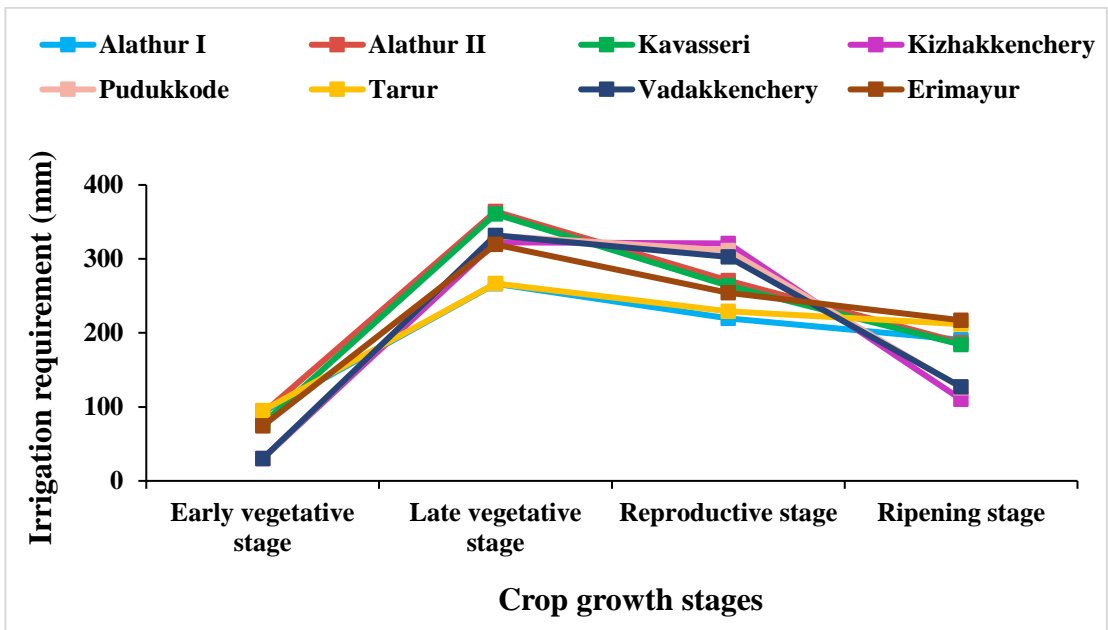


Fig. 5.18. Stagewise irrigation requirement in Alathur block during *mundakan* season 2020-21

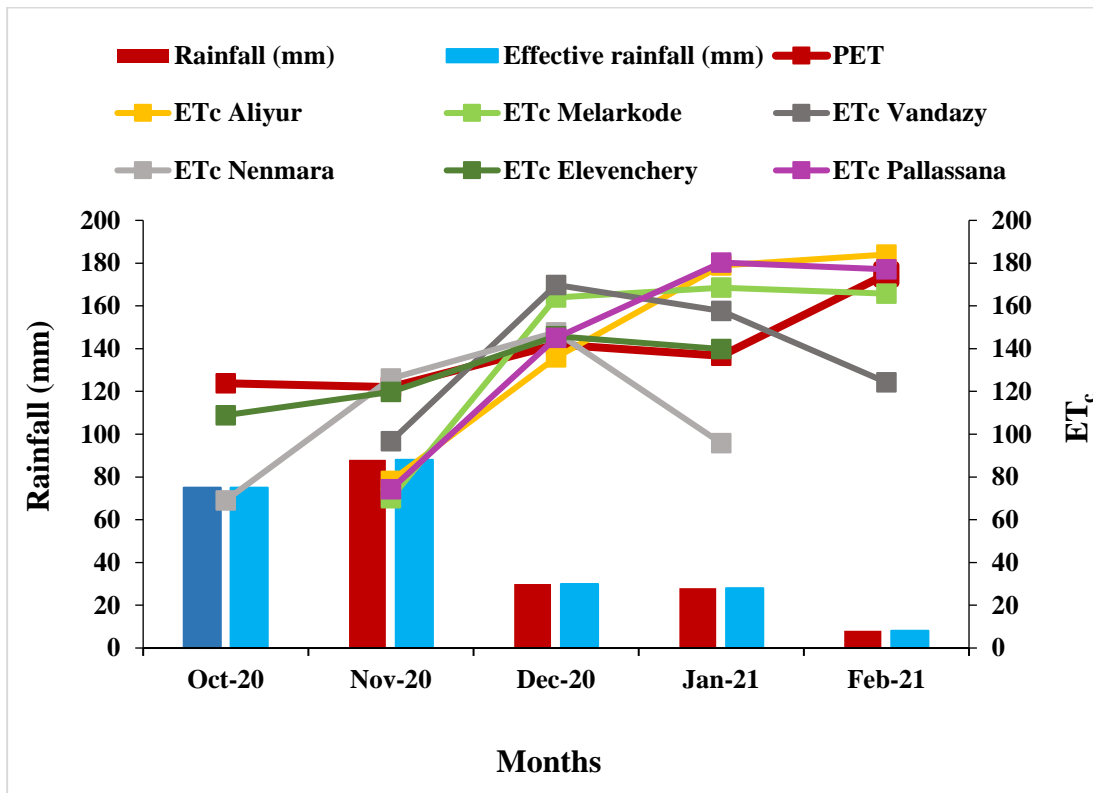


Fig. 5.19. Distribution of monthly rainfall, effective rainfall, reference evapotranspiration and crop evapotranspiration of rice in Nenmara block

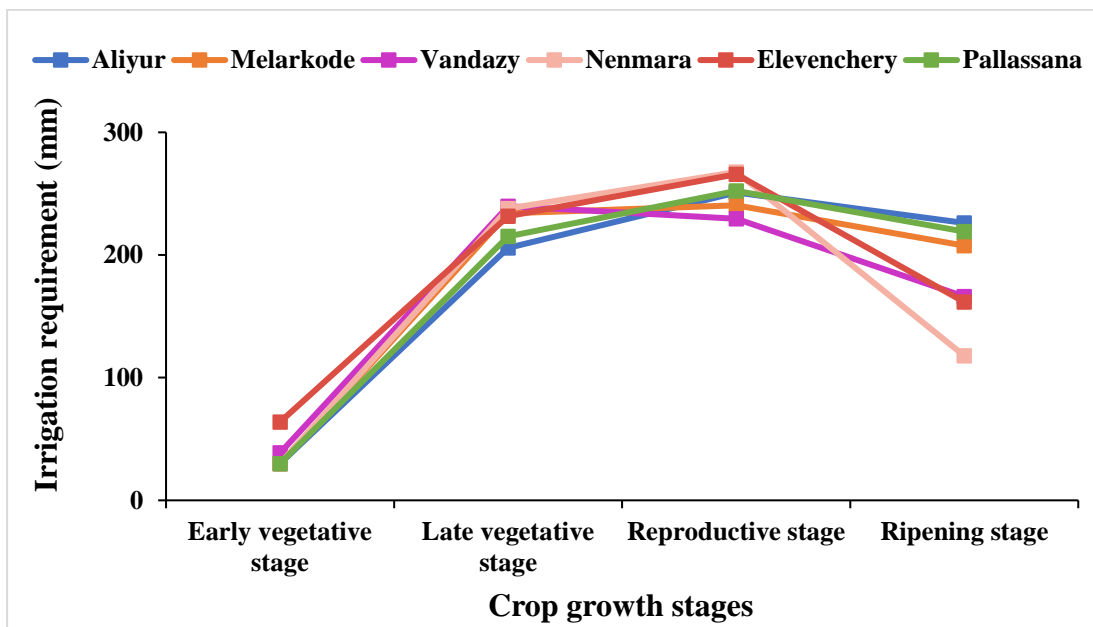


Fig. 5.20. Stagewise irrigation requirement in Nenmara block during mundakan season 2020-21

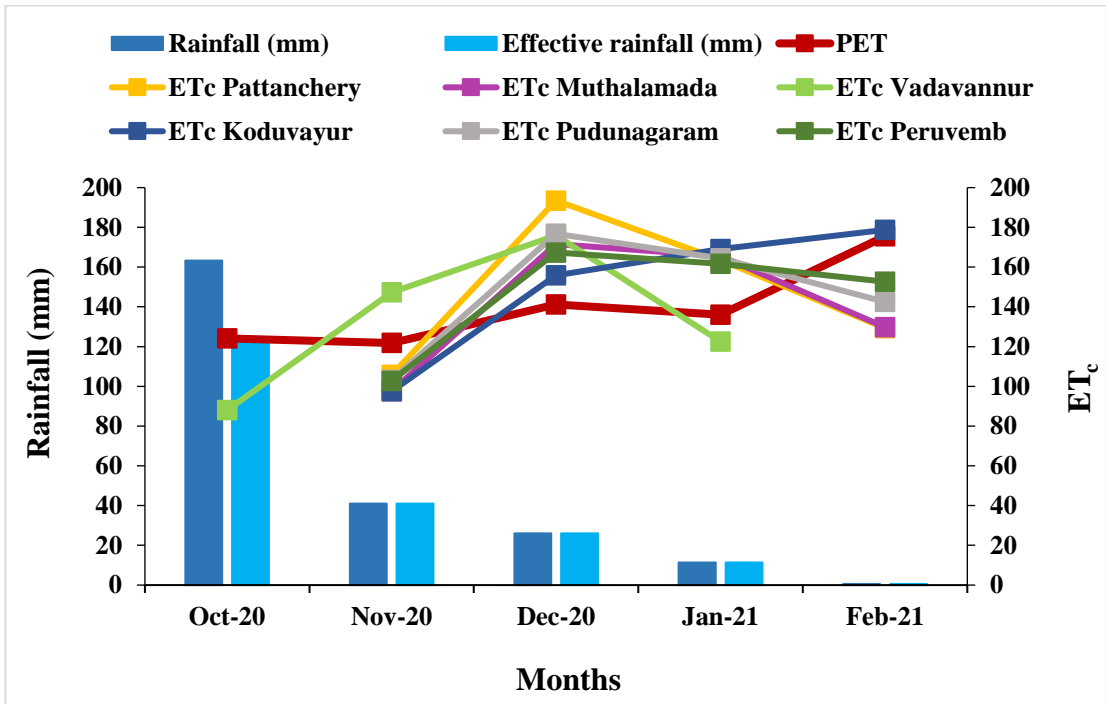


Fig. 5.21. Distribution of monthly rainfall, effective rainfall, reference evapotranspiration and crop evapotranspiration of rice in Kollengode block

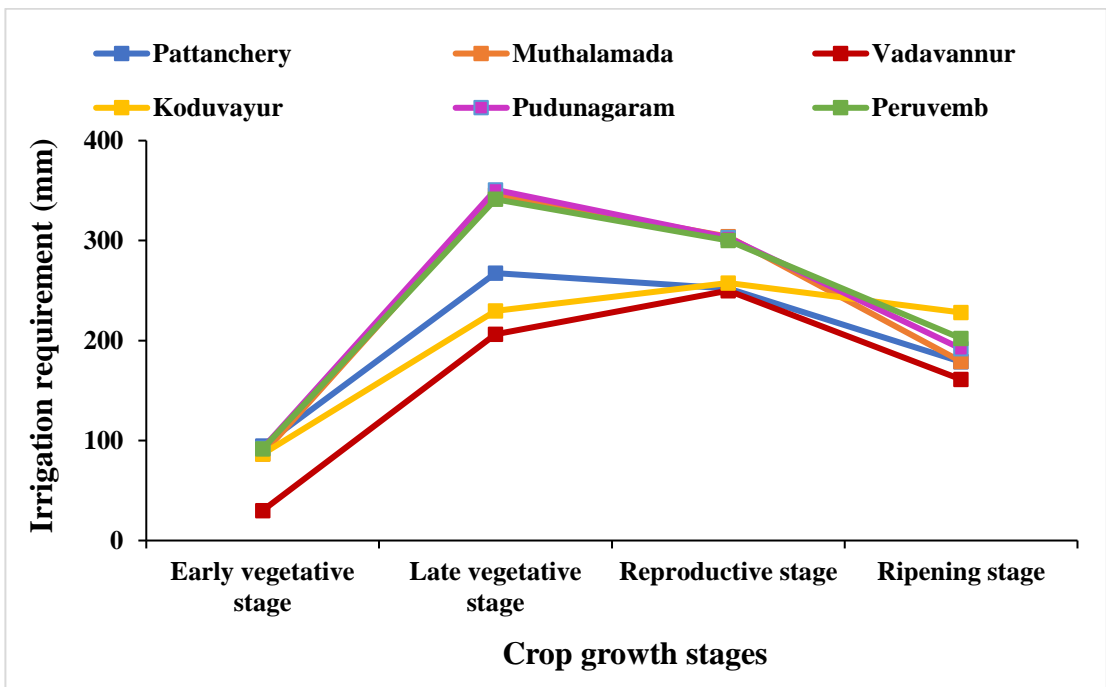


Fig. 5.22. Stagewise irrigation requirement in Kollengode block during mundakan season 2020-21

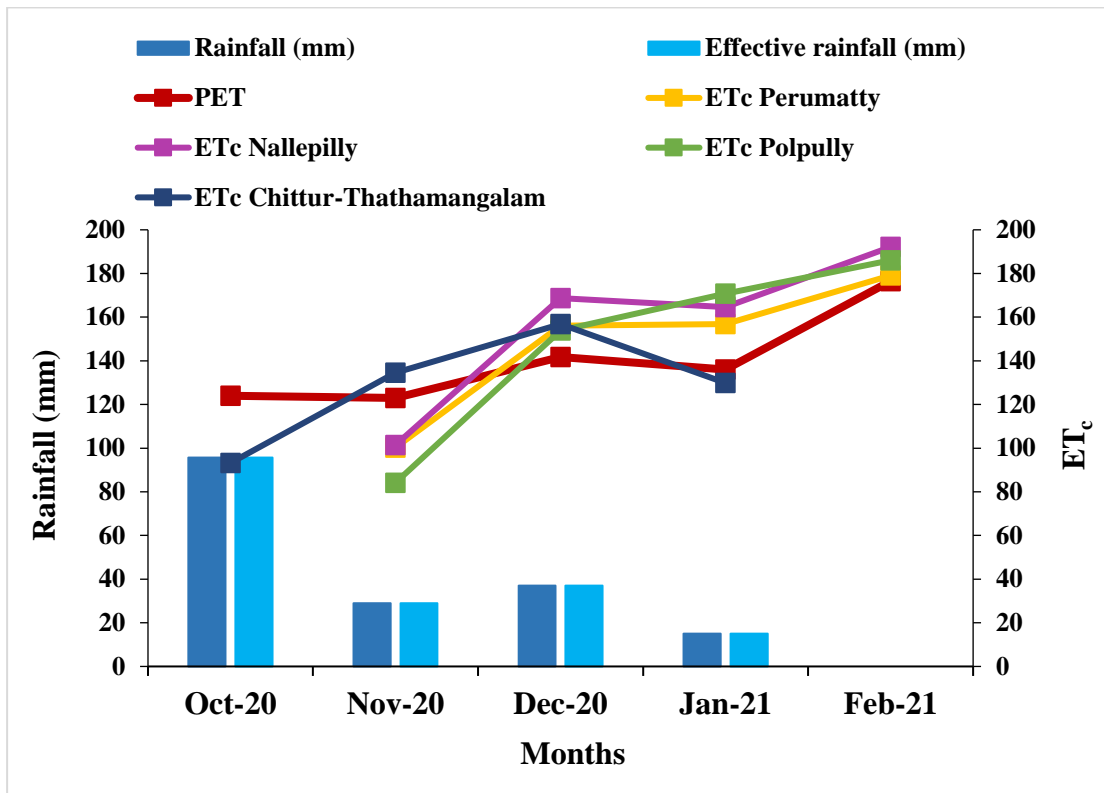


Fig. 5.23. Distribution of monthly rainfall, effective rainfall, reference evapotranspiration and crop evapotranspiration of rice in Chittur block

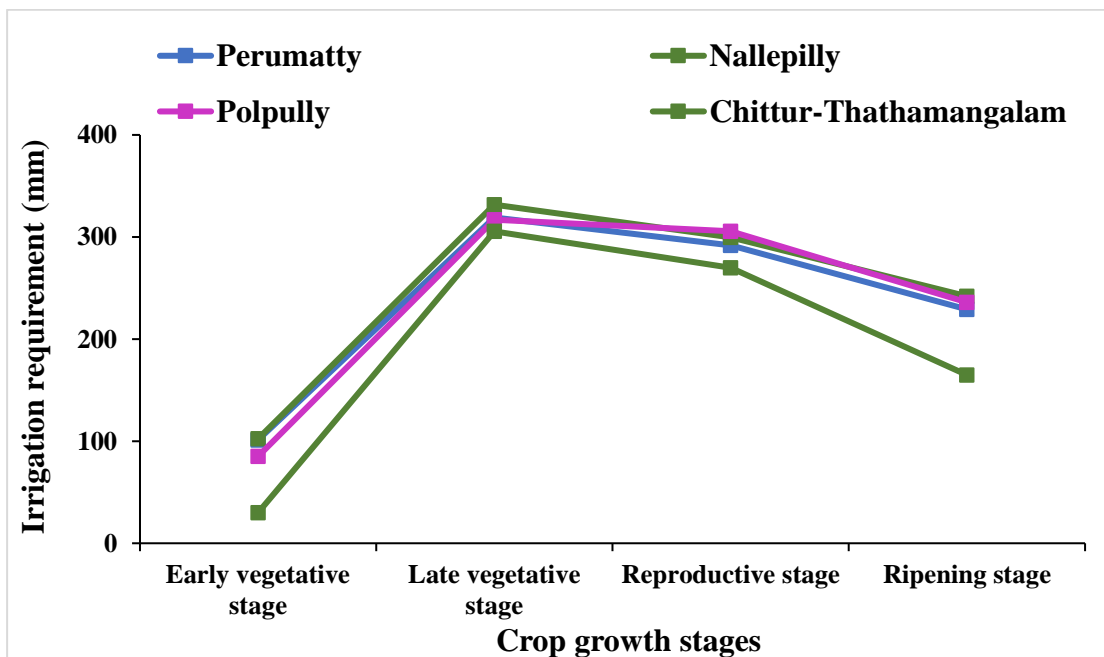


Fig. 5.24. Stagewise irrigation requirement in Chittur block during *mundakan* season 2020-21

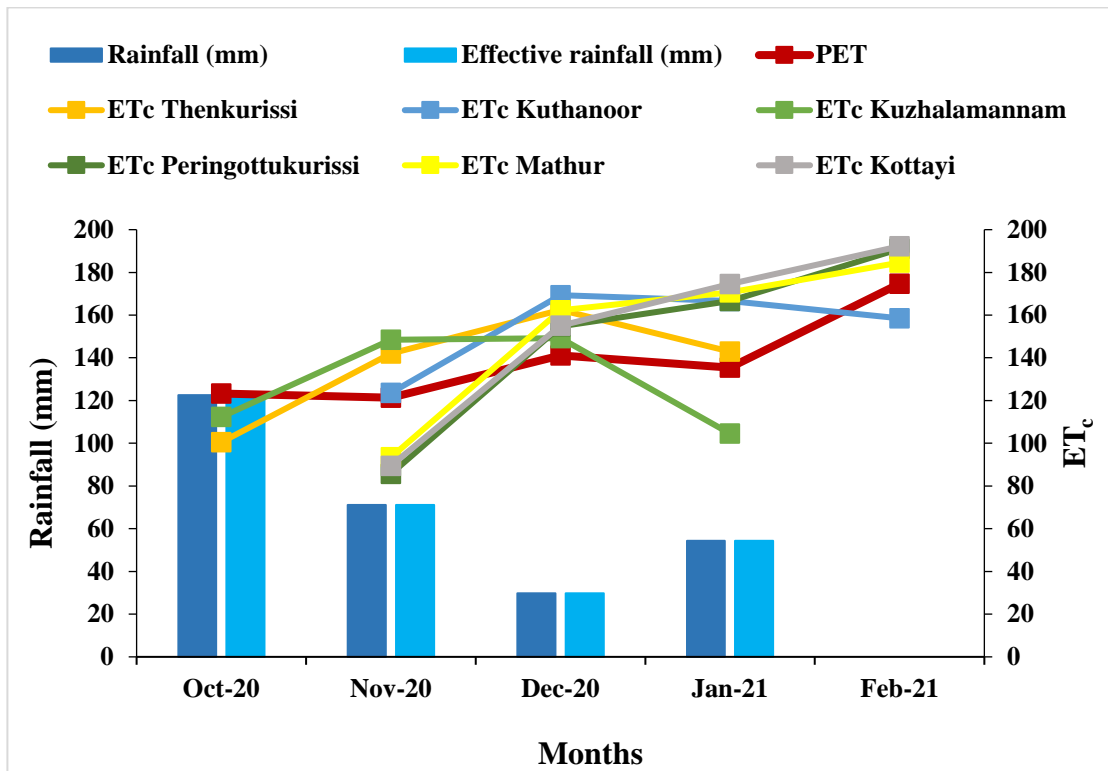


Fig. 5.25. Distribution of monthly rainfall, effective rainfall, reference evapotranspiration and crop evapotranspiration of rice in Kuzhalmannam block

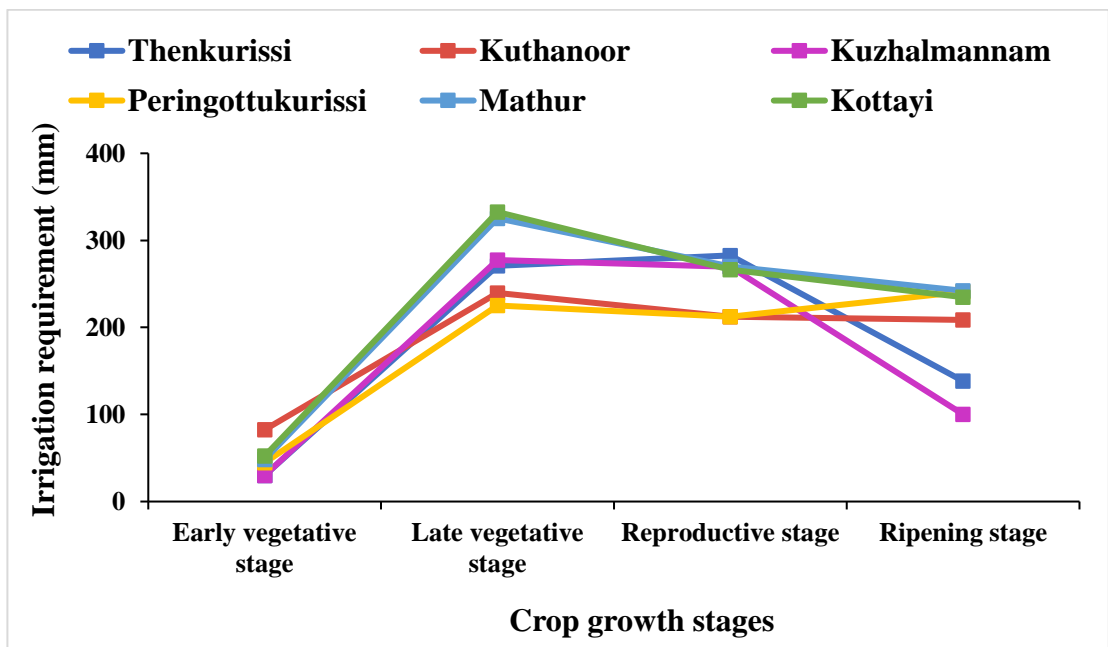


Fig. 5.26. Stagewise irrigation requirement in Kuzhalmannam block during mundakan season

5.3.5. Comparison of K_c values corresponding to rice and non-rice area

K_c maps were developed for the whole study area for all the pixels including rice and non rice areas as well. The rice K_c values obtained from K_c maps showed a definite pattern similar to standard point based K_c values in literature. The K_c value during early vegetative stage corresponding to julian days 305-321 was 0.87, the K_c value of non rice area was also 0.87 during this stage (Fig. 5.27). A slight increase in K_c value to 1.04 was observed in rice area during late vegetative stage (337-353 julian day), but the K_c value in non-rice area remained constant. Towards the reproductive stage of the crop (001-017 julian day) K_c value of rice area further increased to 1.14, whereas in non rice area K_c value of 0.87 was observed. The increase in K_c values in rice area can be attributed to the development of plant canopy/ vegetation cover with the growth of rice plant, which inturn will be reflected in NDVI values. Since, NDVI values were used to develop K_c maps, variation in NDVI will be reflected in K_c values. The maturity stage of the crop (033-049 julian day) showed a decreasing trend in K_c values with 0.93 in rice area and 0.69 in non-rice area, this is due to the reduction in NDVI values as the crop approaches senescence stage.

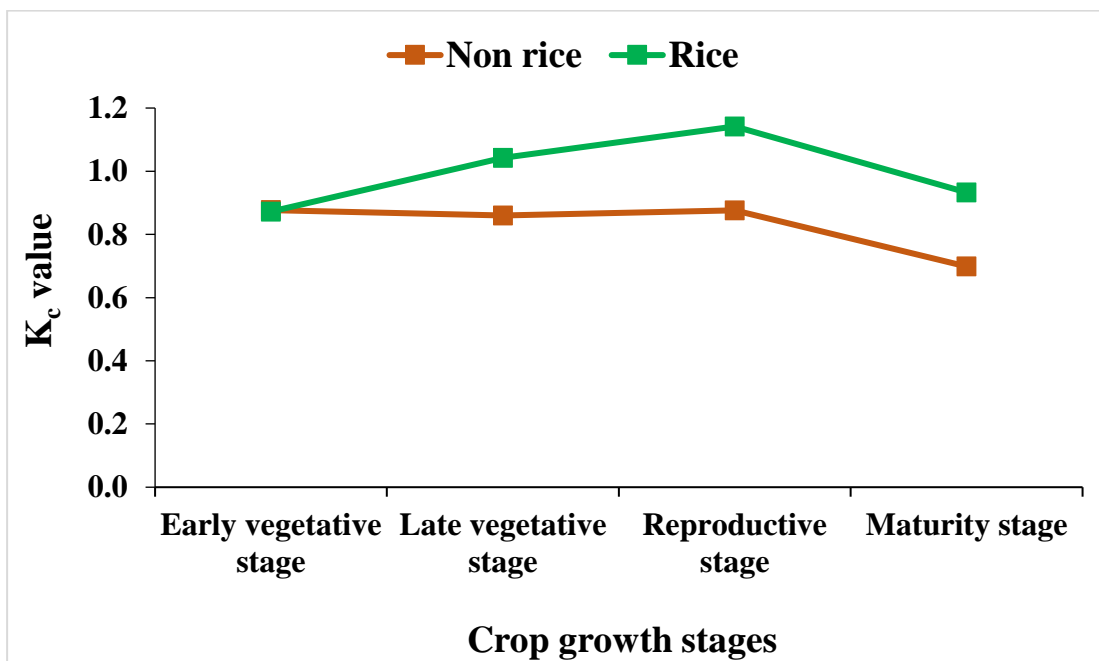


Fig. 5.27. Comparison of K_c values corresponding to rice and non-rice area

In this study, the crop water requirement in rice was estimated based on remote sensing techniques and land based observations during *mundakan* season 2020-21 for five blocks of Palakkad district. Crop coefficient (K_c) maps developed using GIS provided K_c values at regional scale during different stages of crop growth for the study area which helps to estimate crop evapotranspiration with greater accuracy. Crop water demands maps depicting spatial and temporal distribution of irrigation requirement also were made for the whole study area. These maps facilitate the estimation of crop water requirement of a rice field if the geographical coordinates of the location is known. The total crop water requirement during *mundakan* 2020-21 in Palakkad district was estimated in the range of 700-975 mm. Integration of remote sensing & agrometeorological techniques have scope for the estimation of regional scale crop water requirement in a limited time and with less expense.

Summary

6. SUMMARY

Remote sensing products could be effectively used to delineate large homogeneous rice areas as well as fragmented heterogeneous areas. Rice area was delineated using Sentinel-2 images and the total estimated area was 24742.76 ha with an average accuracy of 88.33 % and kappa coefficient 0.766 in five blocks of Palakkad district.

A relationship was established between NDVI derived from satellite data (MODIS images) and K_c values in the form of simple linear regression equation and was validated for the entire crop growth period based on ground truth locations in the study area with an $R^2 = 0.8156$. The K_c value predicted based on satellite derived NDVI values were validated for the training sites in 5 blocks of Palakkad district. The coefficient of determination (R^2) was 0.865 in Alathur block, 0.823 in Nenmara block, 0.840 in Kollengode block, 0.868 in Chittur block, 0.831 in Kuzhalmannam block.

FAO Penman-Montieth method was used in this study to estimate the reference evapotranspiration (ET_o) during the crop period. The block wise ET_o was observed in the range of 123.19-174.94 mm/ month (Alathur block), 122.03-174.83 mm/ month (Nenmara block), 121.8-175.49 mm/ month (Kollengode block), 122.99-176.48 mm/ month (Chittur block) and 121.34-174.69 mm/ month (Kuzhalmannam block).

The crop evapotranspiration was estimated by multiplying crop coefficient (K_c) with the reference evapotranspiration (ET_o). The total crop evapotranspiration (ET_c) during the crop period in Alathur block was in the range of 536.26-611.26 mm, 438.59-577.07 mm in Nenmara block, 533.78-601.05 mm in Kollengode block, 514.34-626.90 mm in Chittur block and 514.49-617.93 mm Kuzhalmannam block. Though the rainfall received during the crop period was effectively utilized, it was not sufficient to compensate crop evapotranspiration fully, so irrigation is required to maintain crop growth in the field.

The irrigation requirement for rice includes water required to compensate crop evapotranspiration and additional water required to maintain standing water in fields. The total irrigation requirement during *mundakan* season 2020-21 in Alathur block was

in the range of 761.56-912.39 mm, in Nenmara block it ranges from 647.59-723.20 mm, 611.18-935.44 mm in Kollengode block, 767.64-975.90 mm in Chittur block and 667-885.75mm in Kuzhalmannam block. The total irrigation requirement of rice was estimated to be in the range of 611-975 mm during *mundakan* season 2020-21 for 5 blocks in Palakkad district.

The crop water demands maps depicting spatial and temporal distribution of irrigation requirement were prepared for the whole study area corresponding to early vegetative stage, late vegetative stage, reproductive stage and maturity stage of the crop. Crop water demand maps facilitate the estimation of crop water requirement of a paddy field if the geographical coordinates of the location is collected using devices like GPS.

References

REFERENCES

- Acheampong, P. K. 1986. Evaluation of potential evapotranspiration methods for Ghana. *GeoJournal*. 12: 409-415.
- Ahmad, L., Parvaze, S., Paravaze, S., and Kanth, R. H. 2017. Crop water requirement of saffron in Kashmir valley. *J. Agrometeorol.* 19 (1): 380-381.
- Ahmad, L., Qayoom, S., Afroza, B., Bhat, O. A., and Mushtaq, N. 2019. Water requirement of solanaceous vegetable crops in Kashmir valley. *Cur. J. App. Sci. Tech.* 35 (4): 1-7.
- Ajith, K., Geethalakshmi, V., Raghunath, K. P., Pazhanivelan, S., and Dheebakaran, G. 2017. Rice yield prediction using MODIS-NDVI (MOD13Q1) and land based observations. *Int. J. Curr. Microbiol. Appl. Sci.* 6 (12): 2277-2293.
- Allen, R. G., Pereira, L. S., Raes, D., and Smith, M. 1998. Crop evapotranspiration: Guidelines for computing crop water requirements. In: *FAO Irrigation and drainage Paper No.56*, Food and Agriculture Organization of the United Nations, Rome, 300p.
- Allen, R. G., Smith, M., Pereira, L. S., and Pruitt, W. O. 1997. Proposed revision to the FAO procedure for estimating crop water requirements. In: Chantzoulakes, K. S. (ed.). *Proceedings of 2nd International Symposium on Irrigation of horticultural crops*, ISHS, *Acta Hort.* 1: 17-33.
- Allen, R. G., Tasumi, M., and Trezza, R. 2007. Satellite-based energy balance for mapping evapotranspiration with internalized calibration (METRIC)—model. *J. Irrig. Drain. Eng.* 133 (4): 380-394.
- Bala, A., Rawat K. S., Misra A. and Srivastava A. 2015. Vegetation indices mapping for Bhiwani district of Haryana (India) through LANDSAT-7ETM+ and remote sensing techniques. *J. Appl. Nat. Sci.* 7 (2): 874-879
- Bandyopadhyay, A. A., Bhadra, N. S., Raghuwanshi and Singh, R. 2009. Temporal trends in estimates of reference evapotranspiration over India. *J. Ecol. Eng.* 14 (5): 508-515.

- Bashir, M. A., Hata, T., Tanakamaru, H., Abdelhadi, A. W., and Tada, A. 2007. Remote sensing derived Crop Coefficient for Estimating Crop Water Requirements for Irrigated Sorghum in the Gezira Scheme, Sudan. *J. Environ. Inform.* 10(1): 47-54.
- Beck, T., Pieter S. A., Atzberger, C., Hogda, K. A., Johansen, B., and Skidmore A. K. 2006. Improved monitoring of vegetation dynamics at very high latitudes: A new method using MODIS NDVI. *Remote Sens. Environ.* 100: 321-334.
- Bruzzone, L., Bovolo, F., Paris, C., Solano-Correa, Y. T., Zanetti, M., and Fernández-Prieto, D. 2017. Analysis of multitemporal Sentinel-2 images in the framework of the ESA scientific exploitation of operational missions. In: *Proceedings of the 2017 9th International Workshop on the analysis of multitemporal remote sensing images (MultiTemp)*, Brugge, Belgium, pp. 1-4.
- Calera A., Campos I., Osann A., D'Urso G., and Menenti M. Review remote sensing for crop water management: from ET modelling to services for the end users. 2017. *Sensors* 17(5): 110.
- Carlson, T., and Ripley, D. 1997. On the Relation between NDVI, fractional vegetation cover, and Leaf Area Index. *Remote Sens. Environ.* 62: 241-252.
- Casa, R., Rossi, M., Sappa, G., and Trotta, A. 2008. Assessing crop water demand by remote sensing and GIS for the Pontina Plain, Central Italy. *Water Resour. Manag.* 23: 1685-1712.
- Chahal, G. B. S., Sood, A., Jalota, S. K., Choudhury, B. U., and Sharma, P. K. 2007. Yield: evapotranspiration and water productivity of rice (*Oryza sativa* L.), wheat (*Triticum aestivum* L.) system in Punjab-India as influenced by transplanting date of rice and weather parameters. *Agric. Water Manag.* 88: 14-27.
- Chattopadhyay, N. and Hulme, M. 1997. Evaporation and potential evapotranspiration in India under conditions of recent and future climate change. *Agric. Forest Meteorol.* 87: 55-73.

- Chavez, J. L., Gowda, P. H., Howell, T. A., Neale, C. M. U., Copeland K. S. 2015. Estimating hourly crop ET using a two-source energy balance model and multispectral airborne imagery. *Irrig. Sci.* 28 (1): 79-91.
- Cihlar, J., Ly, H., Li, Z., Chen, J., Pokrant, H., and Huang, F. 1997. Multitemporal, multichannel AVHRR data sets for land biosphere studies: artifacts and corrections. *Remote Sens. Environ.* 60: 35-57.
- Cohen, J. 1960. A coefficient of agreement for nominal scale. *Educ. Psychol. Meas.* 20: 37-46.
- Cohen, S., Ianetz, A., and Stanhill, G. 2002. Evaporative climate changes at Bet Dagan, Israel, 1964-1998. *Agric. Forest Meteorol.* 111: 83-91.
- Cong, Z. T. and Yang, D. W. 2009. Does evaporation paradox exist in China? *Hydrol. Earth Syst. Sci.* 13: 357-366.
- D'Urso, G. 2001. Simulation and management of on-demand irrigation systems: a combined agrohydrological and remote sensing approach. PhD thesis. Wageningen University, The Netherlands. 175p.
- Dadhwal, V. K. and Ray, S. S. 2000. Crop assessment using remote sensing - Part II: Crop condition and yield assessment. *Indian J. Agric. Economic.* 55 (2): 54-67.
- Dalton J. 1802. Experimental essays on the constitution of mixed gases; on the force of steam of vapour from waters and other liquids in different temperatures, both in a Torricellian vacuum and in air on evaporation and on the expansion of gases by heat. *Mem. Manch. Lit. Philos. Soc.* 5: 535-602.
- de Vries, M. E., Rodenburg, J., Bado, B. V., Sow, A., Leffelaar, P. A., and Giller, K. E. 2010. Rice production with less irrigation water is possible in a Sahelian environment. *Field Crops Res.* 116: 154-164.
- Dharsana, Ashish P., and Pandey R. P. 2013. Analysing trends in reference evapotranspiration and weather variables in the Tons-river basin in Central India. *Stoch. Environ. Res. Risk Assess.* 27: 1407–1421.

- Dinpashoh, Y., Jhajharia, D., Fakheri-Fard, A., Singh, V. P., and Kahya, E. 2011. Trends in reference crop evapotranspiration over Iran. *J. Hydrol.* 399: 422-433.
- Djaman, K., Rudnick, D., Moukoumbi, R., Yonnelle D., Sow, A., and Irmak, S. 2019. Actual evapotranspiration and crop coefficients of irrigated lowland rice (*Oryza sativa* L.) under semiarid climate. *Biosyst. Eng.* 604.
- Duchemin, B., Hadria, R., Erraki, S., Boulet, G., Maisongrande, P., Chehbouni, A., Escadafal, R., Ezzahar, J., Hoedjes, J. C. B., Kharrou, M. H., Khabba, S., Mougnot, B., Olioso, A., Rodriguez, J. C., and Simonneaux, V. 2006. Monitoring wheat phenology and irrigation in Central Morocco: on the use of relationships between evapotranspiration, crops coefficients, leaf area index and remotely-sensed vegetation indices. *Agric. Water Manag.*, 79: 1-27.
- Dutrieux, L. P., Verbesselt, J., Kooistra, L., and Herold, M. 2015. Monitoring forest cover loss using multiple data streams, a case study of a tropical dry forest in Bolivia. *ISPRS J. Photogramm. Remote Sens.* 107: 112-125.
- European Commission. 2018. Cap Explained. Direct Payments for Farmers 2015-2020; EU Publications: Brussels, Belgium.
- FAO. 1992. CROPWAT: a computer programme for irrigation planning and management. Irrigation and Drainage Paper. In: Martin Smith (ed.). *Food and Agriculture Organization of the United Nations*, Rome, Italy. 46 p.
- FAO [Food and Agricultural Organisation]. 2021. Available: www.fao.org (Accessed on 25 Jan 2021).
- Gao, G., Chen D. L., Ren, G. Y., Chen, Y., and Liao, Y. M. 2006. Spatial and temporal variations and controlling factors of potential evapotranspiration in China: 1956–2000. *J. Geogr. Sci.* 16: 3-12.
- Glenn, E. P., Nagler, P. L., and Huete, A. R. 2010. Vegetation index methods for estimating evapotranspiration by remote sensing. *Surv. Geophys.* 31 (6): 531-555.

- González, A., Kjaersgaard, J., Trooien, T., Hay, C., and Ahiablame, L. 2018. Estimation of crop evapotranspiration using satellite remote sensing-based vegetation index. *Adv. Meteorol.*, 2018: 1-12.
- Gowda, T. P., Manjunatha, S. B., Yogesh, T. C. and Sunil, A. S. 2013. Study on Water Requirement of Maize (*Zea mays* L.) using CROPWAT Model in Northern Transitional Zone of Karnataka. *J. Environ. Sci. Comput. Eng. Technol.* 2 (1): 105-113.
- Gromny, E., Lewiński, S., Rybicki, M., Malinowski, R., Krupiński, M., Nowakowski, A., and Jenerowicz, M. 2019. Creation of training dataset for Sentinel-2 land cover classification. In: *Proceedings of the Photonics Applications in Astronomy, Communications, Industry, and High-Energy Physics Experiments*, Wilga, Poland, 111763p.
- Gundekar, H. G., Khodke, U. M., Sarkar, S., and Rai, R. K. 2008. Evaluation of pan coefficient for reference crop evapotranspiration for semi-arid region. *Irrig. Sci.* 26: 169-175.
- Hargreaves, G. L., Hargreaves, G. H., and Riley, J. P. 1986. Irrigation water requirements for Senegal River Basin. *J. Irrig. Drain. Eng.* 1(3): 265-275.
- Hossain, M. B., Yesmin, S., Maniruzzaman, M., and Biswas J. C. 2017. Irrigation scheduling of rice (*Oryza sativa* L.) using CROPWAT model in the western region of Bangladesh. *Agriculturists.* 15(1): 19.
- Huete, A., Didan, K., Miura, T., Rodriguez, E. P., Gao, X., and Ferreira L. G. 2002. Overview of the radiometric and biophysical performance of the MODIS vegetation indices. *Remote Sens. Environ.* 83: 195-213.
- Hunsaker, D. J., Pinter, P. J., and Kimball, B. A. 2005. Wheat basal crop coefficients determined by normalized difference vegetation index. *Irrig. Sci.* 24: 1-14.
- IRRI [International Rice Research Institute]. 2014. Available: <http://www.knowledgebank.irri.org/decision-tools/growthstages-and-important-management-factors>.

- IRRI [International Rice Research Institute]. 2021. IRRI home page. Available: <http://www.knowledgebank.irri.org/> [Accessed 19 Jan. 2021]
- Ishak, A. M., Bray, M., Remesan, R., and Han, D. 2010. Estimating reference evapotranspiration using numerical weather modelling. *Hydrol. Process.* 24: 3490-3509.
- Ivanov Romanenko, A. 1961. Computation of the autumn soil moisture using a universal relationship for a large area. Proceedings, Ukrainian Hydrometeorological Research Institute, Kiev, no. 3.
- Javed, M. A. and Ahmad S. R. 2020. A decision support system for crop water requirement estimation using advanced geospatial techniques. *Pak. J. Agri. Sci.* 57 (4): 981-991.
- Jayanthi, H., Nealea, C. M. U., and Wright, J. L. 2007. Development and validation of canopy reflectance based crop coefficient for potato. *Agric. Water Manag.* 88 (1- 3): 235-246.
- Jhajharia, D., Dinpashoh, Y., Kahya, E., Singh, V. P., and Fakheri-Fard, A. 2011. Trends in reference evapotranspiration in the humid region of North East India. *Hydrol Process*, 26: 421-435.
- Ji, C. 1966. Morphometry From Maps, Essays in Geomorphology, Elsevier Publications, New York. pp. 235-274.
- Justice, D. H., Salomonson, V., Privette, J., Riggs, G., Strahler, A., Lucht, R., Myneni, R., Knjazihhin, Y., Running, S., Nemani, R., Vermote, E., Townshend, J., Defries, R., Roy, D., Wan, Z., Huete, A., van Leeuwen, R., Wolfe, R., Giglio, L., Muller, J.-P., Lewis, P., and Barnsley, M. 1998. The Moderate Resolution Imaging Spectroradiometer (MODIS): land remote sensing for global change research. *IEEE Transactions on Geoscience and Remote Sensing.* 36: 1228-1249.
- Kamble, B., Kilic, A., and Hubbard, K. 2013. Estimating crop coefficients using remote sensing-based vegetation index. *Remote Sens.* 5 (4): 1588-1602.

- Kar, G. and Verma, H. N. 2005. Climatic water balance, Probable rainfall, rice crop water requirements and cold periods in AER 12.0 in India, *Agric. Water Manag.*, 72(1): 15-32.
- KAU [Kerala Agricultural University]. 2016. *Package of Practices Recommendation, Crops* (15th Ed.). Kerala Agricultural University, Thrissur, 393p.
- Kephe, P., Kingsley A., and Brilliant, P. 2021. Challenges and opportunities in crop simulation modelling under seasonal and projected climate change scenarios for crop production in South Africa. *Agric. Food Sec.* 10p.
- Kingra, P. K. and Mahey, R.K. 2009. Comparative evaluation of different methods to compute evapotranspiration at different phenological stages in wheat. *J. Agrometeorol.* 11 (2): 102-108.
- Koksal, E. S. 2008. Evaluation of spectral vegetation indices as an indicator of crop coefficient and evapotranspiration under full and deficit irrigation conditions. *Int. J. Remote Sens.* 29 (23): 7029-7043.
- Korhonen, L., Packalen, P., and Rautiainen, M. 2017. Comparison of Sentinel-2 and Landsat 8 in the estimation of boreal forest canopy cover and leaf area index. *Remote Sens. Environ.* 195: 259-274.
- Kulberg, E. G., Dejonge, K. C., and Chavez J, L. 2017. Evaluation of thermal remote sensing indices to estimate crop evapotranspiration coefficients. *Agric. Water Manag.* 179: 64-73.
- Kumar, K. K., Kumar, K. R., and Rakhecha, P. R. 1986. Comparison of Penman and Thornthwaite methods of estimating potential evapotranspiration for Indian conditions. *Theor. Appl. Climatol.* 38 (37): 140-146.
- Kuo, S., Ho, S., and Liu, C. 2006. Estimation irrigation water requirements with derived crop coefficients for upland and paddy crops in China irrigation association, Taiwan. *Agric. Water Mang.* 82: 433-445.
- Lee J. L. and Huang W. C. 2014. Impact of Climate Change on the Irrigation Water Requirement in Northern Taiwan. *Water* 6 (11): 3339-3361.

- Lopresti, M. F., Bella, C, M, D., and Degioanni, A. J. 2015. Relationship between MODIS-NDVI data and wheat yield: A case study in Northern Buenos Aires province, Argentina, *Inf. Process. Agric.* 2 (2): 73-84.
- Lorite, I. J., Ruiz-Ramos, M. Gabaldón-Leal, C., Cruz-Blanco, M., Porras, R., and Santos, C. 2018. Water management and climate change in semiarid environments: water scarcity and sustainable agriculture in semiarid environment. *Tools, Strategies, and Challenges for Woody Crops.* pp. 3-40.
- Mahi, G. S. and Kingra, P. K. 2018. *Fundamentals of Agrometeorology and Climate Change.* Kalyani Publishers. New Delhi. 401p.
- Maina, M., Amin, M., Rowshon, M. K., Aimrun, W., Samsuzana, A., and Yazid, M. 2014. Effects of crop evapotranspiration estimation techniques and weather parameters on rice crop water requirement. *Australian J. Crop Sci.* 8 (4): 495-501.
- Malenovský, Z., Rott, H., Cihlar, J., Schaepman, M. E., García-Santos, G., Fernandes, R., and Berger, M. 2012. Sentinels for science: potential of Sentinel-1, -2, and -3 missions for scientific observations of ocean, cryosphere, and land. *Remote Sens. Environ.* 120: 91-101.
- Mavi, H. S. 2018. *Introduction to Agrometeorology.* CBS Publishers and Distributors, New Delhi, 275p.
- Mdemu, M. V., Magayane, M. D., Lankford, B., Hatibu, N., and Kadigi, R. M. J. 2004. Conjoining rainfall and irrigation seasonality to enhance productivity of water in rice irrigated farms in the Upper Ruaha River Basin, Tanzania. *Phys. Chem. Earth.* 29: 1119-1124.
- Mehboob, Golam-Islam M., Tariqul A. F. M., and Deshapriya, L. 2016. Rice mapping and monitoring in Sylhet region of Bangladesh using MODIS-NDVI. 26p.
- Meyer, A. 1926. About some connections between climate and soil in Europe. *Chemie der Erde.* 2: 209-347.

- Mishra, P., Tiwari, K. N., Chowdary, V. M., and Gontia, N. K. 2005. Irrigation water demand and supply analysis in the command area using remote sensing and GIS. *J. Hydrol. IAHR.* 28(1-2): 59-69.
- Mkhabela, M. S., Bullock, P., Raj, S., Wang, S., and Yang, Y. 2011. Crop yield forecasting on the Canadian Prairies using MODIS NDVI data. *Agr. forest meteorol.* 151: 385-393.
- Montazar, A., Rejmanek, H., Tindula, G., Little, C., Shapland, T., Anderson, F., Inglese, G., Mutters, R., Linqvist, B., Greer, C. A., Hill, J., and Snyder, R. L. 2017. Crop Coefficient Curve for Paddy Rice from Residual Energy Balance Calculations. *J. Irrig. Drain. Eng.* 143 (2): 4016076.
- Moratiel, R., and Martinez-Cob, A., 2013. Evapotranspiration and crop coefficient of rice (*Oryza sativa* L.) under sprinkler irrigation in a semi-arid climate determined by the surface renewal method. *Irrig. Sci.* 31: 411-422.
- Mosleh, M. K., Hassan. Q. K., and Chowdhury, E. H. 2015. Application of remote sensors in mapping rice area and forecasting its production: A review. *Sensors.* 15: 769-791.
- Mushtaq, M. K., Sharma, L. A., Krishna, B., Mushtaq K., and Mir J. I. 2020. Crop water requirement estimation using pan evaporimeter for high density apple plantation system in Kashmir region of India. *J. Agric. Meteorol.* 22 (1): 86-88.
- Nayak, A. B. 2006. An analysis using Liss III data for estimating water demand for rice cropping in parts of Hirakud command area, Orissa, India. M. Sc. Thesis. International Institute for Geo-information Science and Earth Observation. Indian Institute of Remote Sensing, Dehradun, India.
- Niel, T. G. V. and McVicar, T. R. 2001. Remote Sensing of Rice-Based Irrigated Agriculture: A Review. Rice CRC Technical Report. pp. 1101-1105.
- Noureldin, N. A., Aboelghar, M. A., Saady, H. S., Saady and Ali A. M. 2013. Rice yield forecasting models using satellite imagery in Egypt. *Egypt. J. Remote. Sens. Space Sci.* 16: 125-131.

- Nuarsa, I. W. and Nishio, F. 2007. Relationships between rice growth parameters and remote sensing data. *J. Remote Sens. Earth Sci.* 4: 102-112.
- NWM [National Water Mission]. 2021. NWM home page. Available: <http://nwm.gov.in> [Accessed 15 Jan. 2021]
- Papadakis, J. 1966. *Climates of the world and their agricultural potentialities*. Buenos Aires publishers, Argentina, 174p.
- Papadopoulou, E., Varanou, E., Baltas, E., Dassaklis, A. and Mimikou, M. 2003. Estimating potential evapotranspiration and its spatial distribution in Greece using empirical methods. In; *Proceedings of the 8th International Conference on Environmental Science and Technology* Lemnos Island, Greece, pp. 650-658.
- Parmar, H. V. and Gontia, N. K. 2016. Remote sensing based vegetation indices and crop coefficient relationship for estimation of crop evapotranspiration in Ozal-II canal command. *J. Agrometeorol.* 18 (1): 137-139.
- Pastor-Guzman, J., Atkinson, P. M., Dash, J., and Rioja-Nieto, R. 2015. Spatiotemporal variation in mangrove chlorophyll concentration using Landsat 8. *Remote Sens.* 7 (11): 14530-14558.
- Persello, C., Tolpekin, V. A., Bergado, J. R., and de By, R. A. 2019. Delineation of agricultural fields in smallholder farms from satellite images using fully convolutional networks and combinatorial grouping. *Remote Sens. Environ.* 231: 111253.
- Pesaresi, M., Corbane, C., Julea, A., Florczyk, A. J., Syrris, V., and Soille, P. 2016. Assessment of the added-value of Sentinel-2 for detecting built-up areas. *Remote Sens.* 8: 299.
- Pettorelli, N., Vik, J. O., Mysterud, A., Gaillard, J. M., Tucker, C. J., and Stenseth, N. C. 2005. Using the satellite-derived NDVI to assess ecological responses to environmental change. *Trends Ecol Evol.* 220 (9): 503-510.

- Phiri, D., Simwanda M., Salekin, S., Nyirenda, V. R., Murayama Y., and Ranagalage M. 2020. Sentinel-2 Data for Land Cover/Use Mapping: A Review Remote Sens. 12: 2291.
- Pirmoradian, N. and Davatgar, N. 2019. Simulating the effects of climatic fluctuations on rice irrigation water requirement using AquaCrop, *Agric. Water Manag.* 213: 97-106.
- Prince, S. D. and Goward, S. N. 1995. Global Primary Production: A Remote Sensing Approach. *J. Biogeogr.* 22: 815-835.
- Rao, G. S. L. H. V. P. 2008. Agricultural Meteorology. PHI Learning Private Limited, Delhi, 364p.
- Rawat, K. S., Singh, S. K., Bala, A., and Szaboacute S. 2019. Estimation of crop evapotranspiration through spatial distributed crop coefficient in a semi-arid environment. *Agric. Water Mang.* 213: 922-933.
- Ray S. S. and Dadhwal V. K. 2001. Estimation of crop evapotranspiration of irrigation command area using remote sensing and GIS. *Agric. Water Manag.* 49: 239-249.
- Rayner, D. P. 2007. Wind run changes: the dominant factor affecting pan evaporation trends in *Australia. J. Clim.* 20: 3379-3394.
- Raza, S. M. H., Mahmood, S. A., and Khan, A. A. 2018. Delineation of Potential Sites for Rice Cultivation Through Multi-Criteria Evaluation (MCE) Using Remote Sensing and GIS. *Int. J. Plant Prod.* 12: 1-11.
- Reyes-González, A., Kjaersgaard, J., Trooien, T., Hay, C., Ahiablame L., and Hindawi. 2018. Estimation of crop evapotranspiration using satellite remote sensing-based vegetation index. *Adv. Meteorol.* 12 p.
- Rohwer, C. 1931. Evaporation from free water surface. USDA Tech Null. 217: 1-96.

- Rouse, J. W., Haas, R. H., Schell, J. A., and Deering, D. W. Monitoring vegetation systems in the Great Plains with ERTS, in Third ERTS symposium, NASA, Washington DC, USA. pp. 309-317
- Rydberg, A. and Borgefors, G. 2001. Integrated Method for Boundary Delineation of Agricultural Fields in Multispectral Satellite Images. *IEEE Trans. Geosci. Remote Sens.* 39: 2514-2520.
- Sandhu, R. and Irmak, S. 2019. Assessment of AquaCrop model in simulating maize canopy cover, soil-water, evapotranspiration, yield, and water productivity for different planting dates and densities under irrigated and rainfed conditions. *Agric. Water Manag.* 224: 1-2.
- Saravanan, E. 1994. Agroclimatological studies of Kerala state for application in land use planning, PhD thesis, Cochin University of Science and Technology, Kochi, Kerala, 109p.
- Saxena, R., Tiwari, A., Mathur, P., and Chakravarty, N. V. K. 2020. An investigation of reference evapotranspiration trends for crop water requirement estimation in Rajasthan. *J. Agrometeorol.* 22 (4): 449-456.
- Sentelhas, P., Gillespie, T., and Santos, E. 2010. Evaluation of FAO Penman-Monteith and alternative methods for estimating reference evapotranspiration with missing data in Southern Ontario, Canada. *Agric. Water Manag.* 97: 635-644.
- Sethi, R. R., Sahu, A. S., Kaledhonkar, M. J., Sarangi, A., Rani, P., Kumar, A., and Mandal, K.G. 2014. Quantitative determination of rice cultivated areas using geospatial techniques. *IOSR J. Environ. Sci. Toxicol. Food Technol.* 8: 76-81.
- Sheng, F. K., Lin, B. J., and Shieh, H. J. 2001. International Commission on Irrigation and Drainage, 1st Asian Regional Conference, Seoul.
- Shimada, M., Itoh, T., Motooka, T., Watanabe, M., Shiraishi, T., Thapa, R. and Lucas, R. 2014. New global forest/non-forest maps from ALOS PALSAR data (2007–2010). *Remote Sens. Environ.* 155: 13-31.

- Singh, R. and Irmak, A. 2008. A modified approach for estimation of crop coefficients using satellite remote sensing data. Presented at the 2008 ASABE Annual International Meeting, Providence, Rhode Island, Paper Number: 083542.
- Smith, M. 1992. CROPWAT: a computer programme for irrigation planning and management. Irrigation and Drainage Paper. Food and Agriculture Organization of the United Nations, Rome, Italy, 46 p.
- Spanu, A., Murtas, A., and Ballone, F. 2009. Water use and crop coefficients in sprinkler irrigated rice. *Ital. J. Agron.* 4 (2): 47-58.
- Stephen, V. S. 1997. Selecting and interpreting measures of thematic classification accuracy. *Remote Sens. Environ.*, 62 (1): 77-89.
- Surendran, U., Sushanth, C. M., Mammen, G., and Joseph, E. J. 2015. Modelling the crop water requirement using FAO-CROPWAT and assessment of water resources for sustainable water resource management: A case study in Palakkad district of humid tropical Kerala, India. *Aquat. Procedia.* 4: 1211-1219.
- Tabari, H., Grismer, E. M., and Trajkovic, S. 2011. Comparative analysis of 31 reference evapotranspiration methods under humid conditions. *Irrig. Sci.* 31: 107-117.
- Tabbal, D. F., Bouman, B. A. M., Bhuiyan, S. I., Sibayan, E. B., and Sattar, M. A. 2002. On-Farm strategies for reducing water input in irrigated rice; case studies in the Philippines. *Agric. Water Mang.* 56: 93-112.
- Tasumi, M. and Allen R. G. 2007. Satellite-based ET mapping to assess variation in ET with timing of crop development. *Agric. Water Manag.* 88: 54-62.
- Terjung, W. H., Hayes, J. T., Ji, H. Y., and Ser, B. 1984. Crop water requirements for rainfed and irrigated rice (Paddy) in China. *Arch. Met. Geoph. Biocl.* 34: 181.
- Thomas C. G. 2010. Land Husbandry and Watershed Management. Kalyani Publishers, Ludhiana, 716p.
- Tian, P., Cao, X., Zhang, L., Sun, N., Sun, L., Logan, T., Shi, J., Wang, Y., Ji, Y., Lin, Y., Huang, Z., Zhou, T., Shi, Y., and Zhang, R. 2015. Aerosol vertical

- distribution and optical properties over China from long-term satellite and ground-based remote sensing, *Atmos. Chem. Phys.* 17: 2509-2523.
- Toureiro, C., Serralheiro, R., Shahidian, S., and Sousa, A. 2017. Irrigation management with remote sensing: Evaluating irrigation requirement for maize under Mediterranean climate condition. *Agric. Water Manag.* 184: 211–220.
- Trabert, W. 1896. Performance of Twelve Mass Transfer Based Reference Evapotranspiration Models under Humid Climate. *Meteorol.* 13: 261-263.
- Trajkovic, S. 2009. Comparison of radial basis function networks and empirical equations for converting from pan evaporation to reference evapotranspiration. *Hydrol Process.* 23: 874-880.
- Tyagi, N. K., Sharma, D. K., and Luthra, S. K. 2000. Determination of crop coefficients of rice and sunflower. *Agric. Water Manag.* 45: 41-54.
- Ullasa. M. Y. 2019. Crop Models for Efficient Water Management. doi:10.13140/RG.2.2.14648.80645
- Valipour, M. 2014. Application of new mass transfer formulae for computation of evapotranspiration. *J. Appl. Water Eng. Res.* 2 (1): 33-46.
- van Leeuwen, W. J. D., Huete, A. R., and Laing, T. W. 1999. MODIS vegetation index compositing approach: a prototype with AVHRR data. *Remote Sens. Environ.*, 69: 264 -280.
- Vermote, E., Saleous, E. N., and Justice, C. 2002. Atmospheric correction of the MODIS data in the visible to middle infrared: First results. *Remote Sens. Environ.* 83: 97-111.
- Vicente-Serrano, S. M., Camarero, J. J., Olano, J. M., Martín-Hernández, N., Peña-Gallardo, M., Tomás-Burguera, M., Gazol, A., Azorin-Molina, C., Bhuyan, U., Kenawy A. E., and Ahamad, M. 2016. Diverse relationships between forest growth and the Normalized Difference Vegetation Index at a global scale. *Remote Sens. Environ.* 187: 14-29.

- Vysakh, A., Ajithkumar, B., and Sathish, J. V. 2017. Effect of dates of planting on crop water requirement of rice in Kerala. *J. Agrometeorol.* 51-54.
- WMO [World Meteorological Organisation]. 1966. Measurement and estimation of evaporation and evapotranspiration. Tech Pap. (CIMO-Rep) 83.
- Xiao, W., Xu, S., and He, T. 2021. Mapping Paddy Rice with Sentinel-1/2 and Phenology-, Object-Based Algorithm—A Implementation in Hangjiahu Plain in China Using GEE Platform. *Remote Sens.*13: 990.
- Xu, Y., Yu, L., Feng, D., Peng, D., Li, C., Huang, X., Lu, H. and Gong, P. 2019. Comparisons of three recent moderate resolution African land cover datasets. *Int. J. Remote Sens.* 40: 6185-6202.
- Xue, J. and Su, B. 2017. Significant remote sensing vegetation indices: A review of developments and applications. *J. Sens.*, 1: 1-17.
- Xue, J. and Su, B. 2017. Significant Remote Sensing Vegetation Indices: A Review of Developments and Applications. Article ID 1353691. doi.org/10.1155/2017/1353691
- Yoo, S., Choi, J., and Jang M. 2006. Estimation of crop coefficients from Penman-Montieth and FAO Modified Penman formulas for paddy rice. In: *Proceedings of the Korean society of Agricultural Engineering*, 48 (1): 13-23.
- Zhan, P., Zhu, W., and Li, N. 2021. An automated rice mapping method based on flooding signals in synthetic aperture radar time series. *Remote Sens. Environ.* 252: 112112.
- Zhang, Y., Liu, C., Tang, Y., and Yang, Y. 2007. Trends in pan evaporation and reference and actual evapotranspiration across the Tibetan Plateau. *J. Geophys. Res.* 112: 12110.
- Zhao, Y., Shan, X., and Tang, P. 2014. Spatial consistency analysis and relative geometric correction of low spatial resolution multi-source remote sensing data. *Remote Sens. Tech. Appl.* 29: 155-163.

Appendices

Appendix I

Abbreviations and units used

Abbreviations

AET : Actual evapotranspiration

ET : Evapotranspiration

FCC : False Color Composite

GIS : Geographic Information System

MODIS : Moderate Resolution Imaging Spectroradiometer

NASA : National Aeronautics and Space Administration

NDVI : Normalized Difference Vegetation Index

NOAAA-VHRR : National Oceanic and Atmospheric Administration- Advanced

Very High Resolution Radiometer

PET : Potential evapotranspiration

USGS : United States Geological Survey

VI : Vegetation Indices

Units

mm : millimeter

kg ha⁻¹ : kilogram per hectare

MJ : Mega Joule

% : per cent

°C : degree Celsius

kPa : kilo Pascal

m s⁻¹ : meter per second

Appendix II

Name and address of the farmers in ground truth locations

Blocks	Locations	Name and address of the farmer
Alathur	Alathur I	Muhammed Fuad, S/O Abdul Shukkoor, Kizhakkevedu (H), NH Vanoor, Alathur
	AlathurII	Suresh Baby, S/O Chandran, Kumbalakkode, Alathur
	Kavasseri	K. B. Sreeprasad, Kakampara (H), Erattakulam P.O., Alathur
	Kizhakkenchery	Raju F., Vadakkevedu (H), Chendamkulam, Vambadu, Kizhakkenchery
	Pudukkode	Radakrishnan, Puuvakkodekalam (H), Pudukkode
	Tarur	Arumukhan, Kalathil (H), Pallayil, Tarur
	Vadakkenchery	M. Abdul Majeed, Sena manzil (H), Payyakkundu P. O., Anjimurthimangalam
	Erimayur	Sureshkumar, Maruthurkalam (H), Kunisseri
Nenmara	Aliyur	Narayanan, Mannattukalam (H), Puthanthara, Thiruvazhiyadu
	Melarkode	P. Muraleedharan, Chungath (H), Konnallur, Chittilanchery
	Vandazhy	Kumaran, S/O Krishnan, Valliyode, Vandazhy
	Nenmara	Sudevan, S/O kesavan, Aluvassery, Nenmara P. O.
	Elevenchery	Ramanunni, Ramanilayam(H), Cherapuram, Elevenchery
	Pallassana	P S Unnikrishnan, Pulikkal (H), Kizhakethara, Pallasana

Chittur	Perumatty	Krishnadas, Pavithram (H), Ayyapankavu, Perumatty, Vandithavalam
	Nallepilly	V. N. Sethumadavan, Thottasserykalam, Nallepilly
	Polpully	P K Divakaran, Aramanakkalam (H), Panayur P. O. Polpully
	Chittur- Thathamangalam	K. Mohanan, Polanikalam (H), Thathamangalam
Kuzhalmannam	Thenkurissi	Praseed, Paliyanpattakalam, Thekkumpuram, Vemballur
	Kuthanoor	Rajagopalan, Chalakkodukalam (H), Chembukadu
	Kuzhalmannam	Raja, Manjadi (H), Mochulli P.O., Kuzhalmannam
	Peringottukurissi	Joymon, Vazhakkodukalam (H), Chulanoor
	Mathur	M. Mani, Ponnathuveedu (H), Mathur Agraharam
	Kottayi	Rajan P., Kizhakkekara (H), Post Agraharam, Kottayi
Kollengode	Pattanchery	Sethumadavan, Kannikandathu(H), Chettiyarchella, Nenjode P. O., Pattanchery
	Muthalamada	Sasikumar, S/O Prabhakaran, Manali (H), Kuttyadam, Muthalamada
	Vadavannur	Raveendran, Koottalappadamkulam, Vadavannur
	Koduvayur	Thanka Prakash, Thamikandathu(H), Kannankode, Karipode P O
	Pudunagaram	Narayanankutty, Karimathu (H), Illathukulambu
	Peruvemb	Sachidanadhan, Puthanveedu, Aalyapadamkalam P.O., Pervemb

Appendix III : Weather data during the crop growth period
Weekly weather data of Alathur block during 2020-21

Year	SMW	Tmax (°C)	Tmin (°C)	DTR (°C)	Tmean (°C)	RH 1 (%)	RH 2 (%)	RHmean (%)	WS (km h ⁻¹)	BSS (h)	EVP (mm/ week)	RF (mm)
2020	42	32.1	24.7	7.4	28.4	91	78	84.5	2.8	5.9	9.5	22.3
2020	43	34.3	26.7	7.6	30.5	88	70	79	2	6.4	15.2	22.3
2020	44	34.1	26.2	7.9	30.15	88	68	78	1.8	6	13.8	26.4
2020	45	33.1	24.9	8.2	29	75	57	66	5.7	7.2	19	1.2
2020	46	31.6	23.9	7.7	27.75	73	65	69	6.2	7	18.1	4.2
2020	47	28.6	20.9	7.7	24.75	72	50	61	4.3	8.6	20.8	0
2020	48	30.7	21.4	9.3	26.05	77	63	70	6	7.9	20	0
2020	49	32.7	22.2	10.5	27.45	80	71	75.5	4.8	3.9	12	7.7
2020	50	32.7	22.8	9.9	27.75	75	55	65	5.7	8.6	24.2	0
2020	51	36.3	26.4	9.9	31.35	74	59	66.5	12.1	7.2	21	0
2020	52	35.5	24.5	11	30	75	57	66	9.3	7.7	32.1	0
2021	1	30.4	22.5	7.9	26.45	76	63	69.5	12.8	6.7	19.6	47.7
2021	2	33.2	23	10.2	28.1	80	72	76	5.9	3.3	16.6	0
2021	3	30.8	21.4	9.4	26.1	74	59	66.5	10.3	7.4	26.6	0
2021	4	32.1	22.8	9.3	27.45	76	53	64.5	5.6	8.3	23.1	0
2021	5	32.8	20.8	12	26.8	61	44	52.5	11.2	8.7	36.4	0
2021	6	35.9	23.4	12.5	29.65	61	36	48.5	13.4	9	36.7	0
2021	7	35.8	26.5	9.3	31.15	74	40	57	7.1	9	37.3	0
2021	8	36.9	24.6	12.3	30.75	68	49	58.5	6	8.2	25	1.1
2021	9	33.3	22.9	10.4	28.1	72	33	52.5	8	8.3	32	0

SMW: Standard meteorological week Tmax: Maximum temperature Tmin: Minimum temperature Tmean: Mean temperature DTR: Diurnal temperature range
 RH 1: Forenoon relative humidity RH 2: Afternoon relative humidity RHmean: Mean relative humidity WS: Wind speed BSS: Bright sunshine hours EVP: Evaporation
 RF: Rainfall

Appendix III (Contd.)

Weekly weather data of Nenmara block during 2020-21

Year	SMW	Tmax (°C)	Tmin (°C)	DTR (°C)	Tmean (°C)	RH 1 (%)	RH 2 (%)	RHmean (%)	WS (km h⁻¹)	BSS (h)	EVP (mm/ week)	RF (mm)
2020	42	32.2	24.4	7.8	28.3	91	78	84.5	2.8	5.9	9.5	29
2020	43	33.6	26.3	7.3	29.95	88	70	79	2	6.4	15.2	4
2020	44	33.5	25.8	7.7	29.65	88	68	78	1.8	6	13.8	19
2020	45	33.5	25.3	8.2	29.4	75	57	66	5.7	7.2	19	0
2020	46	31.6	23.4	8.2	27.5	73	65	69	6.2	7	18.1	67
2020	47	27.7	21.2	6.5	24.45	72	50	61	4.3	8.6	20.8	2
2020	48	30.3	20.6	9.7	25.45	77	63	70	6	7.9	20	0
2020	49	32.6	21.6	11	27.1	80	71	75.5	4.8	3.9	12	30
2020	50	31.3	22.5	8.8	26.9	75	55	65	5.7	8.6	24.2	0
2020	51	36.8	26	10.8	31.4	74	59	66.5	12.1	7.2	21	0
2020	52	35.2	24.3	10.9	29.75	75	57	66	9.3	7.7	32.1	0
2021	1	31.5	23.4	8.1	27.45	76	63	69.5	12.8	6.7	19.6	16
2021	2	32.9	22.4	10.5	27.65	80	72	76	5.9	3.3	16.6	12
2021	3	30.6	21.3	9.3	25.95	74	59	66.5	10.3	7.4	26.6	0
2021	4	32.2	22.3	9.9	27.25	76	53	64.5	5.6	8.3	23.1	0
2021	5	31.7	20.4	11.3	26.05	61	44	52.5	11.2	8.7	36.4	0
2021	6	35.3	23.1	12.2	29.2	61	36	48.5	13.4	9	36.7	0
2021	7	36.1	26.1	10	31.1	74	40	57	7.1	9	37.3	0
2021	8	37	24.7	12.3	30.85	68	49	58.5	6	8.2	25	8
2021	9	33.1	22.6	10.5	27.85	72	33	52.5	8	8.3	32	0

SMW: Standard meteorological week Tmax: Maximum temperature Tmin: Minimum temperature Tmean: Mean temperature DTR: Diurnal temperature range
 RH 1: Forenoon relative humidity RH 2: Afternoon relative humidity RHmean: Mean relative humidity WS: Wind speed BSS: Bright sunshine hours EVP: Evaporation
 RF : Rainfall

Appendix III (Contd.)

Weekly weather data of Kollengode block during 2020-21

Year	SMW	Tmax (°C)	Tmin (°C)	DTR (°C)	Tmean (°C)	RH 1 (%)	RH 2 (%)	RHmean (%)	WS (km h⁻¹)	BSS (h)	EVP (mm/ week)	RF (mm)
2020	42	32.4	24.5	7.9	28.45	91	78	84.5	2.8	5.9	9.5	31
2020	43	34.2	26.3	7.9	30.25	88	70	79	2	6.4	15.2	5.2
2020	44	33.6	25.9	7.7	29.75	88	68	78	1.8	6	13.8	22
2020	45	33.5	25.3	8.2	29.4	75	57	66	5.7	7.2	19	0
2020	46	31.5	23.5	8	27.5	73	65	69	6.2	7	18.1	21.6
2020	47	27.5	21.1	6.4	24.3	72	50	61	4.3	8.6	20.8	0
2020	48	30.1	20.5	9.6	25.3	77	63	70	6	7.9	20	0
2020	49	32.4	21.4	11	26.9	80	71	75.5	4.8	3.9	12	24.4
2020	50	31	22.3	8.7	26.65	75	55	65	5.7	8.6	24.2	0.4
2020	51	36.6	25.8	10.8	31.2	74	59	66.5	12.1	7.2	21	0.6
2020	52	35.1	24.2	10.9	29.65	75	57	66	9.3	7.7	32.1	0.6
2021	1	30.3	22.3	8	26.3	76	63	69.5	12.8	6.7	19.6	8.2
2021	2	33.1	22.7	10.4	27.9	80	72	76	5.9	3.3	16.6	3.2
2021	3	30.7	21.1	9.6	25.9	74	59	66.5	10.3	7.4	26.6	0
2021	4	31.8	22.5	9.3	27.15	76	53	64.5	5.6	8.3	23.1	0
2021	5	32.8	20.4	12.4	26.6	61	44	52.5	11.2	8.7	36.4	0
2021	6	35.9	23.1	12.8	29.5	61	36	48.5	13.4	9	36.7	0
2021	7	36.1	26.3	9.8	31.2	74	40	57	7.1	9	37.3	0
2021	8	37.2	24.4	12.8	30.8	68	49	58.5	6	8.2	25	0.6
2021	9	33.7	22.7	11	28.2	72	33	52.5	8	8.3	32	0

SMW: Standard meteorological week Tmax: Maximum temperature Tmin: Minimum temperature Tmean: Mean temperature DTR: Diurnal temperature range
 RH 1: Forenoon relative humidity RH 2: Afternoon relative humidity RHmean : Mean relative humidity WS: Wind speed BSS: Bright sunshine hours EVP: Evaporation
 RF: Rainfall

Appendix III (Contd.)

Weekly weather data of Chittur block during 2020-21

Year	SMW	Tmax (°C)	Tmin (°C)	DTR (°C)	Tmean (°C)	RH 1 (%)	RH 2 (%)	RHmean (%)	WS (km h⁻¹)	BSS (h)	EVP (mm/ week)	RF (mm)
2020	42	32.3	24.6	7.7	28.45	91	78	84.5	2.8	5.9	9.5	5
2020	43	33.8	26.5	7.3	30.15	88	70	79	2	6.4	15.2	10
2020	44	33.8	26.1	7.7	29.95	88	68	78	1.8	6	13.8	8.7
2020	45	33.8	25.6	8.2	29.7	75	57	66	5.7	7.2	19	0
2020	46	32	23.8	8.2	27.9	73	65	69	6.2	7	18.1	22
2020	47	28.1	21.5	6.6	24.8	72	50	61	4.3	8.6	20.8	0
2020	48	30.6	20.7	9.9	25.65	77	63	70	6	7.9	20	0
2020	49	32.7	21.6	11.1	27.15	80	71	75.5	4.8	3.9	12	37
2020	50	31.4	22.4	9	26.9	75	55	65	5.7	8.6	24.2	0
2020	51	36.8	25.9	10.9	31.35	74	59	66.5	12.1	7.2	21	0
2020	52	35.2	24.3	10.9	29.75	75	57	66	9.3	7.7	32.1	0
2021	1	30.3	22.3	8	26.3	76	63	69.5	12.8	6.7	19.6	14
2021	2	33.1	22.7	10.4	27.9	80	72	76	5.9	3.3	16.6	1
2021	3	30.8	21	9.8	25.9	74	59	66.5	10.3	7.4	26.6	0
2021	4	31.9	22.4	9.5	27.15	76	53	64.5	5.6	8.3	23.1	0
2021	5	32.9	20.4	12.5	26.65	61	44	52.5	11.2	8.7	36.4	0
2021	6	36.1	23.1	13	29.6	61	36	48.5	13.4	9	36.7	0
2021	7	36.3	26.3	10	31.3	74	40	57	7.1	9	37.3	0
2021	8	37.4	24.4	13	30.9	68	49	58.5	6	8.2	25	0
2021	9	34	22.7	11.3	28.35	72	33	52.5	8	8.3	32	0

SMW: Standard meteorological week Tmax: Maximum temperature Tmin: Minimum temperature Tmean: Mean temperature DTR: Diurnal temperature range
 RH 1: Forenoon relative humidity RH 2: Afternoon relative humidity RHmean : Mean relative humidity WS: Wind speed BSS: Bright sunshine hours EVP: Evaporation
 RF : Rainfall

Appendix III (Contd.)

Weekly weather data of Kuzhalmannam block

Year	SMW	Tmax (°C)	Tmin (°C)	DTR (°C)	Tmean (°C)	RH 1 (%)	RH 2 (%)	RHmean (%)	WS (km h⁻¹)	BSS (h)	EVP (mm/ week)	RF (mm)
2020	42	32.1	24.4	7.7	28.25	91	78	84.5	2.8	5.9	9.5	11.7
2020	43	33.4	26.2	7.2	29.8	88	70	79	2	6.4	15.2	1.6
2020	44	33.3	25.8	7.5	29.55	88	68	78	1.8	6	13.8	29.5
2020	45	33.2	25.2	8	29.2	75	57	66	5.7	7.2	19	13.6
2020	46	31.3	23.4	7.9	27.35	73	65	69	6.2	7	18.1	17.3
2020	47	27.4	21.1	6.3	24.25	72	50	61	4.3	8.6	20.8	0
2020	48	30.1	20.5	9.6	25.3	77	63	70	6	7.9	20	11.2
2020	49	32.4	21.5	10.9	26.95	80	71	75.5	4.8	3.9	12	29.7
2020	50	31.1	22.4	8.7	26.75	75	55	65	5.7	8.6	24.2	0
2020	51	36.8	25.9	10.9	31.35	74	59	66.5	12.1	7.2	21	0
2020	52	35.1	24.2	10.9	29.65	75	57	66	9.3	7.7	32.1	0
2021	1	30.2	22.3	7.9	26.25	76	63	69.5	12.8	6.7	19.6	53.5
2021	2	32.9	22.6	10.3	27.75	80	72	76	5.9	3.3	16.6	0.9
2021	3	30.5	20.9	9.6	25.7	74	59	66.5	10.3	7.4	26.6	0
2021	4	31.8	22.4	9.4	27.1	76	53	64.5	5.6	8.3	23.1	0
2021	5	32.7	20.4	12.3	26.55	61	44	52.5	11.2	8.7	36.4	0
2021	6	35.8	23.1	12.7	29.45	61	36	48.5	13.4	9	36.7	0
2021	7	35.9	26.4	9.5	31.15	74	40	57	7.1	9	37.3	0
2021	8	37	24.4	12.6	30.7	68	49	58.5	6	8.2	25	0
2021	9	33.4	22.7	10.7	28.05	72	33	52.5	8	8.3	32	0

SMW: Standard meteorological week Tmax: Maximum temperature Tmin: Minimum temperature Tmean: Mean temperature DTR: Diurnal temperature range
 RH 1: Forenoon relative humidity RH 2: Afternoon relative humidity RHmean : Mean relative humidity WS: Wind speed BSS: Bright sunshine hours EVP: Evaporation
 RF : Rainfall

ESTIMATION OF CROP WATER REQUIREMENT IN RICE USING SATELLITE DATA AND GIS

by
CHINNU RAJU
(2019-11-186)

ABSTRACT OF THE THESIS

Submitted in partial fulfillment of the requirement for the degree of

MASTER OF SCIENCE IN AGRICULTURE

Faculty of Agriculture
Kerala Agricultural University



**DEPARTMENT OF AGRICULTURAL METEOROLOGY
COLLEGE OF AGRICULTURE**

VELLANIKKARA, THRISSUR – 680 656

KERALA, INDIA

2021

ABSTRACT

Water shortage is one of the world's most critical issues, and climate change projections suggest that it will get worse in the future. Since, water availability and accessibility are the most significant constraints to agricultural production in water-scarce areas, resolving this issue is crucial. In order to overcome this, farmers must better estimate crop water requirements and use irrigation water more efficiently. Proper irrigation management and water conservation depend on accurate estimation of crop water demands. This study was done to estimate crop water requirement in rice crop during *mundakan* season 2020-21 in Palakkad district of Kerala using remote sensing and land based observations.

Remote sensing technology relies on the spectral signatures of the vegetation and other land covers in an area. In order to proceed with the analysis of remote sensing products, the major rice growing areas were delineated using multi temporal cloud free Sentinel-2 imageries at a spatial resolution of 10 m following iso cluster unsupervised classification. The overall classification accuracy was 88.33 % with a Kappa coefficient of 0.77. Small fragmented heterogeneous rice areas and large homogeneous rice areas were classified equally well.

A commonly used and recommended method for estimating crop water requirements is the use of reference evapotranspiration (ET_o) and crop coefficient (K_c). Under field conditions, standard methods to estimate evapotranspiration (ET) over homogenous surfaces include conventional techniques such as weighing lysimeters that measure the water consumed through ET directly based on a mass balance, or flux measurements using Bowen Ratio or Eddy Covariance instrument systems that measure components of the surface energy balance to estimate evapotranspiration. However, a limitation of these systems is that they provide point measurements that may not adequately represent the ET from fields other than where the measurement is taken. To overcome this problem of estimating ET from multiple fields, satellite-based remote sensing is a useful method for estimating ET on a field-by-field basis at a regional scale

The use of remotely sensed vegetation indices, such as the Normalized Difference Vegetation Index (NDVI) and Soil Adjusted Vegetation Index (SAVI), has

been tested by scientists to predict crop coefficient (K_c) at field and regional scale. In this study, analysis was done to establish a relationship between Normalized Difference Vegetation Index (NDVI) and crop coefficient (K_c) values for the 30 ground truth locations spread over 5 blocks *viz.* Alathur, Nenmara, Kollengode, Chittur and Kuzhalmannam, which represents the major rice growing tract of Palakkad district. A linear equation was set, between NDVI values obtained from MODIS NDVI (MOD13Q1) 16 day composite with a spatial resolution of 250 m and K_c table values collected from literature, and the equation showed a strong relation with an R^2 value of 0.8156. The Normalized Difference Vegetation Index (NDVI) was calculated from reflectance of the red and near infrared bands. K_c values vary from season to season and field to field. Also, K_c depends on crop growth stage, plant density, and irrigation management. Hence, it becomes necessary to test the relationship between NDVI and K_c to confirm crop coefficient under local conditions.

The K_c predicted values during early vegetative were in the range of 0.5-0.8, towards the late vegetative stage, it showed an increasing trend from 0.8 to 1.2, during the reproductive stage the value raised to 1.3, and when the rice crop reached maturity stage K_c values decreased to 0.58. The potential evapotranspiration during different crop growth stages ranged between 120-176 mm. The total crop evapotranspiration during the entire *mundakan* season 2020-21 in the training sites considered for the study was in the range of 500-626 mm. Water lost through crop evapotranspiration is compensated by effective rainfall and water supplied through irrigation. The rainfall received during early vegetative stage *ie;* during October and November months were sufficient to compensate evapotranspiration losses of the rice crop. But irrigation is necessary for sustaining crop growth during late vegetative, reproductive and maturity stages due to the lack of rainfall in the corresponding months so as to compensate crop evapotranspiration. In rice, total irrigation requirement includes water required to compensate crop evapotranspiration and additional water supplied to maintain standing water in the fields. The total irrigation requirement of rice during *mundakan* 2020-21 in Palakkad district was in the range of 611-975 mm.

Crop coefficient (K_c) maps created at a regional scale provided K_c values during various stages of crop growth, allowing for more accurate estimation of crop

evapotranspiration for the research area. Crop water demands maps were also created for the entire study area, demonstrating the spatial and temporal distribution of irrigation requirements. If the geographical coordinates of the place are known, these maps make estimates of crop water requirement of a rice field much easier.

Global warming and climate change may lead to increased frequency of irrigation in the near future. This in turn causes increased the demand of water for irrigation purposes. Information regarding crop specific area under irrigated agriculture and crop growing season are important for efficient use of available water resources. The delineated rice field will provide a clear view of the geographical coverage of irrigation requirements, and the crop water demand maps will show the stage wise irrigation water requirements. The irrigation requirement map prepared for the study area covering 5 blocks of Palakkad district can be used for water resource planning and management. This is particularly useful for understanding inter seasonal variations in irrigation water demand at different geographical and temporal dimensions.